Politecnico di Torino

Master's degree in Petroleum and Mining Engineering

A.Y. 2024/25

Graduation session:

March-April 2025

"Thermal conductivity of lithologies for sizing shallow geothermal systems"

Advisors:

Prof. Alessandro Casasso

Candidate:

MohammadAmin Albooyeh

(ID 289637)

Abstract

As the world looks for cleaner energy solutions, shallow geothermal energy has attracted attention as a renewable energy source that can contribute to replace fossil fuels.

The ability of various geological materials to transport heat plays an important role in the efficiency of operation of ground-source heat pump systems and on their economic feasibility. Studying the thermal properties of rocks is therefore of key importance and, for this purpose, both laboratory and field tests have been conducted.

This thesis explains how the thermal properties of different types of rock rocks are determined and, based on a comprehensive set of results from the literature, the influence of factors such as lithology, mineral composition, moisture levels, and temperature variations was assessed.

By offering a critical review of thermal conductivity measurements, this research contributes to valuable insight that can direct future development in geothermal energy applications.

Acknowledgements

Table of Contents

1 Introduction

Addressing the global issue of climate change has become a top priority worldwide and most nations in the world have signed the Paris Agreement (2015), which seeks to limit global temperature increases to 1.5°C above pre-industrial levels. However, as energy demands continue to rise due to population growth, industrial expansion, and technological innovations, greenhouse gas (GHG) emissions remain a major challenge (1).

In response, renewable energy alternatives to fossil fuels are being explored. One such alternative is represented by geothermal heating and cooling systems, which are recognized for their reliability and sustainability as energy solutions (39).

1.1 Overview of shallow geothermal systems

1.1.1 Geothermal energy basics

Geothermal heat is continuously generated within the Earth due to the natural decay of radioactive materials deep inside the planet. This heat gradually flows outward from the core, often reaching the surface through volcanic activity, though it usually stays trapped beneath the Earth's crust, heating the surrounding rocks and underground water to extremely high temperatures, sometimes reaching several hundred degrees Celsius. If hot water or steam is contained within porous, permeable rocks, forming a geothermal aquifer, the heat can be harnessed (57).
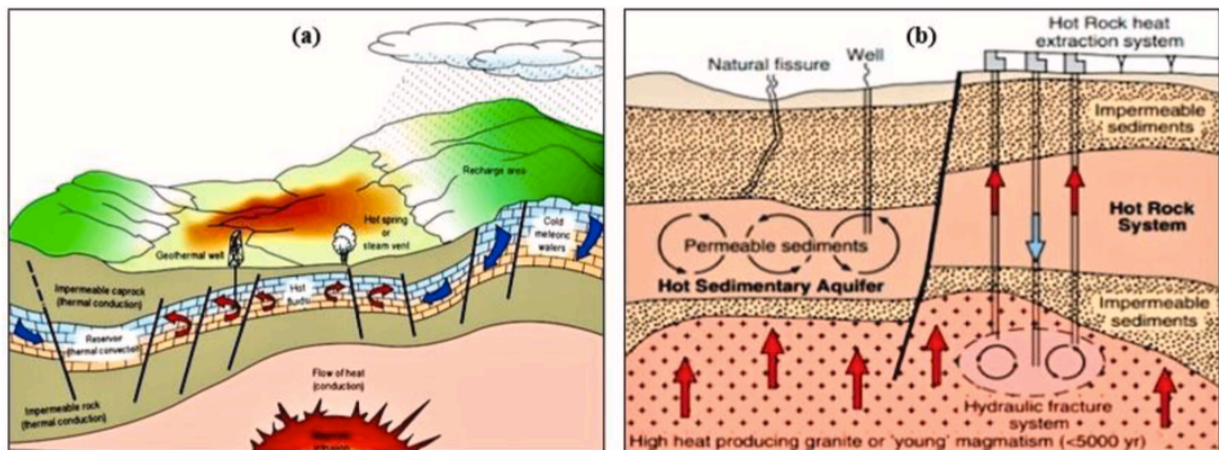
Figure 1: (a) Ideal geothermal system schematic; (b) Hot rock and hot sedimentary aquifer systems (57).

The heat from the Earth's molten core spreads to the surrounding rocks and eventually transfers to underground water reserves through convection. Various technologies are capable of capturing and utilizing this heated water or steam for different applications (Fig. 1) (57).

Temperatures within the Earth's continental crust increase with depth, starting from surface temperatures and gradually rising to around 1000°C at several kilometers depth, while the Earth's core can reach temperatures between 3500°C and 4500°C (69). The total heat flow from the Earth is estimated to be approximately 42×10^{12} W, derived from conduction, convection, and radiation. Out of this, 8×10^{12} W comes from the Earth's crust, which, although comprising only 2% of the Earth's volume, is rich in radioactive materials. The mantle contributes 32.3×10^{12} W, representing 82% of the Earth's volume, while the core contributes 1.7×10^{12} W, making up 16% of the Earth's volume but lacking radioactive materials (20).

1.1.2 Types of Geothermal Systems

The use of shallow geothermal energy has gained traction due to rising fossil fuel prices and its ability to help reduce CO_2 emissions (65). Geothermal systems are typically classified into shallow, medium, and deep categories (Fig. 2). Shallow systems, generally installed at depths of 100–150 meters, utilize the soil and nearby aquifers. Medium-depth systems, found at greater depths, are often associated with hydrothermal resources and are also suitable for underground thermal storage. Deep systems, on the other hand, are linked to petro-thermal resources (56).
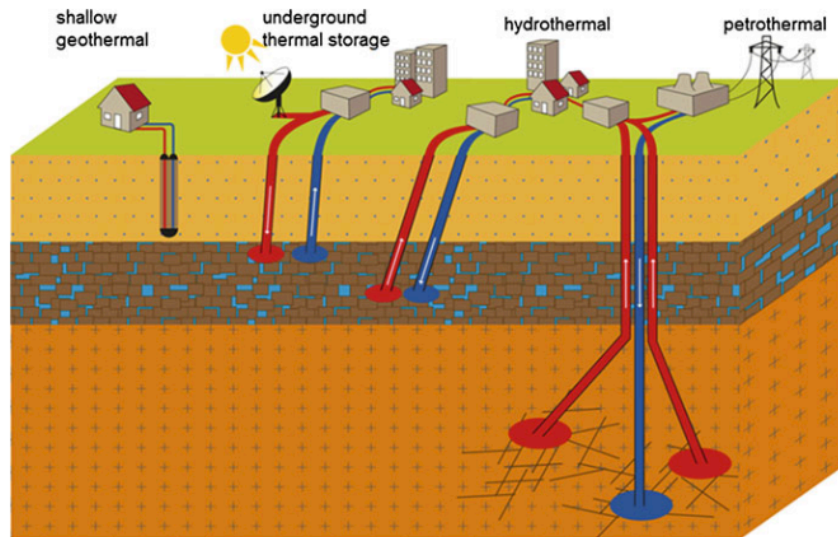
Figure 2: Overview of Geothermal Systems: Shallow, medium, and deep systems (56).

These systems typically consist of three main components: the ground loop, the heat pump, and the indoor loop.

• The ground loop is made up of one or more borehole heat exchangers (BHEs) that either extract heat from the shallow subsurface for heating purposes or inject heat for cooling. This is typically achieved through closed-loop pipes, either vertically or horizontally installed in the ground, with a refrigerant circulating through them.

• The heat pump's role is to increase the low-grade heat extracted from the ground loop to a higher temperature, making it suitable for heating rooms or providing hot water.

• The indoor loop is responsible for transporting and distributing the high-grade heat or cool air throughout the building (56).

1.2   Shallow geothermal system technologies

1.2.1   Ground source heat pumps (GSHPs) and borehole heat exchanger (BHE)

Heat transfer is required for heat or cool places, and a method to achieve this is usually up to 50 to 100 meters, by 50 to 100 meters, by exploiting in thermal energy stored in the ground at the shallow depth. This geothermal energy can be exploited using heat pumps, which convert low-temperature geothermal energy into high temperatures. This process relies on the physical properties of fluids to absorb heat when vaporizing and release heat when condensing (43).

Among the numerous applications of geothermal energy, such as energy production, district heating, greenhouse heating, aquaculture, climate regulation, and bathing, the most common is the use of geothermal heat pumps powered by ground-source heat exchangers (GSHEs) (62).

Ground Source Heat Pumps (GSHPs) transfer heat from the ground to a building through a ground heat exchanger connected to a heat pump. The performance of the GSHP system in specific borhole depends on the thermal conductivity and temperature of the ground. Data from temperature sensors with borhole can provide information about various depth and land temperature on time. As a result, it is important to understand the thermal properties of the ground accurately for the long -term efficiency of the GSHP system (66). The GSHP system is classified into two types: a closed-loop system, where heat is exchanged along the ground through a circulating liquid in a closed loop pipe, and the open loop system, which has groundwater heat pump It is also known as (GWHPS), where heat is exchanged with ground water, which is usually applied to the same aquifer (12).

Open-loop systems consist of several components: a heat exchanger (installed within the building to be heated or cooled), an abstraction well, and an injection well (Fig. 3). In certain cases, the extracted water is not re-injected into the ground but is discharged to the surface, such as in sewage systems. This practice should be done with caution to avoid environmental harm and only when it doesn't risk depleting the aquifer's groundwater.

The advantage of open-loop systems lies in their use of natural water, which can also be used for "free" cooling, drinking, or irrigation, depending on its quality. Additionally, these systems can extract more heat from the ground than geo-exchangers of the same size. For equivalent heating or cooling demand, open-loop systems tend to be more cost-effective, as they require less drilling (43).
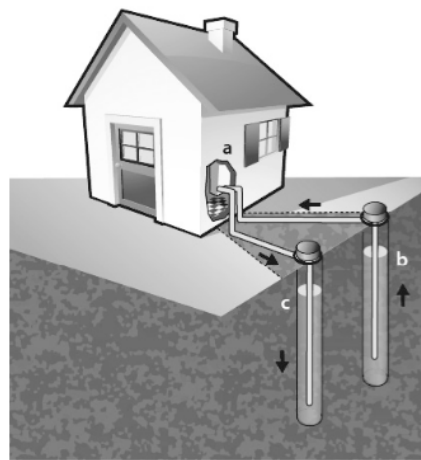
Figure 3: Open Loop GSHP System Details: (a) Heat exchanger, (b) Abstraction well, (c) Injection well (43).

Closed-loop systems, or Ground Coupled Heat Pump (GCHP) systems, involve closed-loop tubing installed in various configurations, such as horizontally in trenches, vertically in boreholes, or as baskets (Figs. 4 and 5). The loop is generally made from high-density polyethylene pipes and filled with a mixture of water and antifreeze. The size of the loop field depends on factors like soil type, moisture content, average ground temperature, and the heat characteristics of the building. Horizontal loops are suitable for areas with adequate surface space for installation, though vertical borehole heat exchangers are more commonly used for heating and cooling buildings (43).
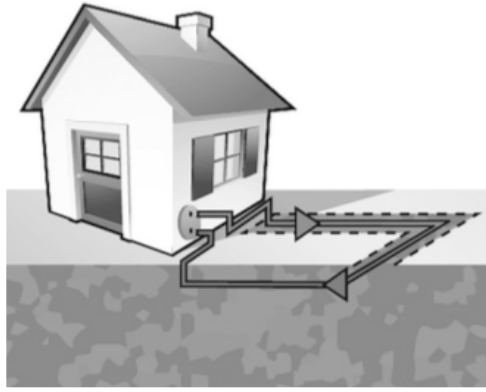
Figure 4: Closed Loop GSHP: Horizontal linear system (43).

Vertical systems typically involve one or more U-pipes or coaxial pipes, especially for deeper boreholes. The boreholes are spaced at least 5-6 meters apart, with their depth determined by ground conditions and the building's needs. For example, a house requiring 10 kW of heating capacity may need three boreholes, each ranging from 80 to 110 meters deep in sedimentary rock. When designed and integrated properly from the outset, these systems can play a significant role in creating modern, low-energy buildings with reduced CO_2 emissions (43).
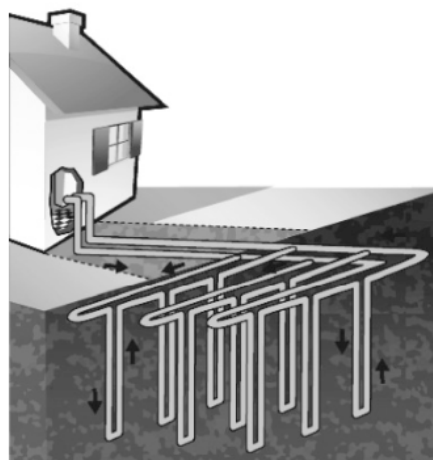
Figure 5: Closed Loop GSHP: Vertical system (43).

The performance of YouTube Borhole Heat Exchanges (BHE) is dependent on the thermal properties of the surrounding geological formation and the grout or backfill used in the borhole. To ensure the accurate design and cost-effectiveness of the GSHP system, it is important to understand

the thermal conductivity of the geological structure and the thermal resistance of BHE (22). A general technique to measure these parameters is the thermal response test (TRT). The data of this test is usually analyzed using the Calvin line source equation, which simplifies the sub -collecting heat transfer process. This method is mainly responsible for conductive heat transfer from BHE, while transport effects are represented through the parameters of effective thermal conductivity and borhole thermal resistance (65).

1.3   Definition and importance of thermal conductivity

Thermal conductivity refers to the ability of a material, such as rock, to transfer heat, and it is a vital parameter when evaluating geothermal potential at a specific location (21). This physical property is crucial for applications involving the movement, exchange, or conversion of thermal energy, and it plays a significant role in designing insulation and various building materials. Thermal conductivity can be calculated using parameters like thermal expansion rate, heat capacity, and density, as shown in the equation below (61,14):

$\lambda = \alpha \rho C_p$ (Equation 1)

The thermal conductivity of rocks is influenced by several factors, including mineral composition, porosity, anisotropy, and the properties of fluids within the pores. These factors cause substantial variations in thermal conductivity among different rock types, such as sedimentary, igneous, and metamorphic rocks.

The mineral composition of rocks directly impacts their thermal conductivity, with certain minerals exhibiting higher conductivity than others. For instance, quartz and hematite have high thermal conductivity, while materials such as clay, gypsum, and organic matter show much lower thermal conductivity (Table 1) (5).

Rock-forming mineral	λ (W m^{-1} K^{-1})	Rock-forming mineral	λ (W m^{-1} K^{-1})
Quartz-α	7.69[a], 7.69[b] 7.7[c]	Magnetite	5.10[a], 4.7–5.3[e], 5.1[b]
Quartz-mean	6.5[d]	Hematite	11.28[a], 11.2–13.9[e]
Zircon	5.54[a], 5.7[e]	Calcite	3.59[a], 3.25–3.9[e]
Serpentine	3.53 $\pm$ 1.28[a], 1.8-2.9[e]	Dolomite	5.51[a], 5.5[b], 5.3[c]
Clay minerals	2.9[f], 1.7[d]	Anhydrite	4.76[a], 4.76[b], 5.4[d]
Feldspar	2.3[g], 2.0[h]	Gypsum	1.26[a], 1.0–1.3[e]
Apatite	1.38 $\pm$ 0.01[a], 1.4[e]	Organic materials	0.25[f], 1.0[c]

Table 1: Thermal conductivity values of different minerals (5).

Typically, the thermal conductivity of geological materials ranges between 0.5 to 8 W·m^{-1}·K^{-1}, and it is significantly affected by rock weathering and water saturation levels, both of which enhance heat transfer through conduction (18, 21). While bedrock (excluding limestone) generally shows higher thermal conductivity, its thermal capacity is often lower compared to looser Quaternary rock layers (18).

To determine the thermal conductivity of rocks indirectly, petrophysical properties, such as porosity, are often used. These properties can be derived from well-logging data in combination with laboratory measurements (21).

1.4 Factors affecting thermal conductivity

1.4.1 Mineral composition

To assess the thermal properties of rocks accurately, understanding the geological, structural, and hydrogeological characteristics of a region at a local scale is essential (18). Thermal conductivity is affected by petrophysical properties like mineral composition, porosity, grain size, cementation degree, pore size and shape, the presence of fractures or cavities, and conditions such as pressure and temperature.

Rocks containing higher concentrations of minerals with high thermal conductivity tend to exhibit increased thermal conductivity. Quartz is particularly significant due to its abundance and its notably high thermal conductivity. In contrast, clay minerals, especially those from the mica group, tend to have low thermal conductivity. For example, sandstones, especially quartz-rich ones, usually have higher thermal conductivity compared to mudstones and claystones (29).

The relationship between mineral composition and thermal conductivity values for different rock types is shown in Figure 6 (70).
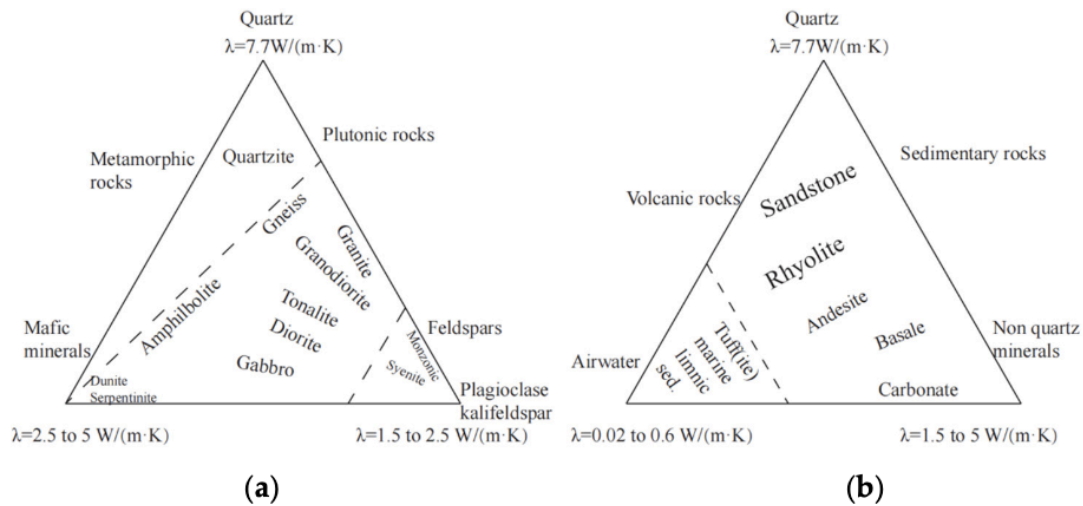
Figure 6: The link between the three primary rock categories and their various mineral components (70).

1.4.2 Porosity and permeability

Porosity and permeability are important characteristics of rocks that are influenced by lithology, depth, stress, and hydrothermal alterations. Typically, these properties decrease with depth due to burial and compaction. However, certain rock types, including volcanic breccias, lava flows, pyroclastic deposits, and some sedimentary rocks like sandstone or limestone, tend to maintain moderate to high primary porosity (up to 30% in sandstone and 70% in pumice) and permeability (ranging from 10^{-14} to 10^{-16} m²).

Volcanic structures show a wide range of primary permeability, from 10^{-9} to 10^{-11} m². Secondary permeability, which arises from fractures, faults, or dissolution features (such as in karstic formations), also plays a significant role in many geothermal systems (Fig. 7). This type of permeability is present in nearly all rock types, including metamorphic, carbonate, and igneous rocks. Secondary permeability allows even low-permeability reservoirs to support productive geothermal systems (34).
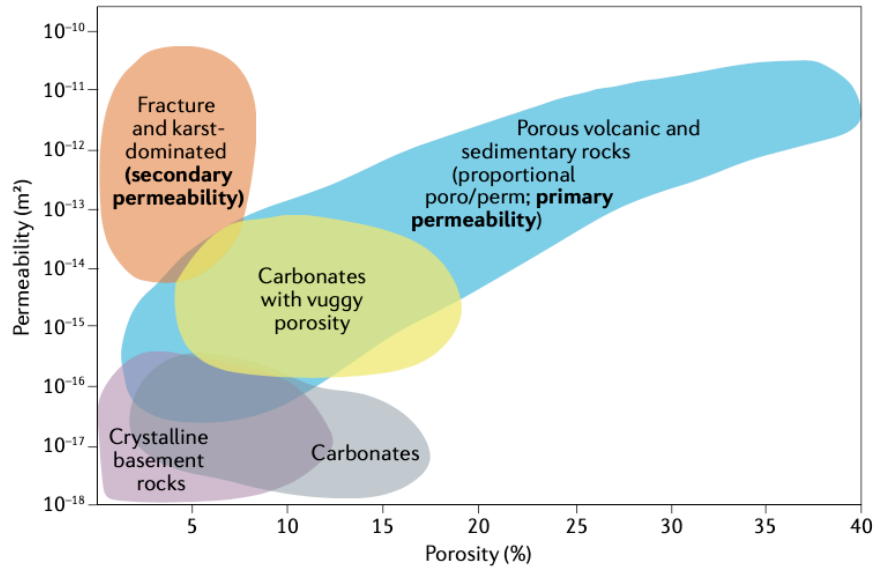
Figure 7: Porosity and permeability relationships in geothermal reservoir formations (34).

1.4.3 Temperature and moisture content

It is important to understand how temperature affects the thermal conductivity (λ) of rocks to study geothermal behavior and thermal evolution in basins. Experimental studies have shown that the λ of carbonate and clastic rocks decreases as temperature rises, while the λ of intrusive and volcanic rocks is relatively unaffected by temperature changes.

Rocks can be categorized into three groups based on the relationship between temperature (T) and λ. The first group, which includes rocks with high λ values (>4.5 W/m·K) at room temperature, shows concave λ-T curves. The second group includes rocks with moderate λ values (2.5–3.5 W/m·K) and linear λ-T curves. The third group contains rocks with low λ values (<2.5 W/m·K), where the λ-T curves are convex. As shown in Figure 8, the λ of four rock types decreases as temperature increases (15).
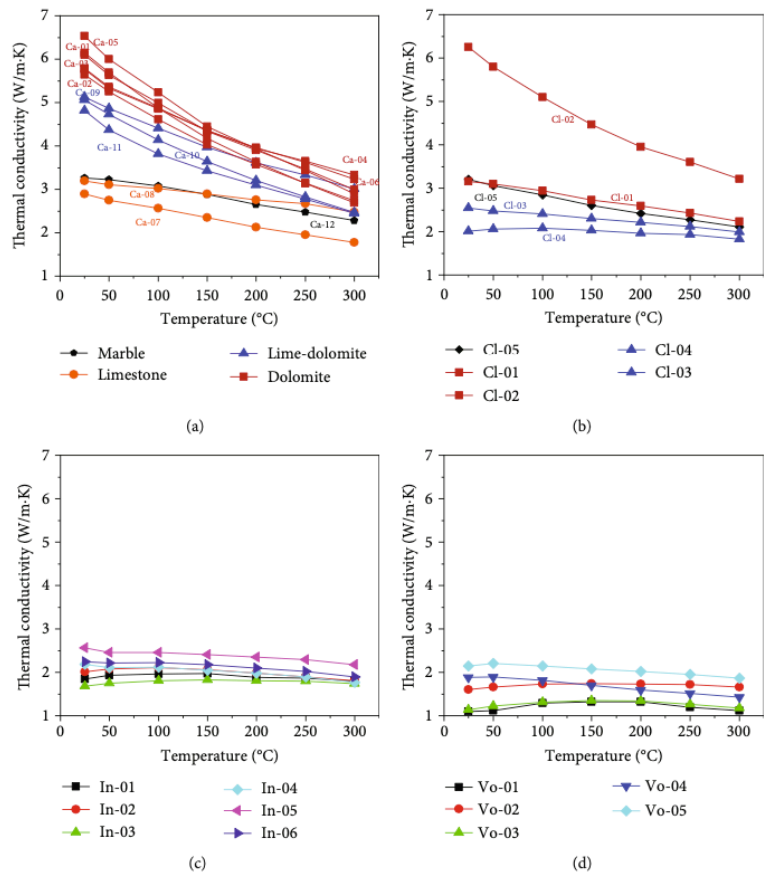
Figure 8: Temperature dependence of λ in four rock types: (a) Carbonates, (b) Clastic rocks, (c) Intrusive rocks, (d) Volcanic rocks (15).

In the design, monitoring, and control of geothermal systems, measuring temperature fields across space and understanding factors like permeability, specific storage, and heat transport (including thermal conductivity and volumetric heat capacity) is crucial (31). Furthermore, the thermal conductivity of soil or rock is influenced by factors such as the properties of the solid, pore fluid, and pore air phases, often measured in terms of density and moisture content (63). Groundwater presence at certain depths can alter the moisture content of the ground, thereby influencing its effective thermal conductivity (25).

1.5 Measuring thermal conductivity

1.5.1 Laboratory methods

1.5.1.1 Steady state methods

Stable-state methods are used to measure the thermal conductivity of the material, when their temperature reaches the balance, meaning they no longer change over time. This allows for the direct application of the rule of the furrier, simplifying the analysis. However, stable-state approaches are often time consuming, it takes hours or even days to assemble a single data point, and they require sophisticated tools and systems to ensure stable heat flow. Measurements are usually performed at an average temperature between the warm and cold ends of the sample, but issues such as contact resistance can complicate accurate measurements. One of the most widely used techniques is the protected hot plate (GHP) method, which is effective for measuring thermal conductivity in solids within the range of 0.01 to 15 W/M ·. In this method, the heat is continuously supplied on one side of the sample by the heat source, and the heat is transferred to the opposite direction through the material, which is connected to a heat sink. After the initial transient period, the temperature and sink of the heat source are stable, and they are monitored by a control system. To reduce the loss of heat to the sides, the guards are placed around the sample. These plates should be flat and made from extreme conductive materials to ensure uniform temperature distribution. They should also have high emissions, especially when measuring materials with low conductivity. It is important to maintain temperature balance between the guard and the sample, with tolerance of about 0.01 ° C to prevent significant lateral heat loss.

The sample size should be large enough (typically a few centimeters) and have a standard shape, either circular or rectangular. Testing usually requires several hours to complete (Fig. 9) (63).
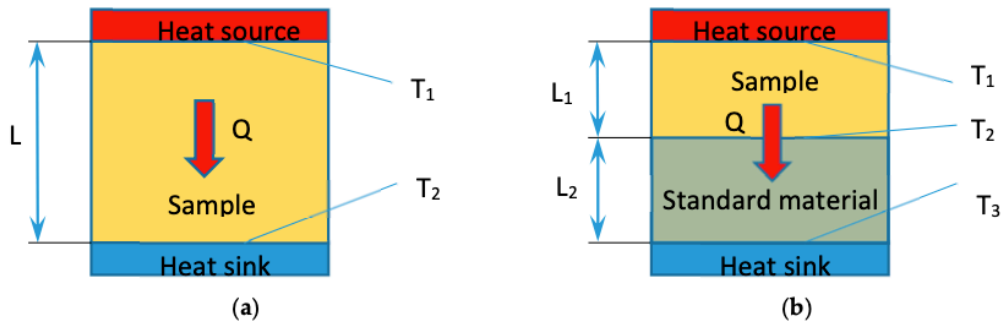
Figure 9: Fundamentals of steady-state methods (63).

Using the temperature difference, the thermal conductivity can be calculated with Fourier's Law as follows (36):

$$\lambda = Q\, d\, /\, A\ \Delta T$$

Where:

- Q is the heat flow in watts (W)
- d is the sample thickness in meters (m)
- A is the cross-sectional area in square meters (m²)
- ΔT is the temperature difference across the sample in kelvins (K)

1.5.1.2   Transient methods

Transient Line-Source (TLS)

This method measures thermal conductivity using the Line-Source technique, which employs a Rheograph High-Pressure Capillary Rheometer (HPCR). The setup allows for measuring the thermal conductivity under various pressures, up to 100 MPa. The system consists of a heating element and a thermocouple enclosed in a needle-shaped casing, with the thermocouple positioned at the center.

To begin, the HPCR cylinder is filled with a non-crosslinking rubber compound to protect the heating element during post-test removal. The needle is then placed in the cylinder, and the temperature is adjusted for testing (Fig. 10). Once thermal equilibrium is reached, a specified amount of energy is dissipated by the needle, and the temperature change (ΔT) is recorded over time from t1 to t2 (36).
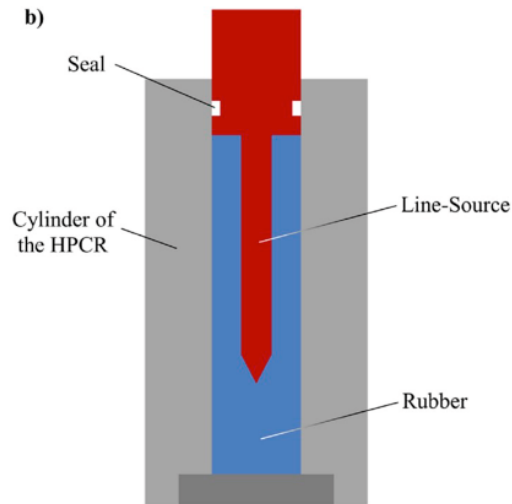
Figure 10: Schematic illustration of the Line-Source method (36).

The thermal conductivity (λ) is then calculated using Fourier's heat transfer equation (Equation 4), incorporating the heat flow per unit length of the needle (ϕ') in watts per meter, the slope of the measured temperature change over a logarithmic time scale in the linear region (C), and a dimensionless calibration factor ($\varkappa$):

$$\lambda = \kappa \, \varphi \, C \, / \, 4 \, \pi \qquad \text{(Equation 4)}$$

$$C = \ln t2/t1 \, / \, \Delta T \qquad \text{(Equation 5)}$$

In these equations, t1 and t2 represent the initial and final time, while ΔT is the temperature difference measured (36).

Transient Plane Source (TPS) Method

The TPS method utilizes a resistive probe that acts both as a heat source and a temperature sensor. The probe is placed in direct contact with the sample's flat surface, which is slightly polished, and a transient heating signal is applied. As the sample heats, the sensor's resistance increases, causing the voltage drop across the sensor to rise. By tracking these changes in temperature over time, the thermal conductivity, diffusivity, volumetric heat capacity, and sample temperature can be determined.

To prevent heat wave reflection at the sample boundaries, the sample must be large enough. Typically, the sample's length should exceed the probe's length by 10% to 20%. The typical minimum sample size is about 20 mm thick and 50–90 mm long, depending on the probe specifications(Fig. 11) (63).

18
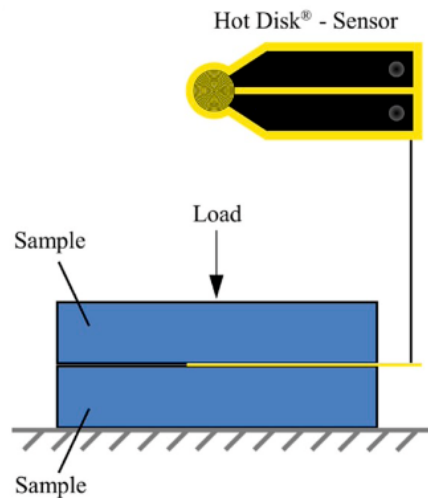
Figure 11: Schematic illustration of the transient Plane-Source (36).

Transient Laser Flash (LFA)

The Laser Flash Apparatus (LFA) is a widely used technique to measure thermal conductivity. This non-contact method uses a high-intensity, short-duration energy pulse, often from a laser, which irradiates the sample from beneath. An infrared detector then records the temperature rise on the sample's rear surface (Fig. 12) (36).
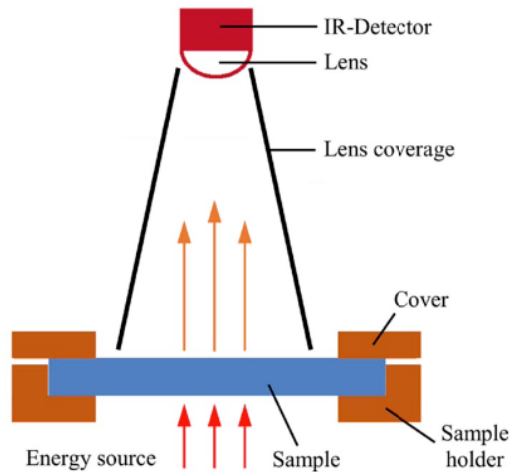
Figure 12: Schematic representation of the transient laser flash method (36).

To calculate the thermal diffusivity, the square of the sample thickness (d) and the half-life of the temperature rise t1/2, which represents the time taken for the temperature to reach half its peak value, are used in the following equation (36):

$$\alpha = 0.1388 \ (d^2 \ / \ t_{1/2})$$

1.5.2 In-situ methods

1.5.2.1 Thermal response test (TRT)

To properly design borehole heat exchangers (BHE) for ground source heat pumps and thermal energy storage systems, it is essential to accurately measure the thermal properties of the ground. These properties, including thermal conductivity, borehole thermal resistance, and undivided ground temperature, directly affect the size, arrangement and depth of the borhole region. The concept of using the thermal response test (TRT) to assess ground thermal properties was first introduced by Mogenseen (1983), while Eklöf and Gehlin (1996) by Eklöf and Gehlin (1996) using Line-SUSMANCON method using the ground thermal Developed a widely adopted process to assess conductivity. Various versions of traditional TRT have been developed, such as the thermal Response Test (ETRT), continuous heating temperature method (CHTM), and thermal response test drilling (TRTWD). The major results of these tests include effective thermal conductivity of the ground and borehole thermal resistance. When evaluating ground heat exchanges (GHX), the effects of grout content and groundwater flow are also important factors (4, 25).

The standard TRT method involves injecting heat into a loop buried underground, and circulating hot water to simulate the final BHE installation. Temperature fluctuations at the inlet and outlet of the heat exchanger, along with the flow rate, are recorded during the test. The duration of the test is generally long, typically lasting at least 50 hours, and the perforation time and costs associated with it are considerable(Fig. 13) (25).
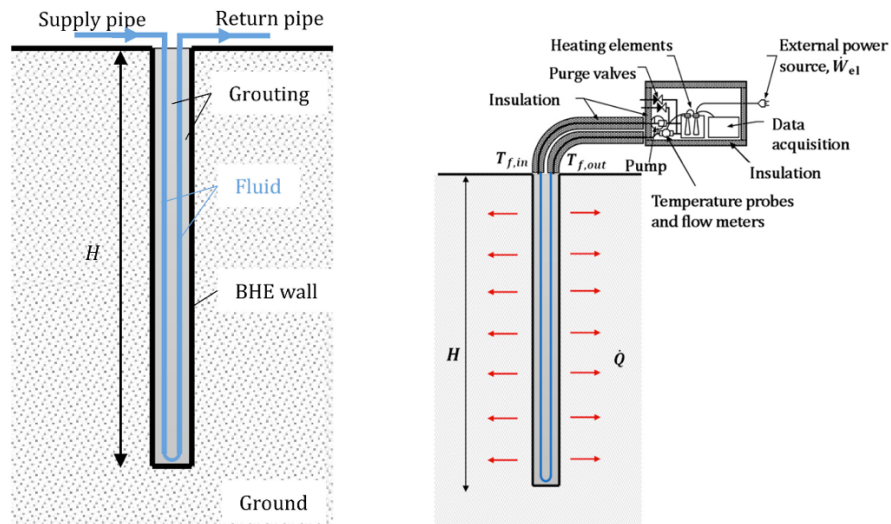
Figure 13: Typical conceptual schematic of TRT, (BHE: Borehole Heat Exchanger) (25).

1.5.2.2 TRT methodology

A typical Thermal Response Test (TRT) unit includes a pump, purge valves, an electric heating element, temperature sensors, a flow meter, and a data logger (Fig. 14). The size of TRT units can vary, ranging from compact suitcase-sized models to larger trailer-mounted systems (49).
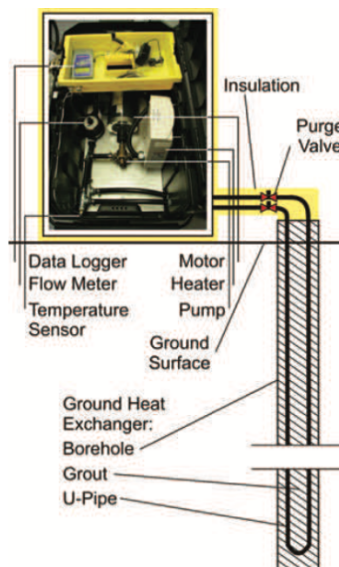
Figure 14: TRT unit developed at Université Laval (49).

The TRT works by analyzing the thermal responses (temperature changes in the circulating fluid at the wellhead) resulting from thermal stimulation, either by extracting or supplying a defined heat flow. The time-dependent changes in average fluid temperature between the heat exchanger's inlet and outlet form the basis of the data. The thermal parameters obtained from the TRT include:

• Effective thermal conductivity of the ground, λ

• Undisturbed ground temperature, T

• Thermal diffusivity of the ground, α (2)

Understanding the underground thermal properties is vital for the optimal design of borehole heat exchangers (BHE). The most critical parameter is the thermal conductivity of the ground, which is site-specific. Thermal contact between the borehole wall and the circulating fluid is influenced by factors such as borehole diameter, pipe size and arrangement, pipe material, and the filling material in the annulus. Efforts are made to reduce the thermal resistance between the borehole wall and the fluid, which is typically referred to as "borehole thermal resistance". Since the mid-1990s, a method has been developed and refined for measuring underground thermal properties directly at the site, using mobile equipment for these measurements, which has been deployed in various countries. The Thermal Response Test (TRT), also known as the 'Geothermal Response Test' (GRT), is a reliable method for measuring both the effective thermal conductivity of the ground and the thermal resistance of the borehole (or the thermal conductivity of the borehole filling) (54).

2 Literature review

2.1 Lithological influences on thermal conductivity

2.1.1 Thermal properties of different lithologies

Understanding the thermal properties of geological materials is important in planning and designing geothermal systems. For the efficient installation of the ground source heat pump (GSHP) system, it is necessary to determine these thermal properties, which can be obtained through field measurement or laboratory tests. Major parameters such as thermal conductivity, thermal capacity and thermal deficiency are important to evaluate geotomical capacity and heat transfer efficiency in various geological materials. Thermal conductivity, in particular, shows significant variations between various lithological types. Within the same type of rock, thermal conductivity increases with depth due to condensation effect. High porcity usually has low thermal conductivity, while higher density increases. There are also significant differences in thermal conductivity in igneous, metamorphic and sedimentary rocks. In addition, when soils or rock samples are saturated, their thermal conductivity usually increases. In order to support the geotomal system design with accurate data, the worldwide study has employed various functioning to map thermal properties of geological materials on many places (60).

2.1.2 Thermal Parameter Analysis: Sampling Methods and Lab Measurements

Since 2003, sharp and more efficient methods have gained popularity globally to measure the thermal properties of rocks (48). This section highlights insight from 16 major studies that use different approaches for such measurements.

2.1.2.1 Applied laboratory approaches

2.1.2.1.1 Rajver et al. (2021)

Rajver and colleagues conducted a study on geological and geothermal characteristics of three alpine pilot regions: Aosta Valley (Italy), Parc Naturel Des Bauges (France), and Municipality of CERKNO (Slovenia). The purpose of research is to assess the geothermal potential of these areas for closed-loop systems, such as Borhole Heat Exchanges (BES). Geological composition varies in sites. The Aosta Valley is mainly made of metamorphic rocks with some granite, while CERKNO and Parc des Bauges

are primarily sedimentary, which is characterized by rapid changes in geological units. These variations significantly affect the geothermal properties of the rocks (48).

Method Description

The Cerkno municipality area:

In the Cerkno municipality area, a total of 16 samples (comprising 30 individual rock specimens) were collected from the town center, and another 16 samples (23 specimens) were sourced from the wider municipality. Measurements focused on thermal conductivity (TC) and thermal diffusivity (TD). For example, Figure 15 illustrates a profile of massive dolomite with high TC values. Other parts of the region showed mixed rock sequences, generally offering good geothermal potential at depths of 100–200 m due to the combination of materials with varying TC values. Table 2 provides a summary of TC measurements for different rock types in the Cerkno area, along with their associated volumetric heat capacities (48).
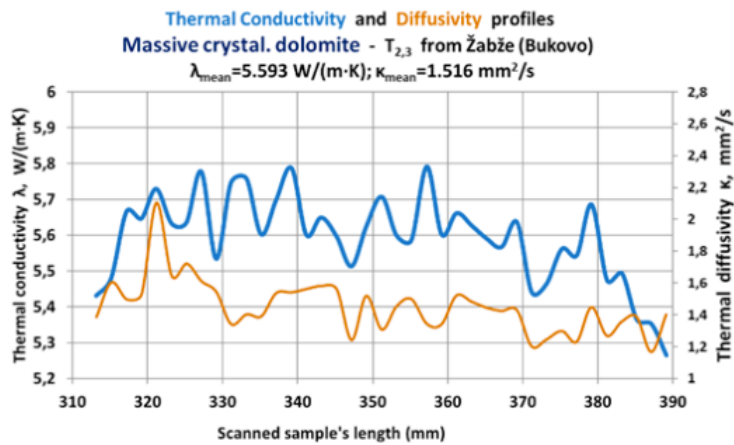
Figure 15: Example of the TC and TD profiles along the sample of massive dolomite (48).

Cerkno area		
Lithology	Thermal conductivity (mean) (W/m·K)	Volumetric Heat capacity (MJ/m³·K)
Dolomite	3.76	2.65
Dolomite	5.6	2.65
Dolomite	5.33	2.65
Dolomitized Limestone	3.03	2.55
Limestone	2.64	2.25
marl to Limestone	1.97	2.25
Limestone	2.36	2.25
Black Limestone	2.01	2.25
Limestone, tectonized	2.51	2.25
Marly Limestone	2.82	2.2
Black Limestone	2.96	2.2
Tuff, lithocrystal	3.18	2.2
Tuff, porphyre	4.04	2.2
Sabdstone & Siltstone	1.95	2.15
Siltstone to mudstone	1.95	2
Sandstone	2.75	2.2
Shaly claystone	1.84	2.05
Quartz conglomerate	4.83	2.2
Quartz sandstone	3.91	2.15
Shaly claystone	1.89	2.25
Siltstone & shaly claystone	1.78	2.1
Siltstone, light brown	3.43	2.05
Tuff sandstone	2.45	3.2
Quartz sandstone	5.3	2.2
Tuff	3	2.2
Tuff	2.32	2.2
Diabase	2.95	2.25
Limestone	2.76	2.25
Dolomite, thin bedded	4.12	2.65
Dolomite, massive crystal	5.59	2.65
Dolomite, bedded	4.84	2.65

Table 2: Measured TC of rock samples from the Cerkno area with associated volumetric heat capacity (48).

The Aosta Valley region:

In the Aosta Valley region, 13 rock samples were collected to represent the main lithologies of the bedrock. These samples were analyzed to determine their thermal conductivity (TC) and heat capacity (calculated from thermal diffusivity, TD). The analysis was conducted using a thermal conductivity scanning (TCS) device at GeoZS, with the results shown in Table 3 and illustrated in Figure 16 (48).
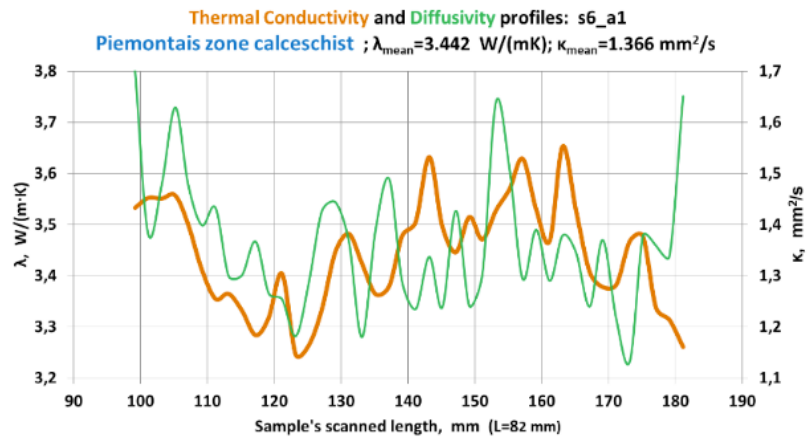
Figure 16: Example of the TC and TD profile along one of the three scanned rock pieces of the sample Piemontais zone calceschist (48).

Aosta			
Lithology	Thermal conductivity (mean) (W/m·K)	Thermal diffusivity (mm²/s)	Heat capacity (MJ/m³·K)
Mont blanc granite	3.12	1.62	1.93
Ultrahelvetic schist	2.82	1.12	2.52
Zone sion courmayeur flysch	3.23	1.14	2.83
Outer brian connals micaschist	4.04	1.04	3.88
Inner brian connals micaschist	3.12	0.94	3.33
Plemontais zone calceschist	3.41	1.27	2.68
Gneiss minuti	3.42	1.42	2.4
metabasalts	2.46	0.81	3.04
Serpentinites	3.41	0.95	3.58
Eclogitic metagranitoids	3.26	1.49	2.19
Metagranitoids	3.44	1.82	1.89
Grand paradis gneiss	3.43	1.32	2.6
Ortogneiss	3.33	1.51	2.21

Table 3: Measured TC and TD and calculated heat capacity of the collected samples from Aosta (48).

The Parc des Bauges:

A cartographic study of the average ground TC was performed for depth between 0 and 100 meters. Seventeen samples, mainly with limestone and molas rocks, were easily collected. In contrast, the marl was difficult to take sample due to their poor performance and low signal, which hinders the sample protection (Fig. 17). Sample rocks mainly include Jurassic and Creteseous-world limestone and marl. Geological structures such as alluvial alluvial, screeds and peacocks, which are poorly induced, were not involved in TC measurements. A remarkable discovery is that, except sample 6, the conductivity for limestone and marl samples was medium to high (> 2.3 w/m · k) (Table 4).
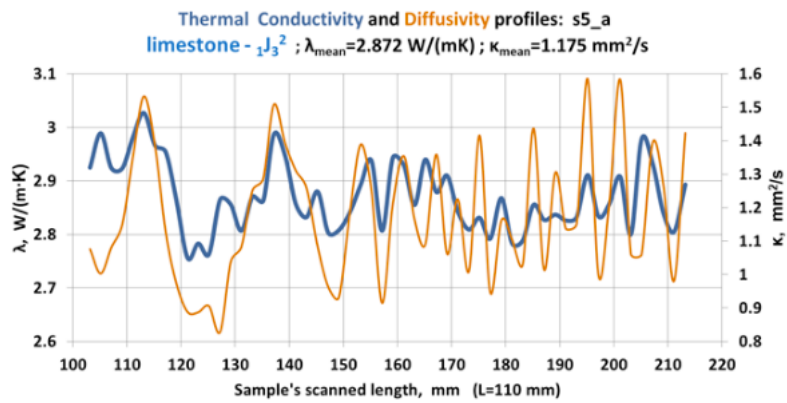
Figure 17: Example of the TC and TD profiles along one of the rock pieces of the sample Limestone of malm age (48).

Parc des Bauges			
Lithology	Thermal conductivity (mean) (W/m·K)	Thermal diffusivity (mm²/s)	Heat capacity (MJ/m³·K)
Molasse sandstone	3.26	1.14	2.86
Limestone	2.77	0.89	3.13
Limestone	2.94	0.95	3.09
Limestone with sand	3.26	0.97	3.37
Limestone	3.34	1.03	3.25
Limestone	2.83	1.16	2.44
Marl & marly limestone	1.26	0.97	1.3
Limestone	2.72	1.23	2.21
marl & marly limestone	2.37	0.56	4.23
Limestone	2.86	1.01	2.83
Limestone / marl with sdand	3.48	0.97	3.61
Limestone	3.38	1.08	3.13
Limestone with slight clay	2.68	0.85	3.15
Limestone	2.84	1.01	2.82
Limestone	2.93	0.94	3.14
Marl / limestone	3.04	1.12	2.72
Marl	2.84	0.89	3.19
Marl	2.94	0.96	3.06

Table 4: Measured TC and TD and calculated heat capacity of the collected samples from Parc des Bauges (48).

The G.POT Method (Casasso and Sethi, 2016)

The G.POT method was applied to evaluate the closed-loop geothermal potential for all three pilot areas, in order to estimate the geothermal potential of Borehole Heat Exchangers (BHEs). This method, applicable for both heating and cooling, assumes that the cyclic application of a sinusoidal thermal load induces a time-dependent thermal alteration of the ground. This alteration continues until a threshold fluid temperature is reached, either minimum or maximum, depending on whether heating or cooling is needed.

The thermal conductivity (TC) of rock samples was measured in the laboratory using thermal conductivity scanning (TCS) method. In terms of mean TC values for bedocks, the Aosta Valley is more homogeneous than the other two regions, serkeons and boys. However, the Aosta Valley also displays higher height variation, leading to the temperature (T0) of the more variable land (T0) than the parc des bauges and more stable conditions in CERKNO.

The key factors influencing geothermal potential are the ground TC and the T0. Higher TC improves geothermal potential, as it reduces the ground's thermal alteration. Similarly, the geothermal potential increases with higher T0 if heating is the goal, as there is a larger margin for cooling the ground. Conversely, for cooling, geothermal potential decreases with higher T0.

The mean TC values range from 2.8 to 4.0 W/(m·K) for rocks from the Aosta Valley, 2.4 to 3.5 W/(m·K) for rocks from Parc des Bauges (with one sedimentary rock sample showing an exception of 1.3 W/(m·K)), and from 1.8 to 5.6 W/(m·K) for rocks from Cerkno. The optical scanning method with the thermal conductivity scanner (TCS) was used for measuring both TC and TD (48).

2.1.2.1.2 Di Sipio et al. (2014)

Di Sipio et al. developed a methodological approach as part of the national VIGOR Project to evaluate the geothermal potential in southern Italy. Calabria, located in the southern part of the country, was selected as the case study region (19).

Method description

The region of Calabria:

The Calabria region is the southernmost part of the Apennine mountain chain and is geologically part of the Calabria-Peloritani Arc (CPA) (Figure 18).
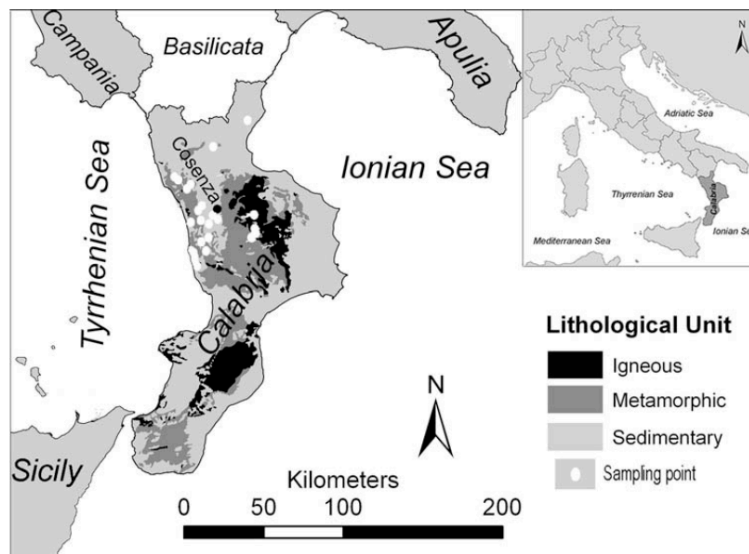
Figure 18: Areal distribution of the igneous, metamorphic and sedimentary rock outcrops in Calabria (scale 1:250.000) highlighting the location of sampling point (dots) (19).

The Calabria series consists of the following geological units (from bottom to top):

• **Mesozoic carbonate complex** - dominated by limestone and dolostone.

• **Liguride complex** - Dating back in Mesozoic and Paliozoic era, characterized by Metamorphos Oceanic Opiolytes.

• **Calabride Complex** - includes pre-alpine, containntal-type high-grade metamorphic rocks (eg, paragonis and ortoginis) and igneous rocks (granite, granodiorite).

• **Plio-quaternaries** - covers sedimentary and sandstone, tectonic boundaries and nappes.

• **Upper Mosinian (Messinian) evaporation deposits** - gypsum and salt, mainly on the Eonian coast, followed by Marli Limustone (19).

His approach included choosing and collecting rock samples to test their physical and thermal properties in the laboratory. The data was then processed through a geographical information system (GIS) to create a geothermal map of the area. The study identified 47 strategraphic structures in Calabria, based on previous geological records. Of these, 10 structures and 70 samples were chosen for analysis, which represent various lithology throughout the region. These include: • 33 samples from sediment rocks, trichic (dolomite and limestone) to plusine (sand and group). • 25 samples from metamorphic rocks vary in metamorphism from low (felite) to high (ganis). • 12 samples from igneous rocks (granite and granodiorite), with separate weathering conditions (19). Geological information for Cailabriya is summarized in Table 5.

Lithology	Thermal conductivity (Dry) (W/m·K)	Number of samples
Granite	2.4	10 granites 3 granodiorites
Sand	1.4	3 cemented sand 2 conglomerate 1 sand
Gneiss	3.2	
Phyllite	3.3	6 gneiss 4 phyllites 2 serpentinite 2 calceschist 2 metabasalt 2 metagabbro
Sedimentary material	1.1	2 conglomerate 2 travertine
Sandstone	1.3	2 sandstone 2 limestone 3 conglomerate 3 gypsum
Clay	1	3 clay 1 marl
Schist	3.4	1 micaschist 1 metasandstone 4 metatonalite
Sedimentary material	1.4	1 sand 2 calcarenite
Dolomitic sedimentary rock	4.3	5 dolomite 1 limestone
Gneiss	3	-
Clay	2	-
Sand	1.3	-
Clay	1.6	-
Sandstone	1.3	-
Sandstone	2.4	-
Evaporite	1.9	-

Calcareous carbonate rock	3.3	-
Sand	1.3	-
Clay	1	-
Clay	2.2	-
Clay	1.6	-
Calcareous carbonate rock	3.3	-
Clay	2	-
Sandstone	1.3	-
Calcareous carbonate rock	1.8	-
Sedimentary material	1.7	-
Sedimentary material	1.5	-
Calcareous carbonate rock	2.8	-
Calcareous carbonate rock	2.7	-
Granofels	2.6	-
Calcareous carbonate rock	4.3	-
Sandstone	1.3	-
Calcareous carbonate rock	2.7	-
Composite genesis rock	2.9	-
Gabbro	2.6	-
Calcareous carbonate rock	2.5	-
Calcareous carbonate rock	3.3	-
Serpentinite	3	-
Migmatite	2.7	-
Conglomerate	1.3	-
Basaltic rocks	1.7	-
Conglomerate	1.9	-
Calcareous carbonate rock	3.2	-
Schist	2.8	-
Calcareous carbonate rock	2.6	-
Conglomerate	2.8	-

Table 5: Description of geological formations as found in the geological map of Italy for Calabria (19).

Sample Preparation

Rock samples, approximately 3 x 3 x 3 cm in size, were dried in a fan-fanfare oven at 70 °C (±5 °C) for 24 hours to prevent mineral changes. After drying, the samples were stored in a dry for 24 hours until they reach a constant weight. To remove air bubbles from porous structures, samples were placed in a vacuum room for 24 hours and gradually at room temperature (20 °C ± 5 °C) under constant pressure for another 24 hours (20 °C ± 5 °C) Was saturated with distilled water.

Thermal Property Tests

Thermal conductivity (TC) and thermal diffusivity (TD) were measured under both dry and wet conditions using two different thermal analyzers:

- **Modified Transient Plane Source (MTPS)** method for rock samples.
- **Transient Line Source (TLS)** method for sediment and unconsolidated materials (Figure 19).

These tests were used to assess the thermal properties of various lithologies, and the results were organized into a GIS database. A total of 29 main lithological categories were identified, with average thermal conductivity (k) values for each category listed in Table 6. In cases where no experimental data were available, bibliographic values were used (19).

Figure 19: Thermal conductivity analyzers composed of interfacial sensor and central unit operating following the modified transient plane source method (a) and the transient line source method (b) (19).

Lithology	Density (gr/cm³)	Porosity (%)	Thermal conductivity perpendicular (Dry) (W/m·K)	Thermal conductivity perpendicular (Saturated) (W/m·K)	Thermal conductivity parallel (Dry) (W/m·K)	Thermal conductivity parallel (Saturated) (W/m·K)
Granite	2.67	29	3.06	3.27	2.7	2.82
Granite	2.62	2.6	2.48	2.69	2.51	2.46
Granodiorite	2.39	11.9	1.92	2.17	1.65	2.31
Granodiorite	2.69	1.7	2.23	2.46	2.49	2.65
Calceschist	2.68	1	3.61	3.62	3.33	3.27
Phyllite	2.75	2.4	2.97	3.29	4.2	4.26
Gneiss	2.77	1	3.28	3.27	3.21	3.44
Gneiss	2.61	1.7	2.56	2.36	2.7	2.87
Metabasalt	2.52	5.8	1.56	2.34	2.99	3.84
Metagabbro	293	3.9	2.72	3.09	2.79	2.94
Metasandstone	2.65	4.7	1.8	2.23	3.16	3.57
Metatonalite	2.69	3.5	2.56	3.28	3.14	3.68
Metatonalite	2.8	1.7	3.39	3.44	2.75	3.23
micaschist	2.6	6.5	3.03	3.18	2.96	2.99
Phyllite	2.68	0.9	3.78	4.03	5.65	5.17
Limestone	1.32	51.6	1.41	2.48	1.42	2.36
Dolomite	2.79	0.2	5.55	6.05	4.08	5.88
Gypsum	2.8	0.1	1.51	1.58	2.36	1.77
Gypsum	2.23	5.5	1.61	1.77	2.07	1.87
Marl	2.12	18.3	1.6	2.49	1.62	2.48
Travertine	1.76	33.5	1.2	2	1.3	2.08

Table 6: Laboratory results of thermal conductivity for selected samples: thermal conductivity measured perpendicular and parallel to layering, in dry and water saturated condition respectively (19).

Geological Variability

Each geological formation in Celibria contains several lithology, formed during different geological periods, and with different degrees of weathering and fracturing. These variations can create local differences in open porcity, which in turn affect the thermal properties of rocks.

Lithological Categories

A simplified stratigraphic model was created based on the lithological descriptions from the soundings, leading to the identification of 29 main lithological categories. These categories were then organized into the GIS database, as shown in Table 7 (19).

Lithology	Thermal conductivity (Dry) (W/m·K)	Thermal conductivity (Saturated) (W/m·K)
Peat	0.4	0.4
Tuff	0.5	0.5
Loam soil	0.7	0.9
Clay	0.9	1.5
Clay and gravel	07	1.6
Silty clay	0.7	1.6
Gravel with clay	0.7	1.6
Basalt	1.7	1.7
Silt	0.5	1.7
Silty sand	0.5	1.7
Silty-clayey sand	0.6	1.7
Gravel	0.4	1.8
Clay and sand	0.8	2
Micaschist	2	2
Conglomerate with clay	1.6	2.1
Shales	2.2	2.2
Breccia	2.2	2.2
Phyllite	2.2	2.2
Sand and gravel	0.5	2.2
Calceschist	2.5	2.5
Marl	2.5	2.5
Sand	0.6	2.6

Calcarenite	2.7	2.7
Sandstone	2.8	2.8
Limestone	2.8	2.8
Conglomerate	2.8	2.8
Gneiss	2.9	2.9
Dolomite	3	3
Granite	3	3

Table 7: Simplified lithological categories derived from the analysis of available stratigraphic soundings (19).

Thermal Conductivity and Anisotropy

To understand how thermal conductivity is affected by factors such as anisotropy and water saturation, 21 samples from the main lithotypes were analyzed (Table 7). The highest thermal conductivity was observed in dolomite and phyllite, both in dry and wet conditions. In these rocks, the mineral components (dolomite in sedimentary rocks and quartz in metamorphic rocks), along with a density greater than 2.5 g/cm³ and low open porosity (<1%), contributed to thermal conductivity values of around 5.5 W/m·K (6.05 W/m·K when wet) and 3.78 W/m·K (4.03 W/m·K when wet), respectively. The lowest thermal conductivity was found in rocks with low density and high porosity, such as travertine (with a density of 1.76×10^3 kg/m³ and porosity of 33.5%), which showed a dry thermal conductivity of only 1.2 W/m·K (19).

2.1.2.1.3 Luo et al (2018)

A geological stratum refers to a distinct rock or soil layer with consistent internal characteristics that set it apart from adjacent layers. A stratigraphic section provides reference data for the strata in a particular sedimentary area. In their study, Luo et al. measured the thermal properties of 116 rock samples collected from 36 formations within the Yangtze Plate in China. This plate, also referred to as the South China Block or South China Subplate, encompasses much of southern China, including Zigui County in Hubei Province, where the samples were collected (Fig. 20) (42).
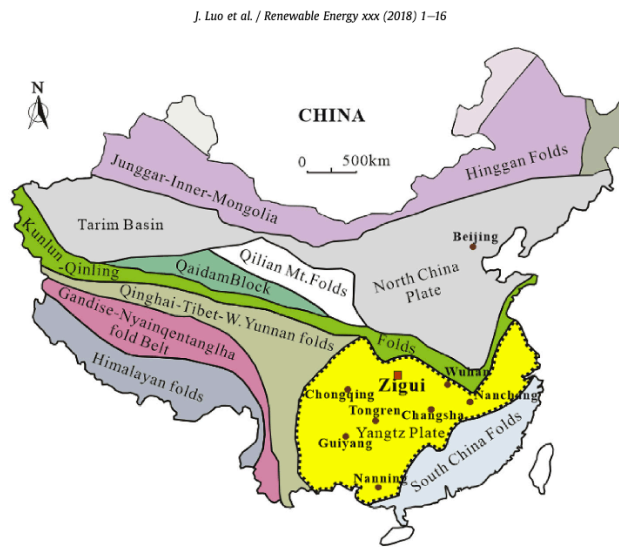
Figure 20: The red dashed line enclosed area is the Yangtze tectonic plate which is the study area for the samples collection in the present study (42).

Method description

The Yangtze Plate is underpinned by a Mesoproterozoic crystalline basement. Its bedrock consists of marine biochemical sedimentary and clastic rocks. In the middle basin and eastern delta, these formations are overlain by Quaternary deposits. The primary geological materials are sedimentary rocks, classified into biochemical and clastic types. Fieldwork involved direct block sampling from exposed outcrops of the Huangling Sedimentary Succession. Samples larger than $10 \times 10 \times 10$ cm were extracted from each geological formation. A total of 116 blocks were gathered from 36 formations, as illustrated in the stratigraphic profile schematic of the Huangling Anticline (Fig. 21) (42).

39

Stratigraphic Unit		Code	Columnar Section	Geological Formtions	Lithology
Group	System				
Mesozoic	Cretaceous	K		Shimen(3)	Upper: Purplish red conglomerate sandstone with gravel sandstone; Lower: Gravel sandstone and siltstone.
				Shimen(2)	
				Shimen(1)	
	Jurassic	J		Niejiashan	Upper: Purplish pink siltstone; Middle: Gray-green quartz sandstone; Lower: Siltstone intercalated with coal.
	Triassic	T		Shazhenxi	Upper: Marl and siltstone, Lower: Limestone and dolomite.
				Badong(5)	
				Badong(4)	
Upper Paleozoic	Permian			Badong(3)	
				Badong(2)	
				Badong(1)	
	Carboniferous	P		Jialinjiang(2)	
				Jialinjiang(1)	
				Wujiapin	Dark gray medium thick bioclastic limestone
		C		Yangxin	
	Devonian			Hezhou	Dark gray quartz sandstone Dark gray thick dolomite
		D		Yuntaiguan	Thick white quartz sandstone
Lower Paleozoic	Silurian	S		Shamao	Upper: Grayish green thick siltstone; Lower: Grayish yellow siltstone.
				Luorepin	
				Longmaxi	
	Ordovician	O		Honghuayuan	Gray thick layered bioclastic limestone and tumorous limestone
				Tongzi	
	Cambrian	∈		Sanyoudong	Upper part: Middle-thick gray dolomite; Middle part: Marl; Lower part: Black thin layer carbonaceous limestone and Shale.
				Qinjiamiao	
				Shilongdong	
				Tianheban	
				Shipai	
				Shuijintuo	
Upper Proterozoic	Sinian System	Z		Dengyin	Upper: Gray-white dolomite, Middle: Dolomite shale, Lower: Moraine conglomerate and quartz sandstone
				Doushantuo(4)	
				Doushantuo(3)	
				Doushantuo(2)	
				Doushantuo(1)	
				Nantuo(2)	
				Nantuo(1)	
Upper Proterozoic				Liantuo(2)	
				Liantuo(1)	
					Gneiss

Figure 21: A stratigraphic profile contains the sedimentary sequence of rock formations of Huangling anticline at Zigui area in Hubei province (42).

40

To measure thermal properties, the rock samples were cut into cylindrical shapes (90 mm in diameter and 60 mm in height). Thermal property measurements were performed using the portable ISOMET 2114 device (Applied Precision Ltd., Slovakia) in accordance with ASTM Standard 5334-08. The device operates by applying a constant heat source via a metal bar in direct contact with the sample surface. The thermal conductivity (λ) is calculated using the following equation and the calculation has an uncertainty of ±5.0%.

$$\lambda = (2 * q / 4\pi) (\ln (t_2) - \ln (t_1) / T_Q (t_2) - T_Q (t_1))$$

Here:

- λ = thermal conductivity ($W \cdot m^{-1} \cdot K^{-1}$),
- q = heating rate (W),
- T = temperature (°C),
- t = time (s),
- subscripts 1 and 2 denote two different measurement times.

Thermal property measurements were conducted under both dry and fully saturated conditions. For the dry state, samples were oven-dried at 110°C for more than 48 hours. For the saturated state, the samples were submerged in water under vacuum conditions for at least 48 hours to ensure full saturation.

The results revealed that dolomite typically exhibits higher thermal conductivity compared to limestone, while silicate minerals have even greater conductivity (Table 8) (42).

Lithology	Thermal conductivity (W/m·K)
Limestone	2.61
Limestone	2.38
Limestone	2.32
Limestone	2.69
Limestone	2.89
Limestone	2.95
Limestone	2.84
Limestone	2.58
Limestone	2.38
Limestone	2.83
Limestone	2.25
Limestone	2.4
Limestone	2.02
Dolomite	4.31
Dolomite	3.89
Dolomite	2.66
Limestone	1.51
Limestone	3.04
Limestone	2.68
Limestone	3.97
Limestone	2.33
Limestone	2.95
Limestone	1.98
Limestone	1.85
Dolomite	2.79
Dolomite	2.74
Dolomite	4.36
Dolomite	4.49
Silicate	3.95
Silicate	3.95

Table 8: Thermal conductivity and mineral constituents of the biochemical sedimentary rocks (42).

Thermal conductivity was found to be quite varying between different lithological types, 0.72 W/m.K to 4.49 W/m.K. Between bio-chemical sedimentary rocks, silicates demonstrated the highest conductivity, followed by dolomite and limestone. These variations are mainly attributed to the difference in mineral composition of rocks (Table 9) (42).

Lithology	Thermal conductivity (Dry) (W/m·K)	Thermal conductivity (saturated) (W/m·K)	Thermal diffusivity (Dry) (m²/s)	Thermal diffusivity (Saturated) (m²/s)	Volumetric Heat capacity (Dry) (MJ/m³·K)	Volumetric Heat capacity (Saturated) (MJ/m³·K)
Sandstone	1.87	2.21	0.9	1.06	2.08	2.09
Silty sandstone	2.63	3.31	1.8	1.44	1.46	2.3
Conglomerate	4.35	5.65	1.96	1.95	2.22	2.9
Silty sandstone	2.02	2.75	1.38	1.2	1.46	2.3
Conglomerate	4.01	5.51	2.06	1.94	1.95	2.84
Sandstone	3.61	5.46	1.85	1.92	1.95	2.85
Sandstone	3.02	5.21	1.85	2.03	1.63	2.57
Sandstone	3.94	5.77	1.92	1.87	2.05	3.09
Sandstone	3.02	4.5	1.58	1.6	1.91	2.81
Sandstone	2.4	3.43	1.28	1.25	1.87	2.75
Shale	1.81	2.21	1.23	1.24	1.47	1.78
Silty Sandstone	2.1	2.94	1.45	1.24	1.45	2.37
Limestone	2.61	3.26	1.52	1.33	1.72	2.46
Sandstone	2.76	4.35	1.42	1.56	1.95	2.79
Sandstone	1.67	2.95	0.99	1.39	1.68	2.12
Sandstone	2.31	3.02	1.32	1.17	1.75	2.58
Dolomite	2.48	3.18	1.25	1.27	1.99	2.5
Dolomite	2.38	3.38	1.59	1.36	1.5	2.49
Limestone	2.69	2.87	1.26	1.19	2.13	2.42
Limestone	2.81	3.23	1.36	1.29	2.06	2.5
Limestone	2.74	2.99	1.5	1.33	1.83	2.25

Dolomite	2.84	3.23	1.83	1.29	1.55	2.5
Sandstone	4.42	5.73	2.43	2.84	1.82	2.02
Sandstone	3.09	3.99	1.61	1.27	1.92	3.13
Sandstone	4.45	5.85	2.31	1.75	1.93	3.35
Mudstone	1.48	2.04	1.01	0.96	1.47	2.12
Shale	2.61	3.65	1.3	1.41	2.01	2.58
Shale	1.64	2.12	1.08	0.99	1.52	2.15
Sandstone	2.98	3.95	1.66	1.46	1.79	2.71
Limestone	2.19	3.04	1.4	1.26	1.56	2.41
Limestone	2.94	3.26	1.35	1.29	2.17	2.52
Limestone	2.22	3.44	1.41	1.32	1.57	2.6
Limestone	2.69	2.96	1.27	1.2	2.12	2.47
Limestone	2.94	3.27	1.35	1.35	2.17	2.43
Limestone	1.9	2.7	1.33	1.3	1.43	2.08
Limestone	2.06	2.58	1.2	1.04	1.72	2.47
Limestone	2.52	2.92	1.22	1.2	2.07	2.43
Limestone	2.37	2.88	1.24	1.22	1.91	2.37
Dolomite	3.51	4.75	2.06	2.11	1.7	2.25
Dolomite	4.59	5.74	2.07	1.88	2.22	3.06
Dolomite	3.89	4.43	2.76	1.53	1.41	2.9
Dolomite	367	5.2	1.87	1.77	1.96	2.94
Dolomite	3.88	4.44	1.8	1.69	2.16	2.62
Dolomite	3.02	4.43	1.79	1.53	1.69	2.9
Mudstone	2.66	3.6	1.45	1.48	1.83	2.44
Limestone	2.51	4.08	1.56	1.51	1.61	2.71

Limestone	3.12	4.06	1.7	1.52	1.83	2.67
Shale	1.62	2.52	0.99	1.1	1.64	2.3
Dolomite	2.57	2.63	1.72	1.23	1.49	2.13
Silicate	3.58	5.35	1.91	1.85	1.87	2.89
Silicate	3.88	4.46	2.07	0.13	1.87	3.5
Dolomite	3.97	5.03	2.11	1.71	1.88	2.95
Dolomite	2.42	2.69	1.29	1.21	1.88	2.22
Limestone	1.83	2.89	1.12	1.21	1.64	2.39
Silicate	2.13	2.79	1.37	1.57	1.56	1.78
Dolomite	2.37	2.67	1.59	1.5	1.49	1.78
Dolomite	2.79	3.73	1.89	1.53	1.48	2.43
Dolomite	2.74	3.29	1.89	1.91	1.45	1.72
Dolomite	4.21	5.27	2.2	1.85	1.91	2.85
Sandstone	2.89	3.78	1.51	1.46	1.92	2.59
Sandstone	2.99	4.02	1.5	1.53	1.99	2.63
Sandstone	3.24	3.37	2.09	1.35	1.55	2.49
Sandstone	3.01	3.26	2.03	1.49	1.48	2.19
Sandstone	2.58	4.28	1.65	1.64	1.56	2.61
Moraine Conglomerate	2.82	3.31	1.37	1.31	2.06	2.52

Table 9: Thermal properties of the rock samples with dry and fully saturated state for different lithological types (42).

2.1.2.1.4   Jon Busby (2016)

Jon Busby calculated soil thermal diffusivity values at 56 locations using temperature data provided by the UK Met Office weather stations. Thermal diffusivity was derived directly from depth-distributed soil temperatures, and thermal conductivity was estimated based on the diffusivity measurements, incorporating additional assumptions about soil texture (11).

Method description

The UK Met Office collects soil temperature figures and archives, which are made available for educational research through the British Atomphyric Data Center (BADC). The temperature reading is recorded at a depth of 5, 10, 20, 30, 50 and 100 cm. To calculate thermal deficiency, at least two depth temperature data is required. From these deviations measurements, approximate thermal conductivity was calculated for 60 sites, between 0.54 and 3.81 W/m.K. The minimum and maximum thermal conductivity was aligned with the lowest and the highest elaborations respectively.

The calculation method relies on the relationship between the depth-dependent decrease in amplitude and increase in phase shift of a transmitted heat pulse in the ground, which is governed by thermal diffusivity. Seasonal temperature cycles spanning several years provided apparent thermal diffusivities, which were used to generate seasonally averaged, site-specific estimates. These estimates can be compared with laboratory measurements or field data obtained using point-measurement methods, such as needle probes.

Thermal conductivity values were estimated from thermal diffusivities using soil texture information. Median values were calculated for three soil types:

- **Sand**: Thermal conductivity of 1.56 $W \cdot m^{-1} \cdot K^{-1}$, thermal diffusivity of 0.9961×10^{-6} $m^2 \cdot s^{-1}$.

- **Loam**: Thermal conductivity of 1.15 $W \cdot m^{-1} \cdot K^{-1}$, thermal diffusivity of 0.7173×10^{-6} $m^2 \cdot s^{-1}$.

- **Clay**: Thermal conductivity of 1.81 $W \cdot m^{-1} \cdot K^{-1}$, thermal diffusivity of 1.0295×10^{-6} $m^2 \cdot s^{-1}$.

The thermal properties calculated using this approach offer valuable inputs for assessing and calibrating modeled datasets, especially in studies related to soil heat transfer (Table 10) (11).

Lithology	Density (gr/cm³)	Porosity (%)	Thermal conductivity (W/m·K)	Thermal diffusivity (10^{-6} m²/s)	Specific heat capacity (J/kg.K)
Loamy soils	1.43	0.42	1.42	0.9003	1102
Sandy clay, clay and silty clay loam to clay	1.25	0.52	0.76	0.4331	1398
Sandy clay, clay and silty clay loam to clay	1.25	0.52	1.43	0.819	1398
Sand to sandy, clayey and silty loams	1.52	0.42	1.48	0.9568	1014
Sandy and loamy soils (limited clay)	1.47	0.42	1.17	0.7698	1030
Loam to clay to sand	1.31	0.44	1.43	0.9537	1144
Sand to sandy silt loam	1.61	0.42	2.55	1.5996	990
Sandy to loamy sand	1.66	0.42	1.45	0.8963	978
Sandy and loamy soils (limited clay)	1.47	0.42	1.17	0.7746	1030
Sandy to sandy loam and sandy clay loam	1.52	0.42	1.65	1.0672	1014
Sandy to sandy loam	1.62	0.4	1.67	1.0354	994
Sand to sandy, clayey and silty loams	1.52	0.42	1.71	1.1091	1014
Sand to sandy, clayey and silty loams	1.52	0.42	1.07	0.6938	1014
Sand to sandy, clayey and silty loams	1.52	0.42	1.23	0.7979	1014
Sand to sandy, clayey and silty loams	1.52	0.42	0.62	0.4002	1014
Sandy and loamy soils (limited clay)	1.47	0.42	3.41	2.2544	1030
Clay, sand, sandy loams	1.32	0.44	1.08	0.7175	1139
Clayey to silty loams (limited sand) to clay	1.24	0.5	1.31	0.7461	1415
Sand to sandy, clayey and silty loams	1.52	0.42	1.7	1.1016	1014
Sandy and sandy–silty loams (little clay)	1.57	0.42	2.46	1.4861	1053
Loam to clay	1.28	0.48	1.79	1.1036	1267
Sandy to loamy sand	1.66	0.42	2.89	1.7815	978
Loam to clay	1.28	0.48	0.68	0.4193	1267
Clayey to silty loams (limited sand) to clay	1.24	0.5	0.82	0.4687	1415

Sandy and loamy soils (limited clay)	1.47	0.42	2.38	1.5739	1030
Clayey to silty loams (limited sand) to clay	1.24	0.5	2.03	1.1571	1415
Sandy clay, clay and silty clay loam to clay	1.25	0.52	1.25	0.7172	1398
Sandy, clayey and silty loams (minimum 20% sand)	1.54	0.42	2.79	1.7971	1008
Loam to clay	1.28	0.48	0.92	0.5663	1267
Loam to clay	1.28	0.48	0.79	0.4894	1267
Clayey to silty loams (limited sand) to clay	1.24	0.5	2.96	1.6848	1415
Sandy to sandy loam and sandy clay loam	1.52	0.42	1.37	0.8872	1014
Loam to clay	1.28	0.48	1.63	1.0071	1267
Loam to clay	1.28	0.48	1.23	0.7568	1267
Sandy to sandy loam and sandy clay loam	1.52	0.42	1.04	0.6754	1014
Sandy to sandy loam and sandy clay loam	1.52	0.42	1.34	0.87	1014
Clayey to silty loams (limited sand) to silty clay	1.35	0.48	1.29	0.7385	1292
Loamy soils	1.43	0.42	0.76	0.4808	1102
Clay, sand, sandy loams	1.32	0.44	0.84	0.5558	1139
Loamy sand to sandy silt loam	1.64	0.44	1.52	0.9003	1027
Loam to clay	1.28	0.48	2.35	1.4517	1267
Sand to sandy, clayey and silty loams	1.52	0.42	2.34	1.5203	1014
Clay, sand, silt, loam	1.31	0.44	1.21	0.8101	1144
Sandy clay, clay and silty clay loam to clay	1.25	0.52	0.99	0.5641	1398
Clay, sand, silt, loam	1.31	0.44	1.19	0.7963	1144
Clayey to silty loams (limited sand) to clay	1.24	0.5	1.81	1.0295	1415
Clay, sand, silt, loam	1.31	0.44	3.07	2.0517	1144
Sand to sandy, clayey and silty loams	1.52	0.42	3.81	2.4691	1014
Sandy clay, clay and silty clay loam to clay	1.25	0.52	1	0.5719	1398

Clay, sand, silt, loam	1.31	0.44	2.14	1.4258	1144
Loam to silty clay	1.38	0.45	3.76	2.3343	1169
Sandy to sandy loam and sandy clay loam	1.52	0.42	2.8	1.8061	1014
Sand to sandy, clayey and silty loams	1.52	0.42	1	0.6487	1014
Sandy and loamy soils (limited clay)	1.47	0.42	1.92	1.271	1030
Loam to clay	1.28	0.48	0.77	0.4757	1267
Loam to sand	1.47	0.4	1.5	0.9842	1039

Table 10: Thermal diffusivities, derived as the mean of accepted amplitude and phase determinations, soil texture from Lawley (2008) and estimated parameters based on the soil texture (11).

2.1.2.1.5 Márquez et al (2016)

Márquez et al. presented a methodology and instrumentation system for indirectly measuring the thermal diffusivity of soil at specific depths by analyzing temperature measurements at those depths. This methodology is designed for applications in the design and sizing of Very Low Enthalpy Geothermal Energy (VLEGE) systems. The proposed method and instrumentation were tested and utilized for designing a VLEGE facility for a chalet with a basement located on the outskirts of Huelva, a city in the southwest of Spain (3).

Method description

The proposed methodology is both simple and cost-effective. It leverages the geotechnical drilling typically required before constructing a house or building to simultaneously measure ground temperatures. These measurements provide actual temperature data and thermal diffusivity values for the desired depth. Figure 22 illustrates the block diagram of the developed instrumentation system, which is used to measure ground temperature. This system can be remotely monitored and controlled using two microcontroller cards connected to a virtual instrument (VI), accessible from any location with an internet connection (3).
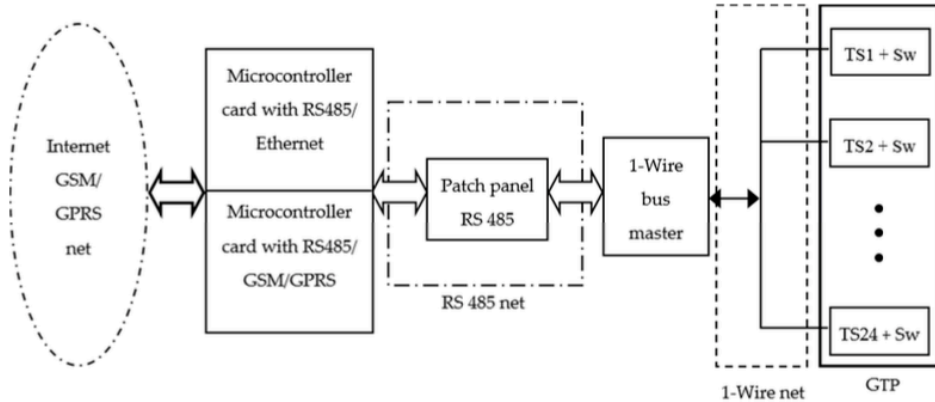
Figure 22: Block diagram of the developed instrumentation system for measuring ground temperature (3).

To enable constant soil temperature measurements at different depths, researchers designed and constructed a ground temperature check (GTP). GTP has a 5-meter-lumb PVC pipe with a diameter of 100 mm. The soil temperature measurement was held in South -West Spain using this probe in

51

about a year. The region has a local climate temperate, affected by the Atlantic Ocean, with an annual average temperature of about 19 ° C. The coldest month is usually January (although it can be December or February) with an average temperature of about 12 ° C, while the hottest month is usually July (or ever August), in which in which the hottest month is usually About 30 ° C is an average temperature. Figure 23 presents the average daily soil temperature recorded at different depths, which ranges from 1 m to 4.8 meters at the duration of the study (3).
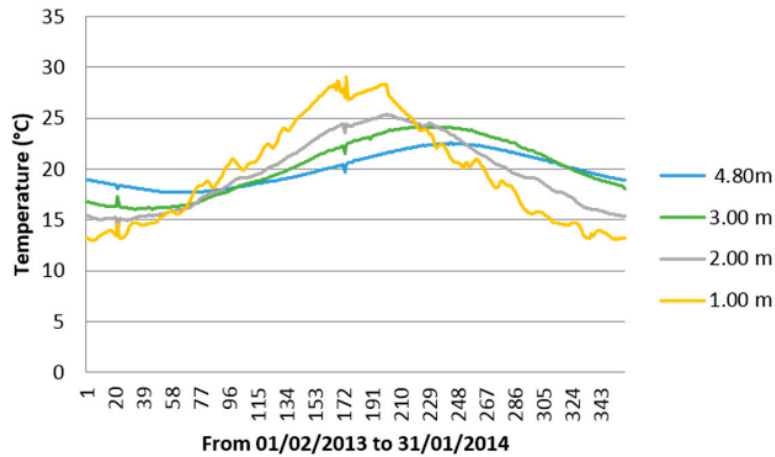
Figure 23: Average daily temperatures at different depths from 1 m to 4.8 m (3).

Table 11 summarizes thermal conductivity, volumetric heat capacity and thermal deficity values for different soil types. The thermal defussity of the soil varies depending on the level of humidity and factors such as gravel and sand structure, with the limitations recorded 0.19×10^{-6} m ×/s to 1.72×10^{-6} m k/s (3).

Lithology	Thermal conductivity (W/m·K)	Thermal diffusivity (10^{-6} m²/s)	Volumetric heat capacity (MJ/m³·K)
Basalt	1.7	0.65	2.6
Greenstone	2.6	0.9	2.9
Gabbro	1.9	0.73	2.6
Granite	3.4	1.13	3
Peridotite	4	1.48	2.7
Gneiss	2.9	1.21	2.4
marble	2.1	1.05	2
Mica schist	2	0.91	2.2
Shale sedimentary	2.1	0.84	2.5
Limestone	2.8	1.17	2.4
Loam	2.1	0.91	2.3
Quartzite	6	2.73	2.2
Salt	5.4	4.5	1.2
Sandstone	2.3	0.82	2.8
Siltstone and argillites	2.2	0.92	2.4
Dry gravel	0.4	0.25	1.6
Water saturated gravel	1.8	0.75	2.4
Dry sand	0.4	0.25	1.6
Water saturated sand	2.4	0.83	2.9
Dry clay / silt	0.5	0.31	1.6
Water saturated clay / silt	1.7	0.5	3.4
Peat	0.4	0.1	3.8

Table 11: Thermal conductivity, volumetric heat capacity and thermal diffusivity fir different kinds of soil (3).

2.1.2.1.6   Fuchs et al (2021)

In non-state conditions, the behavior of sub-state generosity, where temperature fluctuates over time, needs to understand the rate on which the heat is spread. A major parameter for this is the thermal deficiency, which greatly affects this behavior. Fuch et al. Analyzed 40 quartz sandstone samples from different places. Following the initial assessment of the holes and density, he focused on one of the 16 quartz-rich samples, whose porosity ranged from 3% to 35%, to evaluate thermal conductivity and thermal deficiency (26).

Method description

In this study, two methods were employed to measure the thermal properties of rocks at standard conditions (20°C, 1 atm): optical scanning technology (thermal conductivity scanner, TCS) and transient device-based technology (TDB). The primary dataset for this research came from TCS measurements, while tDB measurements (taken from a smaller group of samples) were used to confirm the reliability of the results across methods. The measurements were made on cuboid samples, each with a minimum thickness of 50 mm. In the case of air-saturated conditions, samples were first dried in a vacuum oven at 60°C and under 0.1 bar pressure for 72 hours. Following this, they were cooled for 24 hours in a vacuum desiccator. For saturation with water or n-heptane, the dried samples were evacuated under very low pressure (<0.01 bar at 20°C) for one hour before being soaked for a minimum of 48 hours. Each sample underwent five scanning measurements, each repeated three times for accuracy. The reproducibility of thermal conductivity measurements was typically between 1% and 3%, and between 3% and 5% for thermal diffusivity in both air and water-saturated conditions. A subset of six samples from the TCS cuboids were drilled into 50 mm diameter discs with a thickness of 30 mm for TDB analysis. These measurements, conducted under dry and water-saturated conditions, were repeated five times. The data were then used to determine thermal conductivity and volumetric heat capacity through inverse Monte Carlo analysis based on numerical finite element modeling. The reproducibility for thermal conductivity was 3%–6%, and for volumetric heat capacity, it ranged from 3% to 7% (26).

Thermal diffusivity measurements under air-saturated conditions showed lower values compared to the samples saturated with water. Despite the fact that the thermal diffusivity of air (21×10^{-6} m²/s) is an order of magnitude higher than that of water (0.134×10^{-6} m²/s), the rocks showed higher diffusivity in water-saturated states. This highlights the importance of the saturation medium on the thermal properties of the rocks (Table 12) (26).

Lithology	Density (Dry) (gr/cm³)	Porosity (%)	Thermal conductivity (Dry) (W/m·K)	Thermal conductivity (Saturated)	Thermal diffusivity (Dry) (10^{-6} m²/s)	Thermal diffusivity (Saturated) (10^{-6} m²/s)	Specific heat capacity (J/kg.K)	Volumetric heat capacity (J/kg. m³)
Quartz sandstone	2.509	5.3	5.96	6.75	3.06	3.08	777	1949
	2.578	3.3	6.4	6.94	2.99	3.39	829	2137
	2.235	15.3	3.01	5.37	1.62	2.25	833	1862
	2.424	8.5	4.56	5.9	2.19	2.78	859	2082
	2.489	6.2	5.65	6.31	3	3	758	1887
	2.252	14.5	3.21	5.11	1.95	2.45	730	1644
	2.09	20.9	2.83	4.89	1.66	1.85	795	1662
	2.154	18.5	2.95	4.91	1.66	1.9	825	1777
	1.941	26.6	1.81	3.99	1.06	1.48	881	1710
	2.195	17.6	2.95	5.05	1.91	1.91	704	1545
	1.756	32.1	1.27	3.14	0.96	1.2	753	1322
	1.805	29	1.4	3.7	1.06	1.23	731	1319
	1.802	31.2	1.39	3.42	1.06	1.34	728	1312
	1.828	30.4	1.47	3.42	1.03	1.2	785	1435
	1.937	28	1.38	3.59	1.05	1.31	679	1315
	1.774	35.3	1.09	3.03	0.92	1.24	669	1187

Table 12: Measured Data (Using Air, Water) of Thermal Diffusivity, Thermal Conductivity, and Calculated Data for Volumetric and Specific Heat Capacity (26).

2.1.2.1.7 Stylianou et al (2015)

Cyprus, located in the northeastern Mediterranean, is the third-largest island in the region, covering an area of 9251 km². Geologically, the island consists of four east-west oriented terranes: (a) the Keryneia or Pentadhactylos Range, (b) the Troodos Ophiolite Complex, (c) the Mamonia Complex, and (d) the Mesaoria Plain (or Circum-Troodos Sedimentary Succession). Stylianou et al. investigated the thermal properties of rock samples from different parts of Cyprus (33).

Method description

Given the difficulty of measuring in-sectu, the thermal properties of collected rock samples were measured in a laboratory at room temperature using a portable heat transfer analyzer. Below a depth of 8 meters, the ground temperature in Cyprus remains almost consecutive year, which fluctuates between 18 ° C and 23 ° C depending on the location. This temperature range closely corresponds to laboratory conditions under which measures were held. Thermal property measurement was performed on rock samples in both their dry and water-saint states, using a versatile portable instrument, an isomat 2104 device. The samples were cut into rectangular prisms with flat surfaces measuring 2.5 cm to ensure at least 7×7 cm and and proper fittings for measurement. For each of the 135 samples collected, the three major thermal parameters were measured using Isomat 2104: • Volumetric heat capacity (calculated in the form of density multiplied by specific heat), • Thermal deficiency (α), • thermal conductivity. For dry samples, thermal conductivity values vary from 0.4 to 4.2 WM¯ k¯, while thermal deficiency values vary between 0.3 and 1.9×10^{-6} MIC/S. The specific summer capacity ranged from 0.5 to 1.5 j k¯ kg¯. For water-restrained samples, thermal conductivity remained from 0.6 to 4.5 WM¯ k¯, the thermal defussity remained in the range of 0.3 to 1.9×10^{-6} m k/s, and the specific heat capacity increased from 0.6 to 1.7. J k¯ kg¯ (Table 13) (33).

Lithology	Thermal conductivity (Dry) (W/m·K)	Thermal conductivity (Saturated) (W/m·K)	Thermal diffusivity (Dry) (10^{-6} m²/s)	Thermal diffusivity (Saturated) (10^{-6} m²/s)	Specific Heat capacity (Dry) (J/kg.K)	Specific Heat capacity (Saturated) (J/kg.K)	Number of samples
Calcarenites, sands and gravels	0.9	1.4	0.6	0.7	0.8	1	9
Biocalcarenites, sandstones, gravels, marls, limestone and conglomerates	0.6	1	0.4	0.6	0.9	1.1	3
Biocalcarenites, sandstones, silts, gravels, marls, limestones and conglomerates	0.9	1.3	0.6	0.8	0.8	1	24
Gypsum alternating with chalky marls and marly chalks	1.3	0.9	0.7	0.5	0.7	0.8	5
Biostrome and bioherm reef limestones	1.3	1.6	0.7	0.8	0.8	1	28
Chalks, marls, marly chalks, chalky marls and calcarenites	1.2	1.6	0.7	0.9	0.6	0.8	7
Biostrome and bioherm reef limestone (Terra Member)	1.9	2.2	1.2	1.1	0.7	0.8	6
Chalks, marls, marly chalks with cherts in places as bands or nodules	1.4	1.7	0.8	0.9	0.7	0.9	14
Bentonitic clays interbedded with off-white volcaniclastic sandstones	0.6	1.1	0.6	0.6	0.6	0.9	1
Olivine- and pyroxene-phyric, pillow lavas with occasional sheet flows	1.1	1.3	0.6	0.6	0.7	0.9	2
Pillowed and sheet lava flows with abundant dykes and silts	1.3	1.4	0.7	0.8	0.7	0.8	7

Diabase dykes (>50%) with pillow lava screens, altered to greenschist facies	2.1	2.2	1.1	1.1	0.7	0.8	4
Diabase dykes upto 3 m wide, aphyric and clinopyroxene	2	2	1	1	0.7	0.8	7
Trondhjemites, granophyres, diorites, quartz-diorites and micro granodiorites	3.4	3.6	1.6	1.5	0.8	0.9	1
Isotropic gabbros, uralite gabbros, olivine gabbros and layered melagabbros	2.2	2.8	1.4	1.3	0.6	0.8	3
Websterites, clinopyroxenites, orthopyroxenites and plagioclase bearing pyroxenites	4.2	4.5	1.8	1.9	0.7	0.8	1
Wehrlites and plagioclase-bearing wehrlites, massive or layered	2.9	2.9	1.3	1.3	0.8	0.8	2
Dunites and subordinate clinopyroxene-dunites	2.4	2.3	1.1	1.2	0.8	0.8	1
Tectonized harzburgites with minor dunites and lherzolites	1.7	1.8	0.9	0.8	0.8	0.8	3
Pervasively serpentinized, tectonized harzburgites with minor dunites and lherzolites	2	2.3	1	1.1	0.8	0.9	2

Table 13: Measured values of thermal conductivity, thermal diffusivity and specific heat capacity for geological formation (33).

Lithology	Thermal conductivity (Dry) (W/m·K)	Thermal conductivity (saturated) (W/m·K)	Thermal diffusivity (Dry) (10^{-6} m²/s)	Thermal diffusivity (Saturated) (10^{-6} m²/s)	Specific Heat capacity (Dry) (J/kg·K)	Specific Heat capacity (Saturated) (J/kg·K)	Number of samples
Basalt	1.2	1.4	0.7	0.8	0.7	0.8	4
Calcarenite	1.1	1.5	0.7	0.7	0.7	0.8	23
Chalk	1.4	1.7	0.8	0.9	0.7	0.9	28
Chert	1.7	1.8	0.9	0.9	0.7	0.9	6
Diabase	1.9	2	1	1	0.7	0.8	9
Dunite	2.4	2.3	1.1	1.2	0.8	0.7	1
Gabbro	2.2	2.8	1.4	1.3	0.6	0.8	3
Gypsum	1.3	0.9	0.7	0.5	0.7	0.8	5
Harzburgite	1.7	1.8	0.9	0.8	0.8	0.8	3
Limestone	2.6	2.5	1.5	1.2	0.7	0.8	1
Marl	0.7	1	0.5	0.7	1	1.1	9
Microgabbro	1	1.2	1	0.9	0.7	0.7	4
Olivine-phyric basalt	1	1.2	0.6	0.6	0.7	0.8	2
Plagiogranite	3.4	3.6	1.6	1.5	0.8	0.9	1
Pyroxenite	4.2	4.5	1.8	1.9	0.7	0.8	1
Reef Limestone	1.5	1.8	0.9	0.9	0.6	0.8	14
Sandstone	0.9	1.3	0.9	0.7	0.8	0.8	10
Serpentinite	2	2.3	1	1.1	0.8	0.8	2
Siltstone	0.6	1	0.4	0.6	1.2	1.4	2
Volcanic Breccia	2.1	2.1	1.2	1	0.7	0.8	1
Wehrlite	2.9	2.9	1.3	1.3	0.8	0.8	2

Table 14: Values of thermal conductivity, thermal diffusivity and specific heat capacity for lithology.

(33).

2.1.2.1.8 Balkan et al (2017)

Turkey possesses considerable geothermal potential, but studies on the thermal conductivity of rocks have been scarce. Balkan et al. (2017) reported new thermal conductivity data based on 240 rock samples collected from the western and central Anatolia regions (5).

Method description

The data collection was carried out by the Mineral Research and Exploration General Directorate of Turkey (MTA). In this study, thermal conductivity measurements were taken from 240 rock samples, which were then reported without additional analyses or adjustments. These measurements were performed using a QTM-500 device in MTA's laboratory (Karlı et al., 2006). The QTM-500 follows the ASTM C 1113-90 hot wire method.

Of the 240 samples, 136 were from western Anatolia, and 104 were from central Anatolia. The researchers analyzed 10 different representative rock types from the western region. The majority of the samples were from limestone units, followed by claystone units.

In western Anatolia, the thermal conductivities of the dry samples ranged from 0.7 W/m·K to 3.09 W/m·K. After adjustments for saturation, the values increased significantly (Table 14) (5).

Lithology	Thermal conductivity (Dry) (W/m·K)	Thermal conductivity (saturated) (W/m·K)	Number of samples
Clastic rocks (sandstone)	1.57	3.08	16
Claystone	0.7	1.02	20
Crystallized limestone	3.08	3.49	6
Limestone	2.62	2.98	33
Lacustrine	2.53	2.87	18
Neritic	2.91	3.3	7
Pelagic	3.09	3.51	3
Marl	1.35	1.52	8
Marble	2.93	2.95	9
Schist	2.8	3.19	11
Andesite	1.7	1.99	19
Peridotite	2.52	2.86	3
Tuff	1.11	1.3	11

Table 15: Thermal conductivity values for dry and saturated conditions in western Anatolia (5).

Clastone demonstrated the lowest thermal conductivity of all rock types. In particular, a wide range of conductivity appeared, due to client rocks, mainly sandstones, quartz materials and varying in high holes. In metamorphic rocks, the shist and marble had the thermal conductivity of 3.19 ± 0.93 W/m.K and 2.95 ± 0.4 W/m.K respectively. For igneous rocks, peridotite had an average thermal conductivity of 2.86 ± 0.51 W/m.K, followed by Andesite 1.99 ± 0.68 W/m.K and at Tuff 1.30 ± 0.57 W/m.K. In central Anatolia, the samples were measured directly in saturated conditions, eliminating the need for porosity corrections. The highest mean thermal conductivity value of 5.0 ± 0.98 W/m·K was found for quartzite, which is linked to its high quartz content that facilitates heat transmission. On the other hand, tuff exhibited the lowest mean thermal conductivity of 1.05 ± 0.35 W/m·K, likely due to its high porosity (Table 15) (5).

Lithology	Thermal conductivity (saturated) (W/m·K)	Number of samples
Conglomerate	2.74	3
Crystallized limestone	3.85	14
Limestone	2.64	47
Lacustrine	2.42	13
Neritic	2.88	29
Pelagic	1.83	3
Marl	1.81	7
Marble	3.29	3
Quartzite	5	3
Schist	1.95	2
Andesite	1.8	7
Basalt	1.4	3
Tuff	1.05	9
Granite	4.54	3
Peridotite	2.87	3

Table 16: Thermal conductivity values of saturated conditions and their standard deviations in central Anatolia (5).

2.1.2.1.9   Li et al (2018)

The Tarim Basin, located in the northern part of the Tibetan Plateau in northwestern China, is a major hydrocarbon-rich region and remains a key area for ongoing industrial exploration. Li et al. (2018) collected 101 sedimentary rock samples and measured their thermal properties (69).

Method description

The Tarim Basin consists of an area of 56000 km (216000 mi) and is surrounded by Taranshan mountain in the north, Kunlun Mountains in the south -west and Altin mountain in the south -east. Of the 101 samples, 86 were collected from 16 borhole distributed in the basin, with a depth of 3000 to 6000 meters (9800 to 19700 ft). The remaining 15 samples were taken from the outflow of the north -western margin (image 24) of the basin. The sample set consists of 38 sandstone samples, 31 mudstones, 15 limestone, 8 dolomite, 7 rock salt (evaporation), and 2 groups. The sandstone samples include fine -grain sandstone, siltstone and sandstone, with fine grain sandstone and siltstone major types (69).
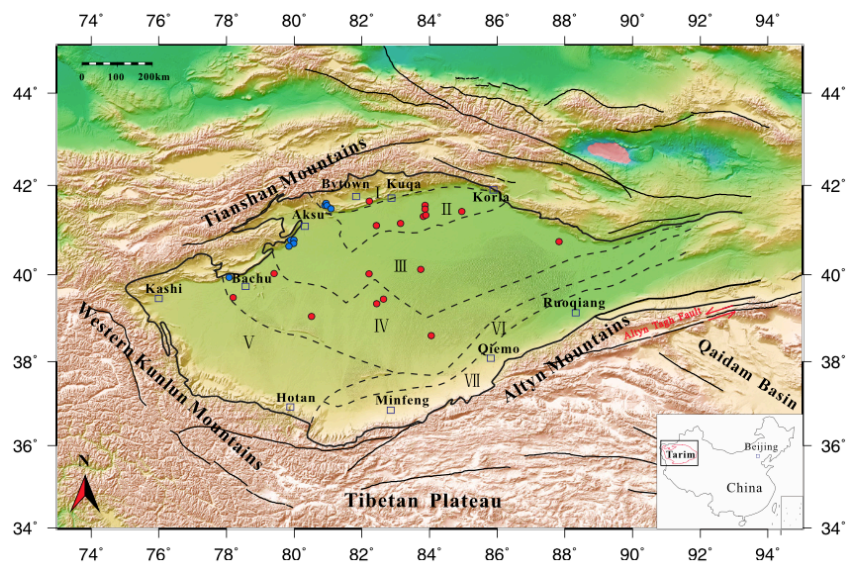
Figure 24: Sketch map showing the tectonic subdivision and sampling locations of the Tarim Basin (69).

Thermal conductivity measurements were performed using the optical scanning method (Popov et al., 1999), at the Institute of Geology and Geophysics, Chinese Academy of Sciences, Beijing, China. The apparatus used was manufactured by a German company and has a measurement range from 0.2 to 25.0 W/m·K with an accuracy of ±3%. This method has been previously applied to other deep drill cores, such as the Vorotilovo core in the Eastern European Platform (Popov et al., 1998), the Kola

Peninsula core (Popov et al., 1999), and the Sulu-Dabie Scientific Drilling Project (He et al., 2008). It is a quick, non-destructive technique that allows continuous measurement. The thermal conductivity of sedimentary rocks in the Tarim Basin varies between 1.08 and 5.35 w/m · K, with an average 2.52 ± 0.99 w/m · K. Rock salt displays the highest medium thermal conductivity, while the lowest in mudstone. For example, sandstone shows a thermal conductivity range of 1.19–4.15 w/m · K, and mudstone is from 1.08–3.54 w/m · K. The wholesale density of these rocks ranges from 2.12 to 2.87 g/cm, on average 2.58 g 0.17 g/cm. Generally, mudstones, sandstones, and group wholesale density are the same, up to 2.54 to 2.63 g/cm, while carbonate rocks - Limstone and dolomite - slightly more density between 2.70 and 2.78 g/cm. Rock salt, however, has the lowest density, an average 2.17 g 0.02 g/cm. At temperatures between 40 ° C and 90 ° C, the specific heat capacity of these rocks and volumetric heat capacity values are presented in Table 16. Mudstone and sandstone display a significant increase with the highest specific heat capacity and temperature, while rock salt shows the lowest value. Limestone and dolomite have moderate specific heat capacity. At 40 ° C, the volumetric heat capacity ranges from 1.61 to 2.79 mj/(m · k), with an average 2.26 mj/(m · · k) (Table 16) (69).

Lithology	Temperature (°C)	Thermal conductivity (mean) (W/m·K)	Thermal diffusivity (10^{-6} m²/s)	Volumetric Heat capacity (MJ/m³·K)
Sandstone	40	2.22	0.98	2.22
	50		0.88	2.45
	60		0.83	2.58
	70		0.8	2.68
	80		0.77	2.76
	90		0.75	2.8
Mudstone	40	2.07	0.81	2.38
	50		0.73	2.64
	60		0.68	2.8
	70		0.63	2.97
	80		0.58	3.15
	90		0.55	3.24
Limestone	40	2.43	0.81	2.28
	50		0.73	2.43
	60		0.68	2.43
	70		0.63	2.42
	80		0.58	2.46
	90		0.55	2.48
Dolomite	40	3.77	1.49	2.44
	50		1.38	2.58
	60		1.35	2.58
	70		1.33	2.58
	80		1.29	2.6
	90		1.25	2.63
Conglomerate	40	3.85	1.87	2.03
	50		1.73	2.18
	60		1.69	2.21
	70		1.66	2.21
	80		1.58	2.27
	90		1.53	2.31
Salt	40	4.51	2.53	1.73
	50		2.38	1.79
	60		2.34	1.79
	70		2.28	1.79

	80		2.19	1.82
	90		2.11	1.85

Table 17: Mean of measured thermal properties of sedimentary rocks in the Tarim basin at different temperature (69).

The thermal deficiency value for sedimentary rocks in the Tarim basin ranges from 0.44×10^{-6} to 2.95×10^{-6} m ×/s at 40 ° C, with an average of 1.12×10^{-6} m k/s (table 16). Rock salt contains the highest thermal defusity, with an average of $2.53 \times 0.40 \times 10^{-6}$ m g/s, followed by group, dolomite and limestone, while mudstone displays the lowest thermal defusity. Additionally, thermal deficiency decreases with rising temperature, which can be attributed to a decrease in the thermal conductivity coupled with an increase in temperature (69) with an increase in volumetric heat capacity.

2.1.2.1.10 Chae et al (2023)

Chae et al. conducted measurements of various mechanical and thermal properties such as density, porosity, specific heat, thermal diffusivity, and thermal conductivity of different rock types, including igneous, metamorphic, and sedimentary rocks, found across South Korea. They also produced distribution maps showing the thermal conductivity of rocks, geothermal gradients, heat flow, and heat production rates based on the basic thermal properties of the region (14).

Method description

The Korean Peninsula located in the eastern part of the Eurasian tectonic plate provides a diverse geology facilitated from different periods, including prequelry metamorphic and plutonic rocks, mesozoic and cedimiatic rocks, as well as quadratic watershed Are. The most common rocks in the region are prequamalian metamorphic rocks and Mesozoic granite, which is more than 47% of the total land area of South Korea simultaneously. In his study, Cha et al. The thermal properties of a total of 3416 rock samples, including density, porcity, specific heat, thermal deficiency and thermal conductivity, were measured. These measurements were performed using the LFA-447 Nano-Flash method (NetzSch, Germany), a laser flash technique. The device was calibrated using a standard sample of pyrokeram 9606, with a thermal conductivity of 4.009 w/mk at 25 ° C. The study found that the average thermal defussity for igneous rocks was 1.29 mm,/s, it was 1.57 mm and/s for metamorphic rocks, and for sedimentary rocks, it was 1.56 mm/s. The high thermal deficiency of

sedimentary rocks is attributed to the significant presence of siltstone (with values from 0.81 to 2.69 mm // second), which has a high thermal expansion coefficient. For metamorphic rocks, this property is affected by the presence of quartzite (1.00–3.48 mm mm/s), phyllite (1.01–2.84 mm mm/s), and scholar (0.82–3.52 mm²/s), which is all high thermal Display deficity. The average specific heat values measured are 0.827 J/GK for igneous rocks, 0.841 J/GK for metamorphic rocks, 0.831 J/GK for sedimentary rocks, are quite similar in three rock types.

To measure density and holes, rock samples were saturated with water. The saturated weight of each sample was recorded, followed by a dry weight at a constant temperature of 103 ° C for 24 hours to determine the dry weight. The results indicated that saturated density of igneous rocks is 1.88 to 3.15 g/cm³, up to 3.23 g/cm³ from metamorphic rocks, and sediment from 2.45 to 3.09 g/cm³, with average density of 2.64 g/cm³, 2.70 g/cm³ and 2.69 g/cm³ respectively.

For thermal conductivity, corrected values for the saturated state ranged from 1.822 to 7.572 W/m.K for granites, with an average of 3.069 W/m.K, and from 1.842 to 8.003 W/m.K for gneisses, with an average of 3.506 W/m.K. The thermal conductivity ranges for igneous rocks, metamorphic rocks, and sedimentary rocks were 1.666–7.52 W/m.K, 1.636–9.053 W/m.K, and 1.778–7.489 W/m.K, respectively, with average values of 3.027 W/m.K, 3.691 W/m.K, and 3.655 W/m.K (Table 17) (14).

Lithology	Thermal conductivity @ room temperature (W/m·K)	Average thermal conductivity (W/m·K)
granite	3.069	Igneous rocke : 3.027
syenite	2.504	
granodiorite	3.066	
diorite	2.663	plutonic rocks : 3.070
gabbro	2.504	
anorthosite	3.167	
felsite	3.165	
dike	3.383	
porphyry	3.171	
rhyolite	3.156	
trachyte	1.977	Volcanic rocks : 2.951
andesite	2.83	
basalt	2.37	
tuff	3.052	
gneiss	3.506	Metamorphic rocks : 3.691
granite gneiss	3.619	
schist	3.917	
phyllite	4.053	
quartzite	5.954	
amphybolite	2.608	
slate	4.559	
hornfels	3.153	
serpentinite	2.645	
conglomerate	3.484	Sedimentary rocks : 3.655
sandstone	3.86	
siltstone	3.102	
shale	3.125	
limestone	3.545	
dolomite	4.286	

Table 18: Thermal conductivity of rocks at room temperature (14).

2.1.2.1.11 García-Noval et al (2024)

Creating a thermal conductivity map of geological structures can be a time-intensive process, but is highly beneficial in determining the optimal location for low-enthusiastic geothermal systems. Such maps help reduce costs and increase the efficiency of geothermal installations. Garcia et neural et al. Used the thermal conductivity of representative rock samples in Ovido (Northwestern Spain) using Sui Thermal Investigation Technique (27).

Method description

Asturias, situated in northwestern Spain, has a rich history as an industrial and mining region. While it lacks medium-to-high enthalpy geothermal resources, shallow geothermal energy offers significant potential. This energy can be harnessed via vertical closed-loop systems in boreholes or open-loop systems utilizing groundwater, owing to the presence of abundant shallow aquifers (García de la Noceda 2020). The region already boasts over 10 MW of installed thermal capacity, distributed across approximately 300 geothermal installations (GEOPLAT 2021). A geological map of Oviedo, compiled from the continuous digital map of Spain (GEODE 2023), illustrates the locations where 22 rock samples were collected from various lithostratigraphic units (Fig. 25) (27).
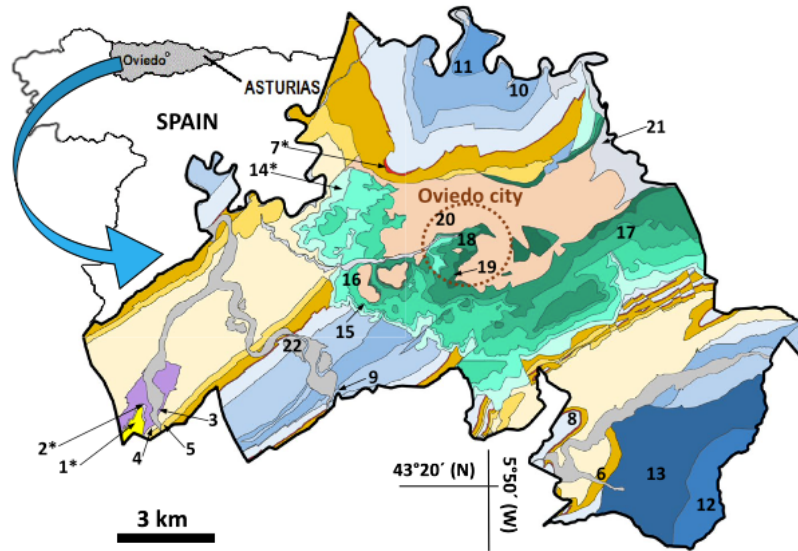
Age		Key	Sample	Formation name
Paleozoic	Ordovician		1	Barrios
	Silurian		2	Formigoso
			3	Furada
	Devonian		4	Rañeces
			5	Moniello
			6	Naranco
	Carboniferous		7	Alba
			8	Barcaliente
			9	Valdeteja
			10	Paquete Folgueras
			11	Paquete Carriles
			12	Paquete Canales
			13	Olloniego
Mesozoic	Cretaceous		14	Ullaga
			15	El Caleyu
			16	Piedramuelle
			17	Otero-Las Tercias
			18	Argañosa
			19	Oviedo
Cenozoic	Tertiary		20	(undifferentiated)
	Quaternary		21	Nora River alluvial
			22	Nalón River alluvial

Figure 25: Geological map and location of the 22 samples taken in the lithostratigraphic units of Oviedo (27).

A total of 26 geological units were studied, from which un-weathered rock samples of at least 20 cm × 20 cm × 20 cm were selected. This dataset included 162 thermal conductivity measurements. The transient thermal needle probe method was employed using the TEMPOS thermal property analyzer (METER). This tool comprises a needle containing both a heating element and a temperature sensor. A constant electric current was passed through the heater for 60 seconds, while the temperature was recorded every second during the heating and subsequent cooling phases (Fig. 26) (27).

Figure 26: Measurement of thermal conductivity by means of a Tempos thermal needle probe device on a boulder sample using a rock sensor (RK-3) and thermal grease (left) and on clayey alluvial sediments using a soil sensor (TR-3) in situ (right) (27).

The study found that limestone was most often sample rock type, which was an accounting for 52% dataset. The thermal conductivity of these limestone samples ranged from 1.14 to 2.95 w/m · K, the average price of 2.25 w/m · ·. Conversely, finely---up rocks, such as Clay and Shells, demonstrated much less thermal conductivity, average 0.85 w/m · k. The rocks with high silica materials, such as sandstones and quartzites, demonstrated the highest thermal conductivity, more than 5 W/M · K, although their values were quite different, with an average 3.61 W/M · K (Table 18). The lowest thermal conductivity in Ovido was seen in structures such as the Nora River (Chaturdhatuk) and the alluvial deposits of the tertiary deposit, where the values were low as 0.2 W/M · K. In contrast, the highest thermal conductivity was recorded in the Barios quartzite, which reached a maximum of 5.35 w/m · K, followed by Paquete Cannes Sandstone, which demonstrated the thermal conductivity of 4.98 w/m · K (27).

Lithology	Thermal conductivity (W/m·K)
Quartz	5.35
Shale	1.6
Sandstone	4.6
Limestone	2.07
Limestone red	1.72
Limestone green	2.48
Sandstone	4.91
Limestone	2.62
Limestone	2.95
Limestone	2.74
Sandstone	1.4
Limestone	2.49
Sandstone	1.94
Sandstone	4.98
Conglomerate	3.52
Sandstone	2.15
Limestone	2.68
Argillite	0.39
Limestone white	2.17
Limestone red	1.94
Limestone	2.04
Limestone	2.89
Limestone	1.65
Clay	0.19
Limestone	1.14
Clay	0.17
Clay	1.11

Table 19: Values of thermal conductivity obtained for each sample (27).

2.1.2.2 Thermal Response Test (TRT) approaches in practice

2.1.2.2.1 Taussi et al. (2021)

Tausi et al. A field conducted to evaluate the geothermal heat exchange capacity of a fluvial ground located in the Lower Metoro Valley, an area within the central epinein of Italy. The purpose of this investigation is to understand and clarify how the heat-exchanges vary throughout the region, using detailed geological and thermal data from public sources. Research focuses on three main objectives: 1. Estimate the rate on which the heat can be removed from the ground. 2. Determining how deep a borehole would need to be drilled to meet a specific energy demand of 4.0 kW. 3. Applying geothemal capacity (G.Pot) models, a tool created by Kasoso and Sethi, to calculate and map geothermal capacity throughout the valley. The findings showed that the geothermal capacity in this valley is largely affected by the type of Bedrek and the presence of water-elaborate sedimentary layers (60).

Method description

The study area located in the foothills of the Marche region is composed of diverse geological layers, including: • Limustone, Marlstone, and Marley Limustone. • Sandstone and siltstone are mixed with marlstone. • Vapor, clay, and silty clay, mixed with sandstone layers. The investigation was limited to the top 100 meters of the sub-collect, as this depth is usually targeted for vertical closed-loop borhole heat exchanges. The approach was structured in three stages, which was based on a method developed by Viesi et al :: 1. Data Collection: Assembleing relevant geological and thermal information. 2. Aptermining map construction: developing visual representation of geothermal features. 3. Geological Possible Analysis: Depending on its physical and thermal characteristics, borhole design and system operation, using the G.Pot model to evaluate the ability of the ground to support low-boggomal geothermal systems. The analysis indicated that geothermal capacity, heat extraction rate, and thermal conductivity value grow as a trick from coastal areas, where sediment is thick, in inland regions, where carbonate rock structures are close to the surface. The thermal properties of rocks were compiled from many sources, as shown in Table 19. The geotherm capacity of the region was between 9.0 and 10.0 MW per year. Additionally, the average borehole depth required to supply a standard domestic energy load of 4.0 kW was about 96 meters, with a depth of 82 to 125 meters depending on the specific site (60).

Lithology	Thermal conductivity (W/m·K)			Volumetric Heat capacity (MJ/m³·K)
	Min Value	Max Value	Recommended Value	
Gravel dry	0.4	0.9	0.4	1.6
Gravel water-saturated	1.6	2.5	1.8	2.4
Sand and gravel moisture dry	1.5	0.9	0.5	1.6
Sand and gravel moisture water saturated	1.6	3	2.2	2.7
Sand dry	0.3	0.9	0.4	1.6
Sand water-saturated	2	3	2.4	2.9
Clay/silt dry	0.4	1	0.5	1.6
Clay/silt water-saturated	11	3.1	17	3.4

Table 20: Thermophysical properties for unconsolidated sediments of the investigated area (60).

Lithology	Thermal conductivity (W/m·K)			Volumetric Heat capacity (MJ/m³·K)
	Min Value	Max Value	Recommended Value	
Argille Azzurre Fm.	-	-	1.91	2.4
Colombacci Fm.	-	-	1.96	2.4
San Donato Fm.	-	-	1.96	2.4
Gessoso Solfifera Fm.	1.15	2.8	1.6	1.2
Tripoli Fm.	-	-	1.96	2.4
Marnoso-Arenacea Fm.	-	-	2.1	2.6
Schlier Fm.	2.01	2.34	2.18	2.5
Bisciaro Fm.	1.3	1.35	1.32	2.4
Sc. Cinerea Fm.	2.1	2.11	2.1	2.5
Sc. Bianca-Rossa-Variegata Fms.	1.82	2.63	2.09	2.4
Marne a Fucoidi Fm.	-	-	2.28	2.5
Maiolica Fm.	2	2.67	2.27	2.4

Table 21: Thermophysical properties for rocks of the investigated area (60).

2.1.2.2.2   Dalla Santa et al. (2020)

Accurate input data about the underground's thermal properties are crucial for designing ground source heat exchanger fields. Dalla Santa et al. developed a comprehensive database of thermal properties by compiling and comparing data from three sources: (1) international guidelines, (2) an extensive review of previous studies, and (3) over 400 direct measurements (17).

Method description

Designing a closed-loop geothermal system requires a detailed understanding of the thermal characteristics of the ground. Key properties include:

1. **Thermal Conductivity**: The material's ability to transfer heat, expressed in W/m·K.

2. **Heat Capacity**: The amount of heat needed to cause a temperature change, expressed in J/K. Specific heat capacity, which accounts for material mass or volume, is typically used.

3. **Thermal Diffusivity**: A measure of heat diffusion during temperature changes, calculated as the ratio of thermal conductivity to heat capacity.

4. **Undisturbed Ground Temperature Profile**: This remains influenced by air temperature in shallow layers but stabilizes below about 10 meters. At greater depths, it increases steadily with the geothermal heat flux.

Within the scope of the **Cheap-GSHP Project**, thermal conductivity and diffusivity were measured using various devices:

- **For rock samples**:
  o The TCi Thermal Conductivity Analyzer (by C-Therm Technologies) at the Institute of Geosciences and Earth Resources in Padova, Italy.
  o The Thermal Conductivity Scanning (TCS) system at Friedrich-Alexander University (FAU) in Erlangen-Nuremberg, Germany.

- **For unconsolidated sediment samples**:
  o The ISOMET 2114 Thermal Properties Analyzer was used for loose sediments at the University of Padova.
  o The TCS system was also applied to over-consolidated clay samples at FAU, Germany.
  o A Taurus Instruments TLP 800 Guarded Hot Plate, specially modified to test gravel samples.

The compiled thermal database is summarized in Table 20 (17).

Rocks	Lithology	From Literature Review Thermal conductivity (W/m·K)				Directly measured Thermal conductivity (W/m·K)				UNIPD-Cheap GSHPs database Thermal conductivity (W/m·K)	
		min	max	Porosity	Volumetric heat capacity (MJ/m³·K)	min	max	Porosity	Volumetric heat capacity	min	max
Sedimentary rocks		0.59	7.7			1.03	4.54			0.59	7.7
	conglomerate	1.5	5.1	2.2-2.7	1.8-2.6			2.43-2.66		1.5	5.1
	sandstone	0.72	6.5	2.2-2.7	1.8-2.6	1.03	4.54	2.7	2.06-2.28	0.72	6.5
	clay-mudstone	0.59	3.48	2.4-2.6	2.1-2.4	1.47	3.21	2.35-2.80	1.80-2.23	0.59	3.48
	limestone	0.6	5.01	2.4-2.7	2.1-2.4	2.42	4.41	2.47-2.78	1.81-2.22	0.6	5.01
	dolomite	0.61	5.73	2.4-2.7	2.1-2.4	1.96	5.22		2.03-2.34	0.61	5.73
	marlstone	1.78	2.9	2.3-2.6	2.2-2.3					1.78	2.9
	gypsum	1.15	2.8	2.2-2.4	2					1.15	2.8
	anhydrite	1.5	7.7	2.8-3.0	2					1.5	7.7
Igneous rocks		0.44	5.86			0.86	3.29			0.44	5.86
	granite	1.49	4.45	2.4-3.0	2.1-3.0	2.02	3.68	2.66-2.73	1.80-2.12	1.49	4.45
	diorite	1.38	4.14	2.9-3.0	2.9	1.99	3.04	2.60-2.71	1.75-2.10	1.38	4.14
	syenite	1.35	5.2	2.5-3.0	2.4	2.2	2.66	2.69	2.02-2.06	1.35	5.2
	gabbro	1.52	5.86	2.8-3.1	2.6	2.41	2.79	2.84	2.08-2.04	1.52	5.86

	rhyolite	1.77	3.98	2.6	2.1	1.89	3.29	2.11-2.5	1.95-2.09	1.77	3.98
	dacite	2	3.91	2.9-3.0	2.9					2	3.91
	andesite	0.64	4.86	2.6-3.2	2.3-2.6	0.96	1.39		1.38-1.57	0.64	4.86
	trachyte	2.2	3.4	2.6	2.1	1.86	1.95	2.33-2.63	1.87-2	1.86	3.4
	basalt	0.44	5.33	2.6-3.2	2.3-2.6	0.86	2.69	2.13-3.02	1.89-2.07	0.44	5.33
	tuff/tuffstone	1.1	2.59							1.1	2.59
Metamorphic rocks		0.65	8.15			1.98	4.43			0.65	8.15
	quartzite schist	1.89	8.15	2.5-2.7	2.1					1.89	8.15
	micaschist	0.65	5.43	2.4-2.7	2.2-2.4	1.98	4.43	2.72-2.76	2.09-2.26	0.65	5.43
	gneiss	0.84	4.86	2.4-2.7	1.8-2.4	3.04	3.89	3.03	2.19-2.2	0.84	4.86
	phyllite	1.5	3.33			1.45	2.94	2.76-2.82	1.41-1.95	1.45	3.33
	amphibolite	1.35	3.9	2.6-2.9	2-2.3					1.35	3.9
	serpentinite	2.41	4.76			2.01	3.72	2.63-2.82	2.1-2.2	2.01	4.76
	marble	0.98	5.98	2.5-2.8	2					0.98	5.98
nconsolidated sediments											
	clean gravel, dry	0.13	0.9	1.8-2.2	1.3-1.6	0.14	0.55			0.14	0.9
	heterometric gravel with sand, wet	0.18	3			0.94	1.33			0.2	3

Material										
medium sand, dry	0.15	0.9	1.8-2.2	1.3-1.6	0.15	0.68		0.41-1.48	0.15	0.9
medium sand, wet	1	2.6	1.9-2.3	2.2-2.8	1.44	2.45		1.53-2.27	1	2.6
silty sand/sandy silt, wet	1.2	2.25			1.24	2.06		1.85-2.48	1.2	2.25
silt, dry	0.26	1.09	1.8-2	1.5-1.6	0.25	0.82		1.37-1.52	0.25	1.09
silt and clayey silt, wet	0.82	2.6	2-2.2	2-2.8	0.93	1.76		1.84-2.43	0.82	2.6
clay, dry	0.25	1.52	1.8-2	1.5-1.6	0.25	1.22		0.49-1.38	0.25	1.52
plastic clay, wet	0.6	1.9	2-2.2	2-2.8	0.87	1.39		0.62-2.67	0.6	1.9
organic materials: peat	0.2	0.7	0.5-1.1	0.5-3.8	0.3	0.66		0.32-0.78	0.2	0.7

Table 22: The UNIPD Cheap-GSHPs thermal database (17).

2.1.2.2.3 Amanzholov et al (2022)

Amanzolov et al. By analyzing the effects of geometric design and soil thermophic properties, a study performed to evaluate the thermal performance of the Borhole Heat Exchanges (Bhes). The team developed an algorithm to solve the mathematical equations of their model and demonstrated numeric simulation using the Comsol multiplicics software (2).

Method description

The study focused on two major parameters: thermal resistance between the soil thermal conductivity and the borhole wall and the circulating fluid. These parameters are required to correctly evaluate the performance of the BES in systems such as ground source heat pump and borhole thermal energy storage (BTES). The test process was divided into two main stages:

1. **Measuring the Ground's Undisturbed Temperature by Depth**

o   This can be done by directly recording the temperature at various depths using sensors placed along the borehole.

o   Alternatively, the temperature change at the inlet and outlet of the BHE can be monitored. The heat transfer fluid (HTF) is circulated for 3–5 hours until temperature changes stabilize, and the inlet and outlet temperatures are nearly the same. This final stabilized value is considered the undisturbed ground temperature.

2. **Measuring Inlet and Outlet Temperatures to Extract Soil and Borehole Properties**

o   Over 5–7 days, data is collected on temperature variations at the inlet and outlet of the BHE to determine the soil's thermal conductivity and the borehole's thermal resistance.

o   If the soil has low thermal conductivity, the inlet/outlet temperatures will rise quickly. However, if the soil's conductivity is high, the temperature rise will stabilize over time.

For testing, a prototype GSHP system was installed at the "Koksai" mosque in Kazakhstan's Almaty region. The subsurface composition down to 180 m includes unconsolidated materials like boulders, gravel, sand, and loam. Two 50 m boreholes were drilled—one for a single U-shaped heat exchanger and another for a double-cross U-shaped design. The gaps between the borehole wall and the heat exchangers were sealed with cement mortar containing 70% water, 24% cement, and 6% bentonite (Fig. 27) (2).
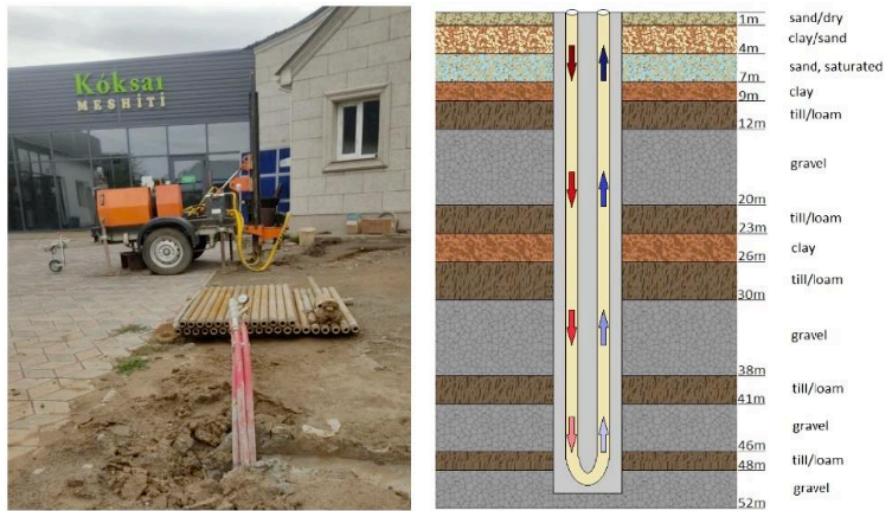
Figure 27: Thermal Response Test at Koksai mosque, Almaty (2).*(1)*

In Almaty, the site's subsurface is made up of approximately 48% gravel, 29% loam, and 23% sand and clay. The thermophysical properties of the soil layers are detailed in Table 21. Based on the thermal response test (TRT) data and predictions from a line-source analytical model, the soil's thermal conductivity was found to be 2.35 W/m·K, and the borehole thermal resistance was calculated as 0.20 m·K/W.

The simulations revealed the following:

- Higher grout material conductivity (0.5–3.3 W/m·K) increased heat extraction.
- Pipe material conductivity above 2.0 W/m·K had no significant impact on heat extraction (tested range: 0.24–0.42 W/m·K).
- A volumetric flow rate above 1.0 m³/h did not alter heat extraction (tested rate: 0.6 m³/h).
- Heat extraction improved as soil thermal conductivity increased (tested range: 0.4–6.0 W/m·K) (2).

Lithology	Depth (m)	Density ϱ, (*103) (kg/m³)	Porosity ϕ (%)	Thermal conductivity λ, (W/m·K)	Volumetric heat capacity ϱc, (MJ/m³·K)
sand, dry	0–1	2	0.31	0.4	1.45
sandy clay	1–4	2.1	0.35	1.6	2.45
sand, moist	4–7	2.1	0.31	1.4	2.5
clay	7–9	21	0.45	1.8	2.4
till/loam	9–12	2.05	0.45	2.4	2
gravel	12–20	2.1	0.26	1.8	2.4
till/loam	20–23	2.05	0.45	2.4	2
clay	23–26	2.1	0.45	1.8	2.4
till/loam	26–30	2.05	0.45	2.4	2
gravel	30–38	2.1	0.26	1.8	2.4
till/loam	38–41	2.05	0.45	2.4	2
gravel	41–46	2.1	0.26	1.8	2.4
till/loam	46–48	2.05	0.45	2.4	2
gravel	48–52	2.1	0.26	1.8	2.4

Table 23: Thermal properties of the underground soil types (2).

2.1.2.2.4   Richard A. Beier (2019)

Richard A. Beer conducted a study on the Borhole Heat Exchanges (BES) to assess the ground and borhole thermal properties at Stillwater, USA. The primary objective was to improve the parameter estimates used with thermal response test (TRT) data while addressing the boundaries of these methods. When specific parameter assessment techniques are applied to evaluate ground thermal conductivity and borhole thermal resistance, the results sometimes show a minimum, shallow decrease. The study of beer demanded a rapid, a rapid, a rapid, a status dynasty for the global minimum, separating the estimate of borhole resistance from the heat capacity as an independent parameter. This allows for more accurate evaluation of ground thermal conductivity and borhole resistance during various heat flow period (6).

Method description

Beier's method was applied to seven TRT datasets. Details of the boreholes used in the study are summarized in Table 22. Boreholes 1, 2, and 3 are located at site A in Stillwater, OK. These boreholes, which penetrate clay and shale layers, have depths of approximately 76 meters. Each borehole has a single U-tube through which circulating water flows. Borehole 1 is surrounded by bentonite grout, while boreholes 2 and 3 use enhanced grout. In Borhole 3, spacers were installed to keep separately along the borehole wall. Borholes 4, 5, and 6 are located in site B in Oklahoma City, OK, where soils have layers of soil, shell and sandstone. Borhole 4 uses standard bentonite grout, while Borhole 5 and 6 are groted with increased grout (Table 22). Each of the borhole 4 and 5 has a YouTube, while the borehole 6 has a double You-tube system, with the utube configured in a parallel flow. The main problem addressed in beer work is the challenge of parameter estimates in TRT data. Using the map of the root medium square error (RMSE) between models predictions and measured temperatures, it was found that traditional methods sometimes showed slow convergence for global minimum. Beer introduced a temperature derived curve to better define three different stages of TRT: borhol-discretion, transition and stable heat-proof period.

 This method allows for more accurate, independent evaluation of borehole resistance and ground thermal conductivity. However, meaningful estimates of the ground's volumetric heat capacity were only possible in a few cases in this study (6).

site A			
Parameter	**Borehole 1, single U-tube**	**Borehole 2, single U-tube**	**Borehole 3, single U-tube**
Lithology	Clay, Sandstone	Clay, Sandstone	Clay, Sandstone
ground thermal conductivity (K_s)	3.32 ± 0.64	3.1 ± 0.39	3.13 ± 0.37
Root Mean Square Error (RMSE oC)	0.266	0.118	0.185
Active U-tube length (m)	75.6	76.2	76.2
Pipe wall thermal conductivity (W/(m.K))	0.4	0.4	0.4
Type of grout	Bentonite	Enhanced	Enhanced
Grout thermal conductivity (W/(m.K))	0.74	1.73	1.73
Grout volumetric heat capacity (kJ/(m³.K))	3500	3000	3000
Fluid volumetric heat capacity (kJ/(m³.K))	4180	4180	4180
Fluid density (kg/m3)	997	997	997
Fluid thermal conductivity (W/(m.K))	0.61	0.61	0.61
Fluid viscosity (kg/(m.s)	0.89 x 10-3	0.89 x 10-3	0.89 x 10-3
Mean heat input rate (W)	2640	2660	2670
Average undisturbed ground temperature (°C)	17.6	17.6	17.6
Duration of test (h)	71.2	50.3	53.2
site B			
Parameter	**Borehole 4, single U-tube**	**Borehole 5, single U-tube**	**Borehole 6, double U-tube**
Lithology	Clay, Shale, Sandstone	Clay, Shale, Sandstone	Clay, Shale, Sandstone
ground thermal conductivity (K_s)	2.22 ± 0.31	2.11 ± 0.16	2.04 ± 0.15
Root Mean Square Error (RMSE)	0.437	0.107	0.158
Active U-tube length (m)	87.8	91.4	91
Pipe wall thermal conductivity (W/(m.K))	0.4	0.4	0.4
Type of grout	Bentonite	Enhanced	Enhanced
Grout thermal conductivity (W/(m.K))	0.74	2.1	2.1
Grout volumetric heat capacity (kJ/(m³.K))	3500	3350	3350
Fluid volumetric heat capacity (kJ/(m³.K))	4180	4180	4180
Fluid density (kg/m³)	996	996	996
Fluid thermal conductivity (W/(m.K))	0.61	0.61	0.61

Fluid viscosity (kg/(m.s)	0.80×10^{-3}	0.80×10^{-3}	0.80×10^{-3}
Mean heat input rate (W)	6100	6090	6090
Average undisturbed ground temperature (°C)	17.2	17.2	17.2
Duration of test (h)	48.2	48.1	48.2

Table 24: Information and parameters for boreholes 1, 2, 3, 4, 5 and 6 at site A and site B (6).

2.1.2.2.5 Zarella et al (2017)

The designing ground source heat pump (GSHP) system is important as decisions made during this phase affect both energy efficiency and installation and cost of operation. Zarela et al. Detected the interpretation of TRT data to evaluate ground thermal conductivity for effective system design. The study took place in Molinela, Bologna, Italy, where several Borhole Heat Exchanges (BES) were tested as part of the cheap-GSHP project funded by the European Union under the horizon 2020 (71).

Method description

The test site is located in Molinella, in the alluvial Po Valley of Bologna province, Emilia-Romagna region, Italy. This area is characterized by flat, alluvial plains formed by alternating layers of coarse sediments like gravel and sand, and finer sediments such as silt and clay. These materials often create sand dikes or horizontal sills. Six different types of BHEs were tested at this site, as listed in Table 23 and 24.

Zarella et al. used an inverse numerical approach that considered the BHE geometry, axial heat transfer, and the effect of surface weather on the ground. The BHEs consisted of four coaxial pipe systems: Boreholes A, F, G, and H. Boreholes F, G, and H were 50 meters deep, while Borehole A was 96 meters deep. All BHEs used high-density polyethylene for the inner pipes, with stainless steel for the outer pipes of Boreholes A, G, and H, and polyvinyl chloride for Borehole F.

For the TRT setup, a closed-loop system was used with the BHE, and a constant heat injection rate was applied. Seven electric resistances, each delivering 1.5 kW, were connected to a tank capable of providing about 10.5 kW of heat. The heat transfer fluid was circulated by a thermally insulated pump (Fig. 28) (71).
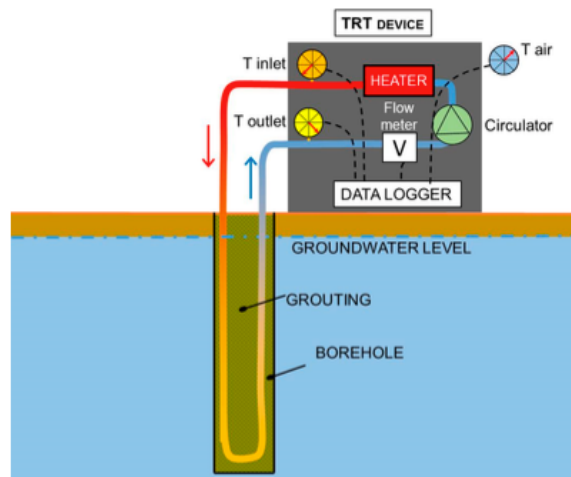
Figure 28: Thermal response test equipment (71).

During the first phase of testing, the electrical resistances were turned off to measure the undisturbed ground temperature. The temperatures of the fluid at the inlet and outlet of the borehole were recorded at one-second intervals for at least 30 minutes. After that, the resistances were turned on, and the standard TRT was performed, recording parameters such as the outside air temperature, fluid temperatures at the borehole inlet and outlet, fluid flow rate, and power consumption by the electric resistances. These measurements were taken every 15 seconds for 72 hours.

The TRT data were analyzed to estimate the ground thermal conductivity using several interpretation methods: the simplified infinite line source model (S-ILSM), the complete infinite line source model (ILSM), the infinite cylinder source model (ICSM), and the inverse numerical approach. The thermal conductivity estimates from the S-ILSM model were generally higher than those from the full ILSM model because the first six hours of data were neglected in the simplified approach. For example, the estimated thermal conductivity ranged from 1.35 W/(m·K) for Borehole G to 1.60 W/(m·K) for Borehole C (which had the same depth). The inverse numerical method yielded a lower value of approximately 1.2 W/(m·K) for Borehole D. Overall, the study found thermal conductivity values between 1.35 and 1.62 W/(m·K) for the same depth, depending on the interpretation method used (71) (Table 23 and 24).

Parameter	Borehole A	Borehole C	Borehole D	Borehole F	Borehole G	Borehole H
Thermal conductivity (W/m.K)	0.4	0.4	0.38	0.4	0.4	0.4
Outside diameter (mm)	32	32	20	32	25	32
Inside diameter (mm)	26	26	14.2	26	21	26
Borehole length (m)	96	50	15	50	50	50
Borehole diameter (mm)	76.1	125	400	101	50	60.3
Thermal conductivity of the grout (m^2/s)		1.6	1.84	1.6		
Thermal diffusivity of the grout (m^2/s)		0.7×10^{-6}	0.86×10^{-6}	0.7×10^{-6}		

Table 25: Characteristics of the coaxial (borehole A, F, G, H), U-tube (borehole C) and the helical shaped pipe (borehole D) borehole heat exchangers (71).

Parameter	Borehole A	Borehole C	Borehole D	Borehole F	Borehole G	Borehole H
Borehole length (m)	96	50	15	50	50	50
λ_{eq} (S-ILSM) (RMSE, °C)	1.49 ± 0.15	1.6 ± 0.13	1.39 ± 0.15	1.43 ± 0.13	1.35 ± 0.13	1.59 ± 0.13
λ_{eq} (ILSM) (RMSE, °C)	1.32 (0.37)	1.58 (0.12)	-	1.2 (0.45)	1.33 (0.31)	1.52 (0.46)
λ_{eq} (ICSM) (RMSE, °C)	1.26 (0.26)	1.5 (0.42)	-	1.2 (0.51)	1.24 (0.48)	1.4 (0.65)
λ_{eq} (CaRM) (RMSE, °C)	1.3 (0.1)	1.51 (0.05)	1.2 (0.06)	1.45 (0.07)	1.35 (0.01)	1.49 (0.03)

Table 26: Equivalent ground thermal conductivity (71).

3   Results

This chapter presents the thermal properties analyzed from 16 tests, including 11 conducted in laboratories and 5 TRT tests, as discussed earlier. The results are organized using various terms and visualized with graphs (refer to Appendix A).

3.1   Analysis of thermal properties

A summary table of the 16 test results has been created, categorized by thermal properties and rock types. The data includes 42 formations grouped into 4 main rock types, as shown in Tables 25 and 26.

Rock types	Lithology	Thermal conduvtivity (Dry) (W/m·K)	Thermal conduvtivity (Saturated) (W/m·K)	Thermal diffusivity (m²/s)	Volumetric heat capacity (MJ/m³·K)
Sedimentary rocks	conglomerate	1.0 - 2.5	2.0 - 5.0	0.1 - 0.3	800 - 1800
	sandstone	1.0 - 4.0	2.0 - 6.0	0.1 - 0.3	800 - 1800
	claystone	1 - 3	2 - 4	0.1 - 0.3	1000 - 2200
	limestone	1.0 - 2.5	2.0 - 4.0	0.1 - 0.4	800 - 2000
	travertine	0.5 - 1.5	1.0 - 3.0	0.05 - 0.1	800 - 2200
	dolomite	2.0 - 4.0	2.5 - 5.5	0.1 - 0.2	800 - 1800
	marl	0.5 - 1.5	1.0 - 3.0	0.05 - 0.1	1200 - 2200
	gypsum	0.2 - 0.5	0.5 - 1.0	0.05 - 0.1	800 - 1400
	clay	0.2 - 1.0	0.5 - 1.5	0.03 - 0.1	800 - 2000
	anhydrite	2.5 - 3.5	3.0 - 5.0	0.1 - 0.2	800 - 1400
Igneous rocks	granite	2.5 - 5.0	3.0 - 6.0	0.5 - 1.0	800 - 1200
	diorite	2.5 - 4.5	3.0 - 6.0	0.5 - 1.0	800 - 1200
	syenite	3.0 - 4.5	3.5 - 6.0	0.5 - 1.0	800 - 1200

	gabbro	3.0 - 6.0	4.0 - 7.0	0.5 - 1.0	800 - 1200
	rhyolite	1.5 - 3.0	2.0 - 4.0	0.3 - 0.5	800 - 1200
	dacite	1.5 - 3.0	2.0 - 4.0	0.3 - 0.5	800 - 1200
	andesite	1.5 - 3.0	2.0 - 4.0	0.3 - 0.5	800 - 1200
	granodiorite	2.5 - 3.5	3.0 - 5.0	0.5 - 1.0	800 - 1200
	trachyte	2.0 - 3.0	2.5 - 4.0	0.5 - 0.8	800 - 1200
	basalt	2.5 - 6.0	4.0 - 7.0	0.5 - 1.0	800 - 1200
	tuff/tuffstone	0.5 - 2.0	1.0 - 3.0	0.05 - 0.1	800 - 2200
Metamorphic rocks	quartzite schist	3.0 - 5.0	3.5 - 6.0	0.5 - 1.0	800 - 1200
	micaschist	2.5 - 4.0	3.0 - 5.0	0.5 - 1.0	800 - 1200
	Calceschist	2.5 - 3.5	3.0 - 5.0	0.5 - 1.0	800 - 1200
	Metatonalite	2.5 - 3.5	3.0 - 5.0	0.5 - 1.0	800 - 1200
	gneiss	2.5 - 4.0	3.0 - 5.0	0.5 - 1.0	800 - 1200
	phyllite	2.5 - 3.5	3.0 - 5.0	0.5 - 1.0	800 - 1200
	amphibolite	2.5 - 4.0	3.0 - 5.0	0.5 - 1.0	800 - 1200
	serpentinite	2.5 - 3.0	3.0 - 5.0	0.5 - 1.0	800 - 1200
	marble	2.0 - 3.0	2.5 - 5.0	0.5 - 1.0	800 - 1200
Unconsolidated sediments	clean gravel, dry	1.0 - 2.0	1.5 - 2.5	0.1 - 0.3	800 - 2000
	heterometric gravel with sand, wet	1.0 - 2.0	2.0 - 4.0	0.1 - 0.3	800 - 2000
	sand, dry	0.15 - 0.50	0.25 - 0.80	0.01 - 0.05	800 - 2000
	sand, moist	0.20 - 0.70	0.30 - 1.0	0.01 - 0.05	800 - 2000
	medium sand, wet	0.10 - 0.50	0.20 - 0.80	0.01 - 0.05	800 - 2000

	silty sand/sandy silt, wet	0.10 - 0.50	0.20 - 0.80	0.01 - 0.05	800 - 2000
	silt, dry	0.10 - 0.25	0.15 - 0.35	0.01 - 0.05	800 - 2000
	silt and clayey silt, wet	0.15 - 0.30	0.20 - 0.40	0.01 - 0.05	800 - 2000
	clay, dry	0.15 - 0.25	0.20 - 0.50	0.01 - 0.05	800 - 2000
	plastic clay, wet	0.20 - 0.40	0.25 - 0.60	0.01 - 0.05	800 - 2000
	till/loam	0.10 - 0.30	0.15 - 0.40	0.01 - 0.05	800 - 2000
	organic materials: peat	0.05 - 0.25	0.10 - 0.30	0.01 - 0.05	1500 - 2500

Table 27: Thermal properties for various rock types

Rock types	Lithology	Density gr/cm3	Porosity (%)	Grain/particle size (mm)
Sedimentary rocks	conglomerate	2.68	20 - 30	2 - 256 (pebble to boulder-sized)
	sandstone	2.65	10 - 20	0.625 - 2 (sand-sized grains)
	claystone	2.4	10 -15	< 0.004 (clay-sized particles)
	limestone	1.32	5 - 10	<1 mm - 2 mm (fine to medium)
	Travertine	1.76	30 -40	<0.5 - 2 mm (fine to medium)
	dolomite	2.79	5 - 10	0.01 - 1 mm (fine to medium)
	marl	2.12	10 - 20	<0.004 - 0.06 mm (clay to silt-sized)
	gypsum	2.23	5 - 10	0.01 - 2 mm (fine to medium)
	clay	2.1	20 - 30	<0.004 mm (clay-sized)
	anhydrite	3.12	1 - 5	0.01 - 1 mm (fine to medium)
Igneous rocks	granite	2.67	1 - 5	1 - 5 mm (medium to coarse)
	diorite	2.86	1 -5	1 - 5 mm (medium to coarse)

	syenite	2.7	1 - 5	1 - 5 mm (medium to coarse)
	gabbro	2.93	1 -5	1 - 5 mm (medium to coarse)
	rhyolite	2.6	10 - 20	<1 mm (fine-grained)
	dacite	2.43	10 - 20	<1 mm (fine-grained)
	andesite	2.52	10 - 20	<1 mm (fine-grained)
	Granodiorite	2.39	5 - 10	1 - 5 mm (medium to coarse)
	trachyte	2.68	10 - 20	<1 mm (fine-grained)
	basalt	2.52	1 - 5	<1 mm (fine-grained)
	tuff/tuffstone	2.25	30 -50	<2 mm (ash-sized and small clasts)
Metamorphic rocks	quartzite schist	2.53	1 - 5	0.1 - 5 mm (medium to coarse)
	micaschist	2.6	1 - 5	0.1 - 5 mm (medium to coarse)
	Calceschist	2.68	5 - 10	0.1 - 5 mm (medium to coarse)
	Metatonalite	2.69	1 - 5	1 - 5 mm (medium to coarse)
	gneiss	2.77	1- 5	1 - 5 mm (medium to coarse)
	phyllite	2.75	1 - 5	<0.1 mm (fine-grained)
	amphibolite	2.86	1 - 5	0.1 - 3 mm (fine to medium)
	serpentinite	2.67	1 - 10	0.1 - 1 mm (fine-grained)
	marble	2.75	1 - 5	0.1 - 5 mm (fine to coarse)
Unconsolidated sediments	clean gravel, dry	2.1	20 - 30	2 - 64 mm (gravel-sized)
	heterometric gravel with sand, wet	2.1	25 - 40	2 - 64 mm (mixed sizes)
	sand, dry	2	30 40	0.0625 - 2 mm (sand-sized)
	sand, moist	2.1	30 -40	0.0625 - 2 mm (sand-sized)
	medium sand, wet	1.8	30 -40	0.25 - 0.5 mm (medium sand)

silty sand/sandy silt, wet	1.87	30 - 50	0.004 - 0.0625 mm (silt-sized)
silt, dry	1.43	30 - 40	0.004 - 0.0625 mm (silt-sized)
silt and clayey silt, wet	1.72	30 - 50	<0.0625 mm (silt to clay-sized)
clay, dry	1.2	20 - 30	<0.004 mm (clay-sized)
plastic clay, wet	1.68	20 - 30	<0.004 mm (clay-sized, plastic)
till/loam	2.05	20 - 30	Mixed, 0.001 mm (clay) - 2 mm (sand)
organic materials: peat	0.52	70 - 95	Highly variable, <0.004 mm to 10+ mm

Table 28: Density, porosity, and grain size of different rock types

3.1.1 Density and porosity

The relationship between dry thermal conductivity, density, and porosity is shown in Figures 29 and 30.
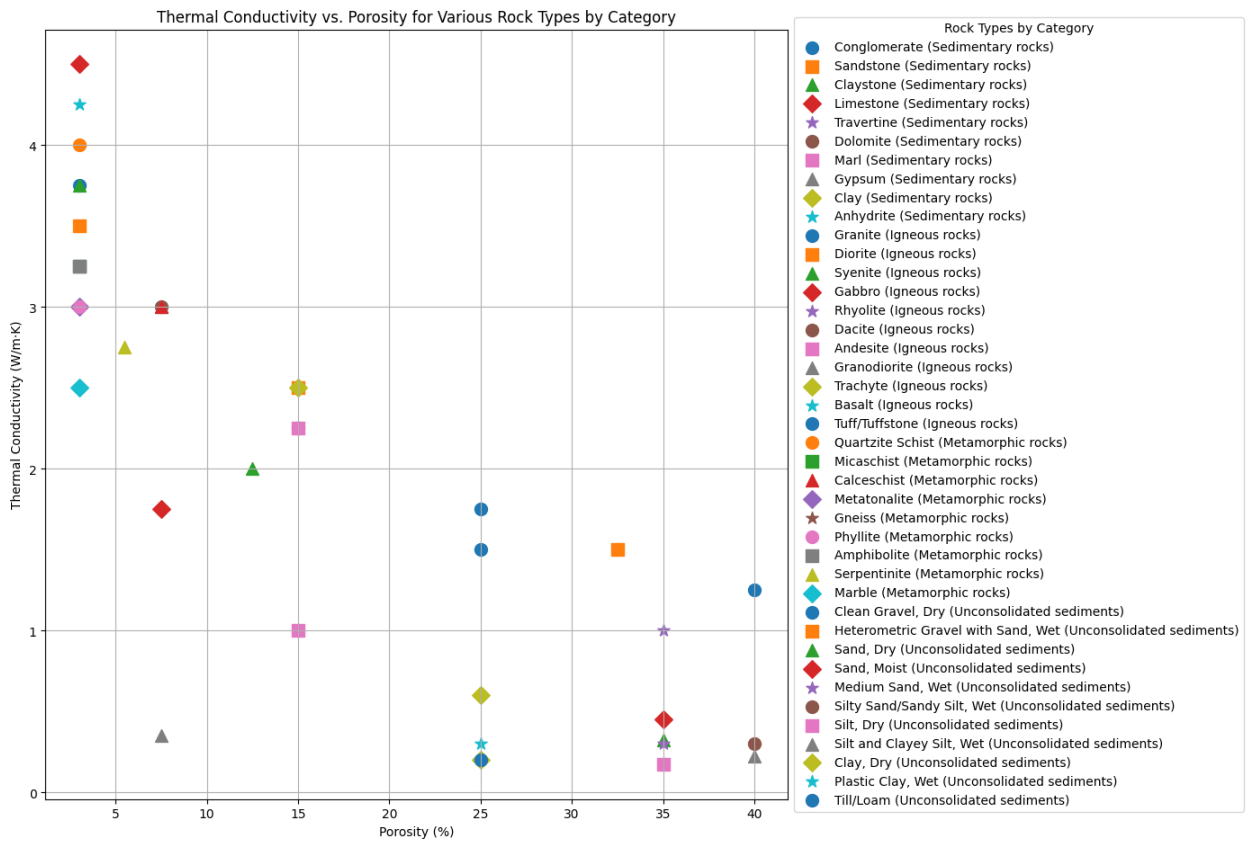
Figure 29: Thermal conductivity vs. porosity

Each data point in Figure 29 represents a specific rock type from four main groups: sediment, igneous, metamorphic, and disinterested sediment. In general, high -porcelain rocks also have high thermal conductivity as empty spaces in the rock facilitate heat transfer. However, some exceptions, such as "clay" and "gypsum", show high holes but low conductivity due to their unique mineral composition, which oppose heat transfer.
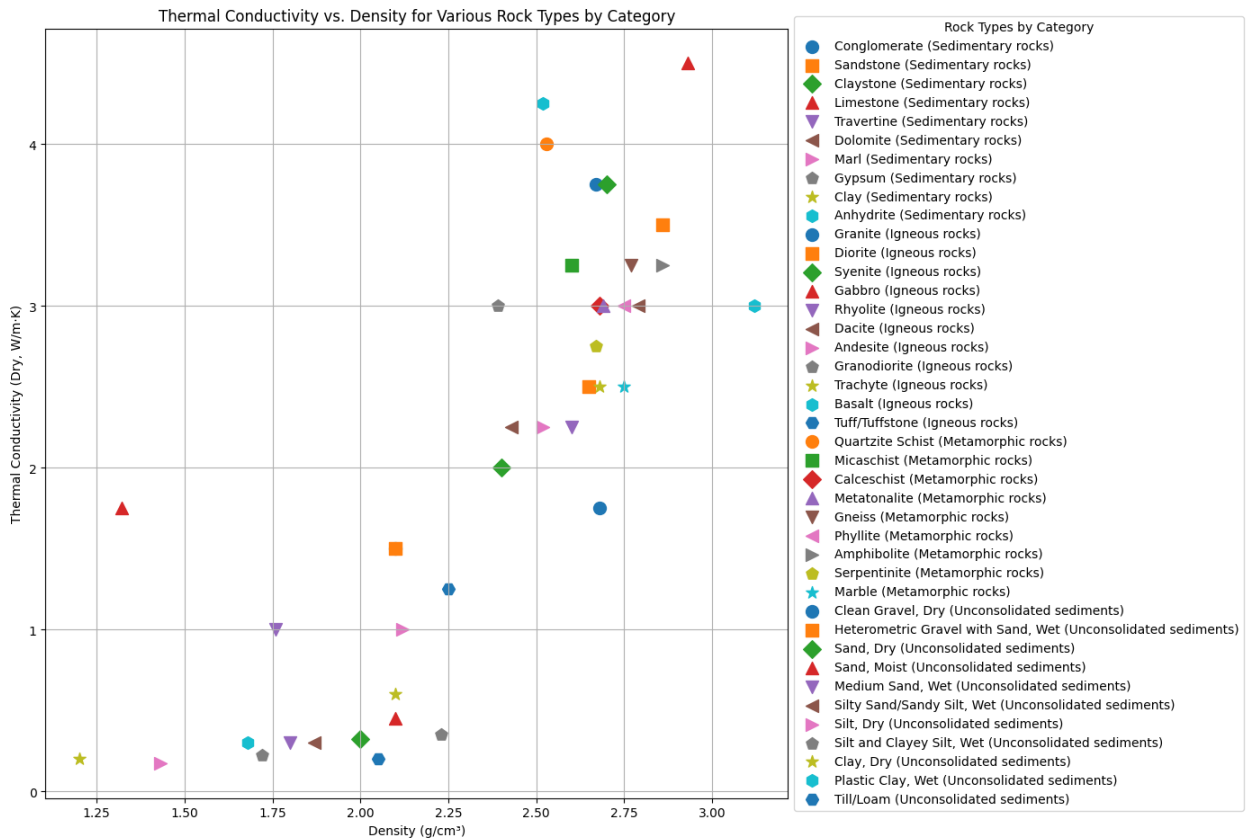
Figure 30: Thermal conductivity vs. density

Figure 30 suggests that dense rocks usually contain high thermal conductivity, meaning that they move heat more efficiently. However, exceptions such as "weight silt and clay silt" have low density, but still due to their mineral structure, significant conductivity is displayed. Rocks such as "granite" and "gabro" display high density and conductivity, making them excellent for geothermal applications.

3.1.2 Thermal conductivity

Figure 31 shows thermal conductivity values for rocks both dry and saturated both dry and saturated.
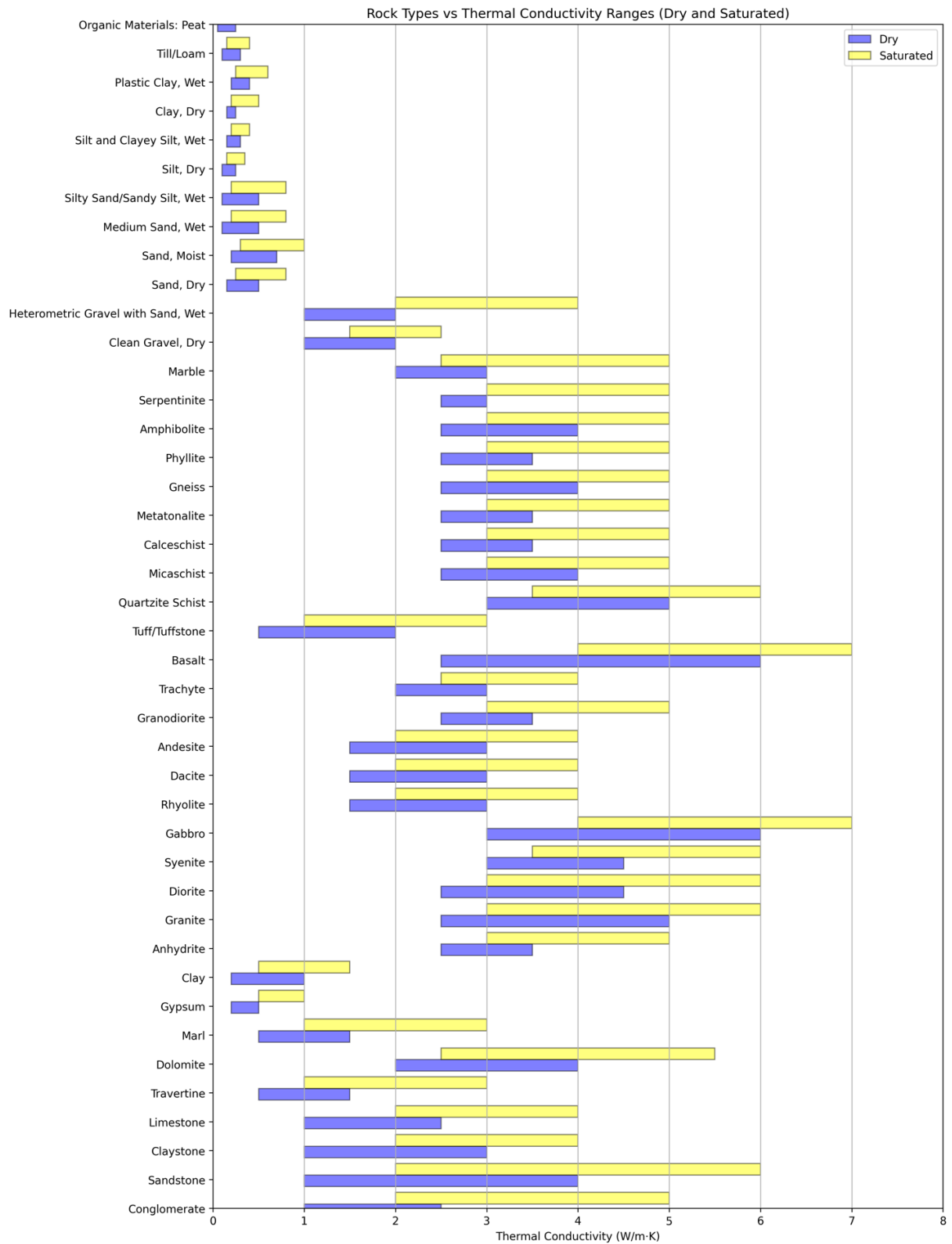
Figure 31: Thermal conductivity under dry and saturated conditions

This chart highlights that the thermal conductivity usually increases when the rocks are saturated, as water increases heat transfer. For example, rocks such as "granite" and "basalt" show a significant increase in conductivity when water is present. Conversely, due to their mineral characteristics, rocks like "Pete" and "Clay" are less conductive even when saturated. Intensive rocks such as "Gabro" and "Basalt", continuously maintain high conductivity, while biological materials such as "Peat" remain a bad heat conductor (17).
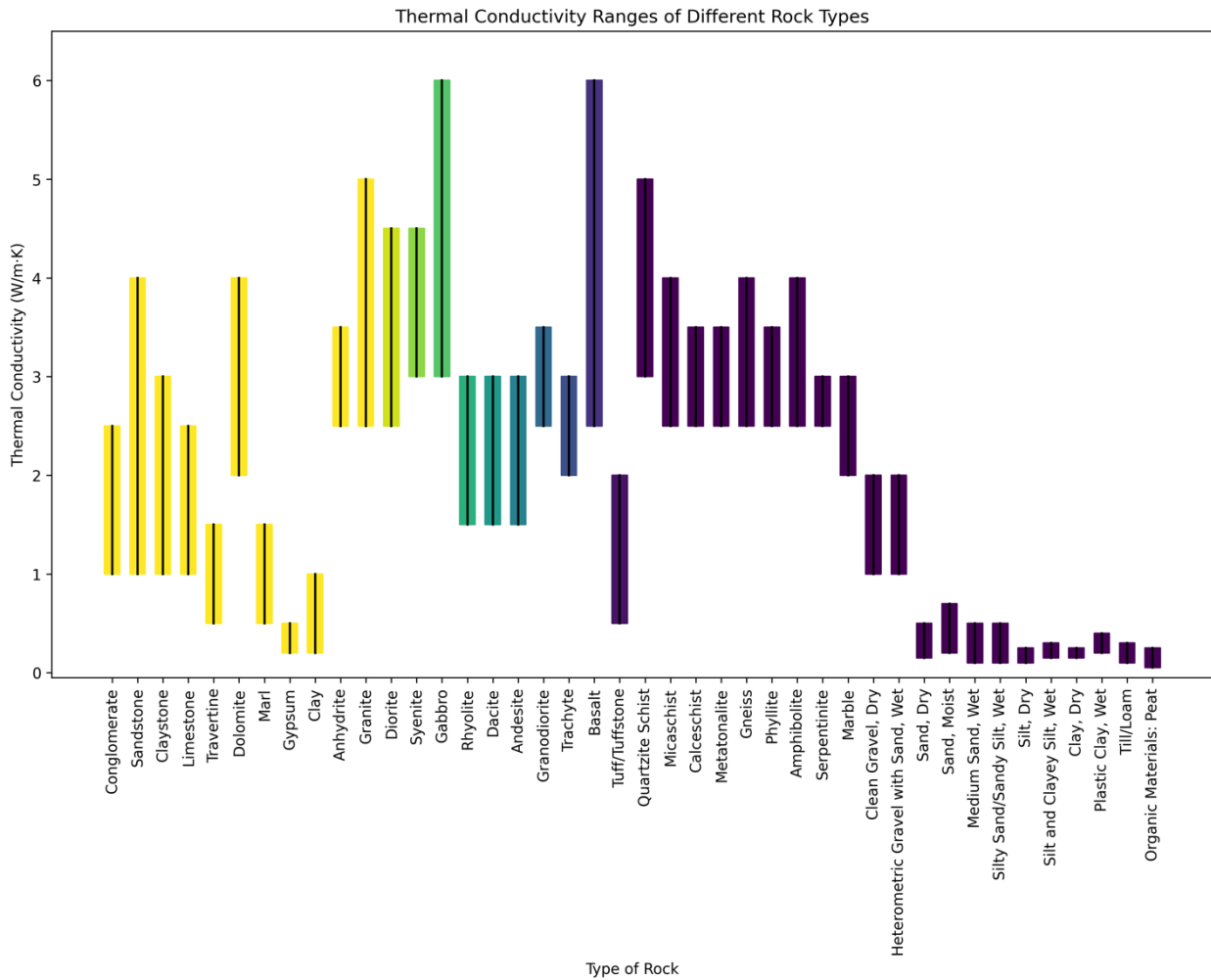
Figure 32: Thermal conductivity ranges for various rock types

The sedimentary rocks perform a wide range of thermal conductivity, affected by factors such as texture, cementation and water content. The rocks of the infiltration (eg, "granite" and "gabro") usually have a higher conductivity than extruscious such as "basalt" due to their low porcines and specific mineral composition. In metamorphic and plutonic rocks, thermal conductivity is determined more than their mineral makeup (eg, quartz) compared to Porosity (Fig. 32).

3.1.3   Thermal diffusivity

Thermal deficity measures how the heat soon runs through a material, which is expressed in M of/S. Granite, rocks such as "" dyrite, "and" basalt "have high proliferation, while soft materials such as" clay "and" silt "have low values. Metamorphic rocks, including "quartzite," "phytalite," and "shist", also perform high proliferation due to their mineral composition (14).
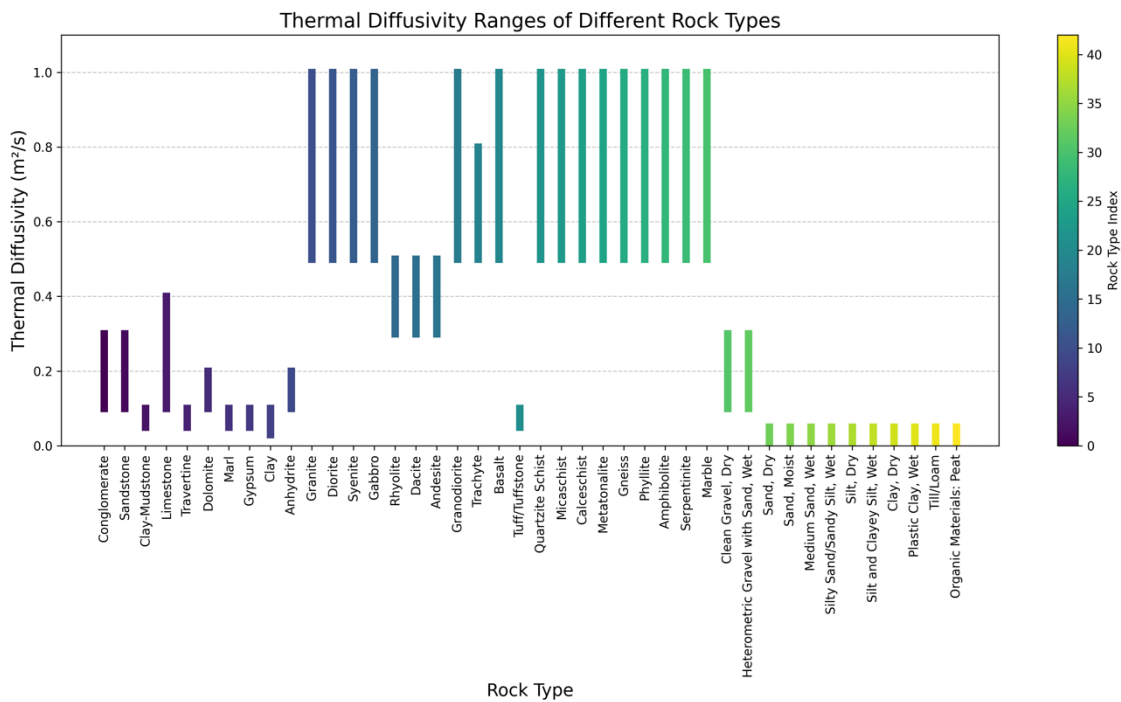

Figure 33: Thermal diffusivity ranges for various rock types

As shown in Figure 33, rocks with high proliferation, such as "granite" and "gabro," move the heat efficiently, making them ideal for geothermal systems. In contrast, rocks such as "clay" and "sand" are better suited to insulation due to their low deviation. Spread rocks such as "limestone" and "sandstone" fall into the medieval, making them versatile for heat transfer and insulation.

95
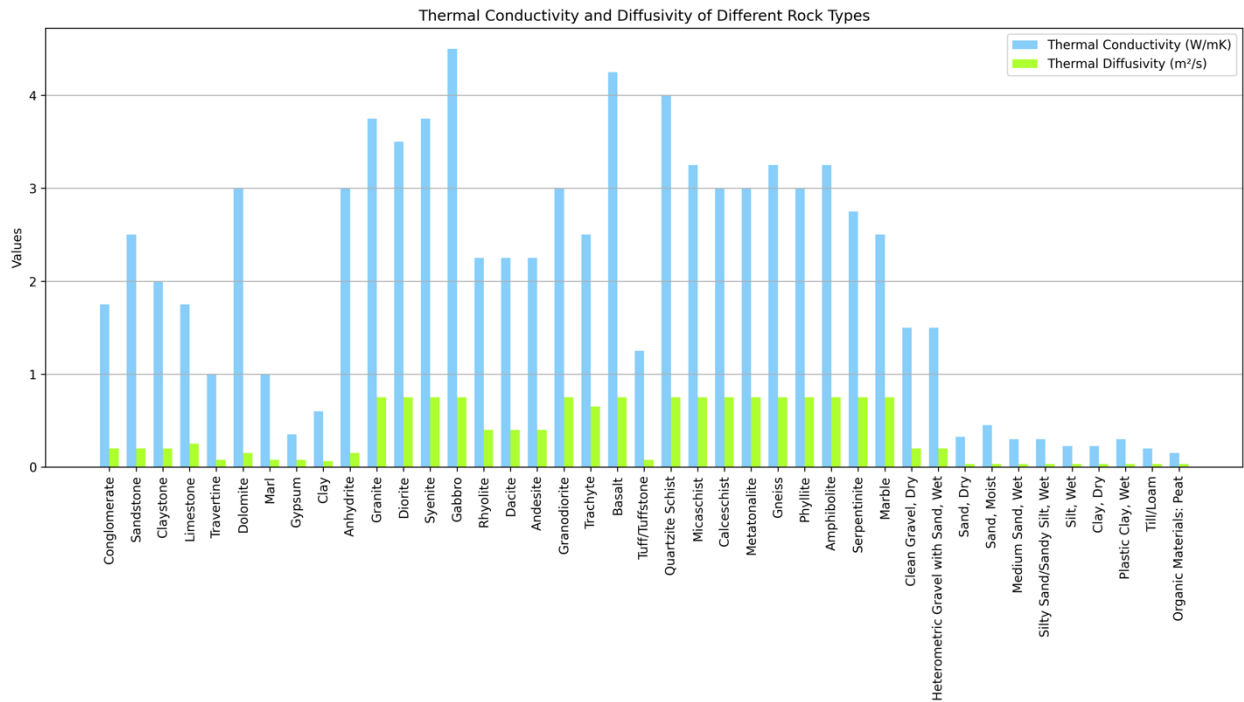
Figure 34: Thermal conductivity and diffusivity of different rock types

Low density and high-porosity rocks usually perform low thermal deficiency. Rocks like "Granite," "Gabro," and "Quartzite Shist" are well suited to geotomical applications due to their efficient heat transfer properties. On the other hand, unrelated rocks, such as wet sand and soil, are more suitable for insulation due to their low conductivity and proliferation (Fig. 34).

3.1.4 Volumetric Heat Capacity

Volumetric heat capacity indicates how much energy is required to raise the temperature of 1 cubic meter of material by 1°C. The ranges for various rock types are illustrated in Figure 35.
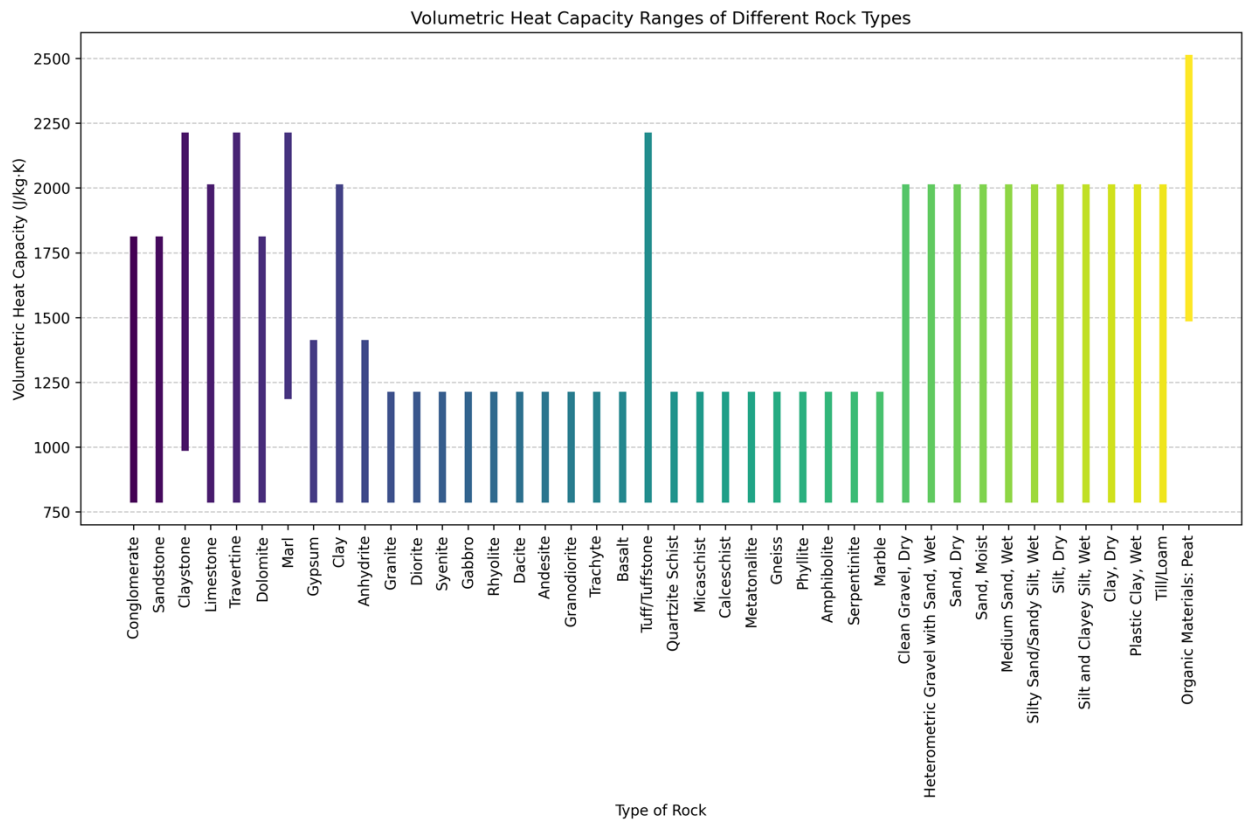
Figure 35: Volumetric heat capacity ranges of various rock types

Rocks like "Peat" have high heat capacity, which makes them slowly storing and releasing heat. This makes them valuable for heating and cooling systems where heat storage is necessary. In this chapter, we examined several charts to understand the thermal properties of different rock types. These insights are valuable to designing shallow geomal systems by comparing thermal conductivity, proliferation and heat capacity among the types of rock.

4 Conclusion

The purpose of this thesis is to check the thermal conductivity of different types of rocks and soil (lithology), which compared to various thermal measurement methods.

- Thermal conductivity in various lithology: This research has shown that different rocks and soil have different thermal properties. For example, dense rocks like granite have high thermal conductivity, whereas soil and rocks with soft textures and high holes have low thermal conductivity.

- Difference in thermal conductivity measurement methods: This study examined various methods to measure the thermal conductivity of rocks and soil. These methods include laboratory testing and thermal response test (TRT). The results indicated that each method has its own specific benefits and limitations: laboratory testing, offering high accuracy in controlled conditions, are not representative of the real in-situ conditions; on the other hand, TRT provides an in-situ measurement of thermal conductivity in natural conditions, which over time gives more realistic data about system behavior. However, this method may be affected by specific environmental conditions and is much more expensive and time-consuming. Therefore, choosing the right method depends on the unique conditions of the project and can affect accuracy and design costs.

Thermal properties of lithology significantly affect the design and adaptation of geothermal systems. Considering the difference in thermal conductivity between various rocks and soils, geothermal systems can be designed to adapt both economic and functional. In addition, the selection of appropriate methods to measure thermal properties and consider local characteristics can help reduce the cost and increase the efficiency of geothermal systems.

References

1. Ahmed AA, Assadi M, Kalantar A, Sliwa T, Sapińska-Śliwa A. A Critical Review on the Use of Shallow Geothermal Energy Systems for Heating and Cooling Purposes. Energies. 2022 Jun 10;15(12):4281.

2. Amanzholov T, Seitov A, Aliuly A, Yerdesh Y, Murugesan M, Botella O, et al. Thermal Response Measurement and Performance Evaluation of Borehole Heat Exchangers: A Case Study in Kazakhstan. Energies. 2022 Nov 14;15(22):8490.

3. Andújar Márquez J, Martínez Bohórquez M, Gómez Melgar S. Ground Thermal Diffusivity Calculation by Direct Soil Temperature Measurement. Application to very Low Enthalpy Geothermal Energy Systems. Sensors. 2016 Feb 29;16(3):306.

4. Bae S, Nam Y, Choi J, Lee K, Choi J. Analysis on Thermal Performance of Ground Heat Exchanger According to Design Type Based on Thermal Response Test. Energies. 2019 Feb 18;12(4):651.

5. Balkan E, Erkan K, Şalk M. Thermal conductivity of major rock types in western and central Anatolia regions, Turkey. Journal of Geophysics and Engineering. 2017 Aug 1;14(4):909–19.

6. Beier RA. Insights into parameter estimation for thermal response tests on borehole heat exchangers. Science and Technology for the Built Environment. 2019 Sep 14;25(8):947–62.

7. Bertani R. GEOTHERMAL ENERGY: AN OVERVIEW ON RESOURCES AND POTENTIAL.

8. Boban L, Miše D, Herceg S, Soldo V. Application and Design Aspects of Ground Heat Exchangers. Energies. 2021 Apr 11;14(8):2134.

9. Bozdağ Ş, Turgut B, Paksoy H, Dikici D, Mazman M, Evliya H. Ground water level influence on thermal response test in Adana, Turkey. Int J Energy Res. 2008 Jun 10;32(7):629–33.

10. Bozzoli F, Pagliarini G, Rainieri S, Schiavi L. Estimation of soil and grout thermal properties through a TSPEP (two-step parameter estimation procedure) applied to TRT (thermal response test) data. Energy. 2011 Feb;36(2):839–46.

11. Busby J. Thermal conductivity and diffusivity estimations for shallow geothermal systems. QJEGH. 2016 May;49(2):138–46.

12. Casasso A, Sethi R. Assessment and Minimization of Potential Environmental Impacts of Ground Source Heat Pump (GSHP) Systems. Water. 2019 Jul 29;11(8):1573.

13. CESEN SpA, Europäische Kommission, editors. Blue book on geothermal resources: a strategic plan for the development of European geothermal sector. Luxembourg: Office for Official Publ. of the European Communities; 1999. 527 p. (Altener).

14. Chae BG, Park ES, Kim HC. Basic analysis of rock mechanical and thermal properties in South Korea. Rock Mechanics Bulletin. 2023 Jul;2(3):100060.

15. Chen C, Zhu C, Zhang B, Tang B, Li K, Li W, et al. Effect of Temperature on the Thermal Conductivity of Rocks and Its Implication for In Situ Correction. Luo X, editor. Geofluids. 2021 May 3;2021:1–12.

16. Christodoulides P, Vieira A, Lenart S, Maranha J, Vidmar G, Popov R, et al. Reviewing the Modeling Aspects and Practices of Shallow Geothermal Energy Systems. Energies. 2020 Aug 18;13(16):4273.

17. Dalla Santa G, Galgaro A, Sassi R, Cultrera M, Scotton P, Mueller J, et al. An updated ground thermal properties database for GSHP applications. Geothermics. 2020 May;85:101758.

18. Di Sipio E, Chiesa S, Destro E, Galgaro A, Giaretta A, Gola G, et al. Rock Thermal Conductivity as Key Parameter for Geothermal Numerical Models. Energy Procedia. 2013;40:87–94.

19. Di Sipio E, Galgaro A, Destro E, Teza G, Chiesa S, Giaretta A, et al. Subsurface thermal conductivity assessment in Calabria (southern Italy): a regional case study. Environ Earth Sci. 2014 Sep;72(5):1383–401.

20. Dickson MH, UNESCO, editors. Geothermal energy: utilization and technology. Paris: UNESCO; 2003. 205 p. (Renewable energies series).

21. Ekeopara PU, Nwosu CJ, Kelechi FM, Nwadiaro CP, ThankGod KK. Prediction of Thermal Conductivity of Rocks in Geothermal Field Using Machine Learning Methods: a Comparative Approach. In: Day 3 Wed, August 02, 2023 [Internet]. Lagos, Nigeria: SPE; 2023 [cited 2024 Dec 11]. p. D032S028R002. Available from: https://onepetro.org/SPENAIC/proceedings/23NAIC/3-23NAIC/D032S028R002/526025

22. Esen H, Inalli M. In-situ thermal response test for ground source heat pump system in Elazığ, Turkey. Energy and Buildings. 2009 Apr;41(4):395–401.

23. Fahlén P. 170 PUBLICATIONS 6,322 CITATIONS SEE PROFILE.

24. Franco A. A Routine Thermal Response Test (TRT) for Estimating Soil Thermal Properties in Connection with Geotechnical Analysis [Internet]. ENGINEERING; 2019 [cited 2024 Dec 11]. Available from: http://www.preprints.org/manuscript/201902.0091/v1

25. Franco A, Conti P. Clearing a Path for Ground Heat Exchange Systems: A Review on Thermal Response Test (TRT) Methods and a Geotechnical Routine Test for Estimating Soil Thermal Properties. Energies. 2020 Jun 9;13(11):2965.

26. Fuchs S, Förster H, Norden B, Balling N, Miele R, Heckenbach E, et al. The Thermal Diffusivity of Sedimentary Rocks: Empirical Validation of a Physically Based $\alpha - \varphi$ Relation. JGR Solid Earth. 2021 Mar;126(3):e2020JB020595.

27. García-Noval C, Álvarez R, García-Cortés S, García C, Alberquilla F, Ordóñez A. Definition of a thermal conductivity map for geothermal purposes. Geotherm Energy. 2024 May 29;12(1):17.

28. Goetzl G, Dilger G, Grimm R, Hofmann K, Holecek J, Cernak R, et al. Strategies for Fostering the Use of Shallow Geothermal Energy for Heating and Cooling in Central Europe - Results from the Interreg Central Europe Project GeoPLASMA-CE.

29. Hajto M, Przelaskowska A, Machowski G, Drabik K, Ząbek G. Indirect Methods for Validating Shallow Geothermal Potential Using Advanced Laboratory Measurements from a Regional to Local Scale—A Case Study from Poland. Energies. 2020 Oct 21;13(20):5515.

30. Heim E, Laska M, Becker R, Klitzsch N. Estimating the Subsurface Thermal Conductivity and Its Uncertainty for Shallow Geothermal Energy Use—A Workflow and Geoportal Based on Publicly Available Data. Energies. 2022 May 18;15(10):3687.

31. Hermans T, Nguyen F, Robert T, Revil A. Geophysical Methods for Monitoring Temperature Changes in Shallow Low Enthalpy Geothermal Systems. Energies. 2014 Aug 11;7(8):5083–118.

32. Ilbeygi A, Biglarian H, Hakkaki-Fard A. A versatile method for estimating grout and ground thermal properties in a thermal response test. Applied Thermal Engineering. 2023 Oct;233:121152.

33. Iosif Stylianou I, Tassou S, Christodoulides P, Panayides I, Florides G. Measurement and analysis of thermal properties of rocks for the compilation of geothermal maps of Cyprus. Renewable Energy. 2016 Apr;88:418–29.

34. Jarzyna JA, Baudzis S, Janowski M, Puskarczyk E. Geothermal Resources Recognition and Characterization on the Basis of Well Logging and Petrophysical Laboratory Data, Polish Case Studies. Energies. 2021 Feb 6;14(4):850.

35. Jolie E, Scott S, Faulds J, Chambefort I, Axelsson G, Gutiérrez-Negrín LC, et al. Geological controls on geothermal resources for power generation. Nat Rev Earth Environ. 2021 Apr 6;2(5):324–39.

36. Kerschbaumer RC, Stieger S, Gschwandl M, Hutterer T, Fasching M, Lechner B, et al. Comparison of steady-state and transient thermal conductivity testing methods using different industrial rubber compounds. Polymer Testing. 2019 Dec;80:106121.

37. Kudrewicz R, Papiernik B, Hajto M, Machowski G. Subsalt Rotliegend Sediments—A New Challenge for Geothermal Systems in Poland. Energies. 2022 Feb 4;15(3):1166.

38. Kumar L, Hossain MdS, Assad MEH, Manoo MU. Technological Advancements and Challenges of Geothermal Energy Systems: A Comprehensive Review. Energies. 2022 Nov 30;15(23):9058.

39. Lee C, Park M, Park S, Won J, Choi H. Back-analyses of in-situ thermal response test (TRT) for evaluating ground thermal conductivity: Back-analysis of in-situ TRT. Int J Energy Res. 2013 Sep;37(11):1397–404.

40. Lee C, Park M, Nguyen TB, Sohn B, Choi JM, Choi H. Performance evaluation of closed-loop vertical ground heat exchangers by conducting in-situ thermal response tests. Renewable Energy. 2012 Jun;42:77–83.

41. Lund JW. Development and Utilization of Geothermal Resources. In: Goswami DY, Zhao Y, editors. Proceedings of ISES World Congress 2007 (Vol I – Vol V) [Internet]. Berlin, Heidelberg: Springer Berlin Heidelberg; 2008 [cited 2024 Dec 11]. p. 87–95. Available from: http://link.springer.com/10.1007/978-3-540-75997-3_13

42. Luo J, Qiao Y, Xiang W, Rohn J. Measurements and analysis of the thermal properties of a sedimentary succession in Yangtze plate in China. Renewable Energy. 2020 Mar;147:2708–23.

43. Manzella A. Geothermal energy. Cahen D, Cifarelli L, Ginley D, Slaoui A, Terrasi A, Wagner F, editors. EPJ Web Conf. 2017;148:00012.

44. McDaniel A, Tinjum J, Hart DJ, Lin YF, Stumpf A, Thomas L. Distributed thermal response test to analyze thermal properties in heterogeneous lithology. Geothermics. 2018 Nov;76:116–24.

45. Miocic JM, Schleichert L, Van De Ven A, Koenigsdorff R. Fast calculation of the technical shallow geothermal energy potential of large areas with a steady-state solution of the finite line source. Geothermics. 2024 Jan;116:102851.

46. Pang Z, Kong Y, Shao H, Kolditz O. Progress and perspectives of geothermal energy studies in China: from shallow to deep systems. Environ Earth Sci. 2018 Aug;77(16):580, s12665-018-7757-z.

47. Perego R, Pera S, Galgaro A. Techno-Economic Mapping for the Improvement of Shallow Geothermal Management in Southern Switzerland. Energies. 2019 Jan 16;12(2):279.

48. Rajver D, Casasso A, Capodaglio P, Cartannaz C, Prestor J, Maragna C, et al. Shallow Geothermal Potential with Borehole Heat Exchangers (BHEs): Three Case Studies in the Alps.

49. Raymond J, Therrien R, Gosselin L, Lefebvre R. A Review of Thermal Response Test Analysis Using Pumping Test Concepts. Groundwater. 2011 Nov;49(6):932–45.

50. Roka R, Figueiredo A, Vieira A, Cardoso J. A systematic review on shallow geothermal energy system: a light into six major barriers. S&R. 2022 Dec 1;46(1):e2023007622.

51. Sáez Blázquez C, Farfán Martín A, Martín Nieto I, Gonzalez-Aguilera D. Measuring of Thermal Conductivities of Soils and Rocks to Be Used in the Calculation of A Geothermal Installation. Energies. 2017 Jun 10;10(6):795.

52. Sailer E, Taborda DMG, Keirstead J. Assessment of Design Procedures for Vertical Borehole Heat Exchangers.

53. Sanner B. Shallow geothermal energy – history, development, current status, and future prospects.

54. Sanner B, Hellström G, Gehlin S, Spitler J. Thermal Response Test, Current Status and World-Wide Application.

55. Sanner DB. SHALLOW GEOTHERMAL SYSTEMS, GROUND SOURCE HEAT PUMPS. GROUND SOURCE HEAT PUMPS.

56. Shao H, Hein P, Sachse A, Kolditz O. Geoenergy Modeling II: Shallow Geothermal Systems [Internet]. Cham: Springer International Publishing; 2016 [cited 2024 Dec 11]. (SpringerBriefs in Energy). Available from: http://link.springer.com/10.1007/978-3-319-45057-5

57. Sharmin T, Khan NR, Akram MS, Ehsan MM. A State-of-the-Art Review on Geothermal Energy Extraction, Utilization, and Improvement Strategies: Conventional, Hybridized, and Enhanced Geothermal Systems. International Journal of Thermofluids. 2023 May;18:100323.

58. Sipio ED, Galgaro A, Destro E, Giaretta A, Chiesa S. Thermal conductivity of rocks and regional mapping.

59. Spitler JD, Gehlin SEA. Thermal response testing for ground source heat pump systems—An historical review. Renewable and Sustainable Energy Reviews. 2015 Oct;50:1125–37.

60. Taussi M, Borghi W, Gliaschera M, Renzulli A. Defining the Shallow Geothermal Heat-Exchange Potential for a Lower Fluvial Plain of the Central Apennines: The Metauro Valley (Marche Region, Italy). Energies. 2021 Feb 1;14(3):768.

61. Thomas J, Frost RR, Harvey RD. THERMAL CONDUCTIVITY OF CARBONATE ROCKS.

62. Vespasiano G, Cianflone G, Taussi M, De Rosa R, Dominici R, Apollaro C. Shallow Geothermal Potential of the Sant'Eufemia Plain (South Italy) for Heating and Cooling Systems: An Effective Renewable Solution in a Climate-Changing Society. Geosciences. 2023 Apr 5;13(4):110.

63. Vieira A, Alberdi-Pagola M, Christodoulides P, Javed S, Loveridge F, Nguyen F, et al. Characterisation of Ground Thermal and Thermo-Mechanical Behaviour for Shallow Geothermal Energy Applications. Energies. 2017 Dec 3;10(12):2044.

64. Wagner R, Clauser C. Evaluating thermal response tests using parameter estimation for thermal conductivity and thermal capacity. J Geophys Eng. 2005 Dec 1;2(4):349–56.

65. Wagner V, Bayer P, Kübert M, Blum P. Numerical sensitivity study of thermal response tests. Renewable Energy. 2012 May;41:245–53.

66. Wang W, Wang G, Liu F, Liu C. Characterization of Ground Thermal Conditions for Shallow Geothermal Exploitation in the Central North China Plain (NCP) Area. Energies. 2022 Oct 8;15(19):7375.

67. Waples DW, Waples JS. A Review and Evaluation of Specific Heat Capacities of Rocks, Minerals, and Subsurface Fluids. Part 1: Minerals and Nonporous Rocks. Natural Resources Research. 2004 Jun;13(2):97–122.

68. White M, Vasyliv Y, Beckers K, Martinez M, Balestra P, Parisi C, et al. Numerical investigation of closed-loop geothermal systems in deep geothermal reservoirs. Geothermics. 2024 Jan;116:102852.

69. Xianglan Li, Shaowen Liu, Changge Feng. Thermal properties of sedimentary rocks in the Tarim Basin, northwestern China. 2018 November;10.1306/11211817179.

70. Ye X, Yu Z, Zhang Y, Kang J, Wu S, Yang T, et al. Mineral Composition Impact on the Thermal Conductivity of Granites Based on Geothermal Field Experiments in the Songliao and Gonghe Basins, China. Minerals. 2022 Feb 15;12(2):247.

71. Zarrella A, Emmi G, Graci S, De Carli M, Cultrera M, Santa G, et al. Thermal Response Testing Results of Different Types of Borehole Heat Exchangers: An Analysis and Comparison of Interpretation Methods. Energies. 2017 Jun 13;10(6):801.

72. Zhang J qi, Zhu C qing. Analysis of thermal properties of main sedimentary rocks in the Beijing area. Unconventional Resources. 2024;4:100104.

(1–72)

Appendix A

All of the graphs shown in Chapter 3 were created by using the Matplotlib library in python.

Thermal conductivity VS porosity (Figure 29):

```python
import matplotlib.pyplot as plt
import numpy as np


# Porosity and Thermal Conductivity for each rock type
rock_data = {
    "Sedimentary rocks": {
        "Conglomerate": {"Porosity": (20, 30), "Thermal Conductivity": (1.0, 2.5)},
        "Sandstone": {"Porosity": (10, 20), "Thermal Conductivity": (1.0, 4.0)},
        "Shale": {"Porosity": (10, 15), "Thermal Conductivity": (1.0, 3.0)},
        "Limestone": {"Porosity": (5, 10), "Thermal Conductivity": (1.0, 2.5)},
        "Travertine": {"Porosity": (10, 40), "Thermal Conductivity": (0.5, 1.5)},
        "Dolomite": {"Porosity": (5, 10), "Thermal Conductivity": (2.0, 4.0)},
        "Marl": {"Porosity": (10, 20), "Thermal Conductivity": (0.5, 1.5)},
        "Gypsum": {"Porosity": (30, 50), "Thermal Conductivity": (0.2, 0.5)},
        "Clay": {"Porosity": (20, 30), "Thermal Conductivity": (0.2, 1.0)},
        "Anhydrite": {"Porosity": (1, 5), "Thermal Conductivity": (2.5, 3.5)}
    },
    "Igneous rocks": {
        "Granite": {"Porosity": (1, 5), "Thermal Conductivity": (2.5, 5.0)},
        "Diorite": {"Porosity": (1, 5), "Thermal Conductivity": (2.5, 4.5)},
        "Syenite": {"Porosity": (1, 5), "Thermal Conductivity": (3.0, 4.5)},
        "Gabbro": {"Porosity": (1, 5), "Thermal Conductivity": (3.0, 6.0)},
        "Rhyolite": {"Porosity": (10, 20), "Thermal Conductivity": (1.5, 3.0)},
        "Dacite": {"Porosity": (10, 20), "Thermal Conductivity": (1.5, 3.0)},
        "Andesite": {"Porosity": (10, 20), "Thermal Conductivity": (1.5, 3.0)},
        "Granodiorite": {"Porosity": (5, 10), "Thermal Conductivity": (2.5, 3.5)},
        "Trachyte": {"Porosity": (10, 20), "Thermal Conductivity": (2.0, 3.0)},
        "Basalt": {"Porosity": (1, 5), "Thermal Conductivity": (2.5, 6.0)},
        "Tuff/Tuffstone": {"Porosity": (30, 50), "Thermal Conductivity": (0.5, 2.0)}
    },
    "Metamorphic rocks": {
        "Quartzite Schist": {"Porosity": (1, 5), "Thermal Conductivity": (3.0, 5.0)},
        "Micaschist": {"Porosity": (1, 5), "Thermal Conductivity": (2.5, 4.0)},
        "Calcschist": {"Porosity": (1, 5), "Thermal Conductivity": (2.5, 3.5)},
        "Metavolcanite": {"Porosity": (1, 5), "Thermal Conductivity": (2.5, 4.0)},
        "Gneiss": {"Porosity": (1, 5), "Thermal Conductivity": (2.5, 4.0)},
```

```python
        "Serpentinite": {"Porosity": (1, 5), "Thermal Conductivity": (2.5, 3.0)},
        "Marble": {"Porosity": (1, 5), "Thermal Conductivity": (2.0, 3.0)}
    },
    "Unconsolidated sediments": {
        "Clean Gravel, Dry": {"Porosity": (20, 30), "Thermal Conductivity": (1.0, 2.0)},
        "Heterograde Gravel & Sand, Wet": {"Porosity": (25, 40), "Thermal Conductivity":
(1.0, 2.0)},
        "Sand, Dry": {"Porosity": (30, 40), "Thermal Conductivity": (0.15, 0.50)},
        "Sand, Wet": {"Porosity": (30, 40), "Thermal Conductivity": (0.20, 0.70)},
        "Medium Silt, Wet": {"Porosity": (30, 40), "Thermal Conductivity": (0.18,
0.50)},
        "Silty Sand/Sandy Silt, Wet": {"Porosity": (30, 50), "Thermal Conductivity":
(0.10, 0.50)},
        "Dry, Dry": {"Porosity": (30, 40), "Thermal Conductivity": (0.10, 0.25)},
        "Silt and Clayey Silt, Wet": {"Porosity": (30, 50), "Thermal Conductivity":
(0.15, 0.30)},
        "Clay, Dry": {"Porosity": (20, 30), "Thermal Conductivity": (0.15, 0.25)},
        "Plastic Clay, Wet": {"Porosity": (20, 30), "Thermal Conductivity": (0.20,
0.40)},
        "Till/Loam": {"Porosity": (20, 30), "Thermal Conductivity": (0.10, 0.30)}
    }
}


# Initialize the figure
plt.figure(figsize=(14, 10))

markers = ['o', 's', 'D', '^', 'v', '<', '>', 'p', 'h', 'H', '+', 'x', 'X', 'd']

# Plot each rock type
for category, rocks in rock_data.items():
    for i, (rock, properties) in enumerate(rocks.items()):
        porosity_mid = np.mean(properties["Porosity"])
        conductivity_mid = np.mean(properties["Thermal Conductivity"])

        plt.scatter(porosity_mid, conductivity_mid, marker=markers[i % len(markers)],
s=100, label=f"{rock} ({category})")

# Customize plot
plt.xlabel("Porosity (%)")
plt.ylabel("Thermal Conductivity (Dry, W/m-K)")
plt.title("Thermal Conductivity vs. Porosity for Various Rock Types by Category")
```

```python
plt.legend(loc='center left', bbox_to_anchor=(1, 0.5), title="Rock Types by Category")
plt.grid(True)
plt.tight_layout()
plt.show()
```

Thermal conductivity VS density (Figure 30):

```python
import matplotlib.pyplot as plt
import numpy as np

# Density and Thermal Conductivity for each rock type
rock_data = {
    "Sedimentary rocks": {
        "Conglomerate": {"Density": 2.68, "Thermal Conductivity": (1.0, 2.5)},
        "Sandstone": {"Density": 2.65, "Thermal Conductivity": (1.0, 4.0)},
        "Shale": {"Density": 2.4, "Thermal Conductivity": (1.0, 3.0)},
        "Limestone": {"Density": 2.71, "Thermal Conductivity": (1.0, 2.5)},
        "Travertine": {"Density": 1.8, "Thermal Conductivity": (0.5, 1.5)},
        "Dolomite": {"Density": 2.79, "Thermal Conductivity": (2.0, 4.0)},
        "Marl": {"Density": 2.2, "Thermal Conductivity": (0.5, 1.5)},
        "Gypsum": {"Density": 2.3, "Thermal Conductivity": (0.2, 0.5)},
        "Clay": {"Density": 2.2, "Thermal Conductivity": (0.2, 1.0)},
        "Anhydrite": {"Density": 2.95, "Thermal Conductivity": (2.5, 3.5)}
    },
    "Igneous rocks": {
        "Granite": {"Density": 2.67, "Thermal Conductivity": (2.5, 5.0)},
        "Diorite": {"Density": 2.85, "Thermal Conductivity": (2.5, 4.5)},
        "Syenite": {"Density": 2.65, "Thermal Conductivity": (3.0, 4.5)},
        "Gabbro": {"Density": 3.0, "Thermal Conductivity": (3.0, 6.0)},
        "Rhyolite": {"Density": 2.4, "Thermal Conductivity": (1.5, 3.0)},
        "Dacite": {"Density": 2.6, "Thermal Conductivity": (1.5, 3.0)},
        "Andesite": {"Density": 2.7, "Thermal Conductivity": (1.5, 3.0)},
        "Granodiorite": {"Density": 2.69, "Thermal Conductivity": (2.5, 3.5)},
        "Trachyte": {"Density": 2.39, "Thermal Conductivity": (2.0, 3.0)},
        "Basalt": {"Density": 2.9, "Thermal Conductivity": (2.5, 6.0)},
        "Tuff/Tuffstone": {"Density": 2.25, "Thermal Conductivity": (0.5, 2.0)}
    },
    "Metamorphic rocks": {
        "Quartzite Schist": {"Density": 2.53, "Thermal Conductivity": (3.0, 5.0)},
        "Micaschist": {"Density": 2.6, "Thermal Conductivity": (2.5, 4.0)},
        "Calcschist": {"Density": 2.7, "Thermal Conductivity": (2.5, 3.5)},
        "Metavolcanite": {"Density": 2.69, "Thermal Conductivity": (2.5, 4.0)},
        "Gneiss": {"Density": 2.77, "Thermal Conductivity": (2.5, 4.0)},
        "Amphibolite": {"Density": 2.86, "Thermal Conductivity": (2.5, 3.5)},
        "Serpentinite": {"Density": 2.67, "Thermal Conductivity": (2.5, 3.0)},
        "Marble": {"Density": 2.6, "Thermal Conductivity": (2.0, 3.0)}
    },
    "Unconsolidated sediments": {
        "Clean Gravel, Dry": {"Density": 2.1, "Thermal Conductivity": (1.0, 2.0)},
        "Heterograde Gravel & Sand, Wet": {"Density": 2.1, "Thermal Conductivity":
(1.0, 2.0)},
        "Sand, Dry": {"Density": 2.0, "Thermal Conductivity": (0.15, 0.50)},
        "Sand, Wet": {"Density": 2.1, "Thermal Conductivity": (0.20, 0.70)},
        "Medium Sand, Wet": {"Density": 1.8, "Thermal Conductivity": (0.10, 0.50)},
        "Silty Sand/Sandy Silt, Wet": {"Density": 1.87, "Thermal Conductivity": (0.10,
0.50)},
        "Silt, Dry": {"Density": 1.43, "Thermal Conductivity": (0.10, 0.25)},
```

```
            "Silt and Clayey Silt, Wet": {"Density": 1.72, "Thermal Conductivity": (0.15,
0.30)},
            "Clay, Dry": {"Density": 1.68, "Thermal Conductivity": (0.15, 0.25)},
            "Plastic Clay, Wet": {"Density": 1.68, "Thermal Conductivity": (0.20, 0.40)},
            "Till/Loam": {"Density": 2.05, "Thermal Conductivity": (0.10, 0.30)}
    }
}

# Initialize the figure
plt.figure(figsize=(14, 10))

markers = ['o', 's', 'D', '^', 'v', '<', '>', 'p', 'h', 'H', '+', 'x', 'X', 'd']

# Plot each rock type
for category, rocks in rock_data.items():
    for i, (rock, properties) in enumerate(rocks.items()):
        conductivity_mid = np.mean(properties["Thermal Conductivity"])

        plt.scatter(properties["Density"], conductivity_mid, marker=markers[i %
len(markers)], s=100, label=f"{rock} ({category})")

# Customize plot
plt.xlabel("Density (g/cm³)")
plt.ylabel("Thermal Conductivity (Dry, W/m-K)")
plt.title("Thermal Conductivity vs. Density for Various Rock Types by Category")
plt.legend(loc='center left', bbox_to_anchor=(1, 0.5), title="Rock Types by Category")
plt.grid(True)
plt.tight_layout()
plt.show()
```

Thermal conductivity in both dry and saturated conditions if different rock types (Figure 31):

```
import matplotlib.pyplot as plt
import matplotlib.patches as patches

# Data with dry and saturated thermal conductivity ranges
data = [
    ("Conglomerate", 1.0, 2.5, 2.0, 5.0), ("Sandstone", 1.0, 4.0, 2.0, 6.0),
("Claystone", 1.3, 3.2, 4.0),
    ("Limestone", 1.0, 2.5, 2.0, 4.0), ("Travertine", 0.5, 1.5, 1.3, 3.0),
("Dolomite", 2.0, 4.0, 2.5, 5.5),
    ("Marl", 0.5, 1.5, 1.0, 3.0), ("Gypsum", 0.2, 0.5, 0.5, 1.0), ("Clay", 0.2, 1.0,
2.5, 3.0),
    ("Anhydrite", 2.5, 3.5, 3.0, 5.0), ("Granite", 2.5, 5.0, 3.0, 6.0), ("Diorite",
2.5, 4.5, 3.0, 6.0),
    ("Syenite", 3.0, 4.5, 3.5, 6.0), ("Gabbro", 3.0, 6.0, 4.0, 7.0), ("Rhyolite", 1.5,
3.0, 2.0, 4.0),
    ("Dacite", 1.5, 3.0, 2.0, 4.0), ("Andesite", 1.5, 3.0, 2.0, 4.0), ("Granodiorite",
2.5, 3.5, 3.0, 5.0),
    ("Trachyte", 2.0, 3.0, 2.5, 4.0), ("Basalt", 2.5, 6.0, 4.0, 7.0),
("Tuff/tuffstone", 0.5, 2.0, 1.0, 3.0),
    ("Quartzite Schist", 3.0, 5.0, 4.0, 6.0), ("Micaschist", 2.5, 4.0, 3.0, 5.0),
    ("Calcschists", 2.5, 3.5, 3.0, 5.0), ("Metavolcanite", 2.5, 3.5, 3.0, 5.0),
("Gneiss", 2.5, 4.0, 3.0, 5.0),
    ("Phyllite", 2.5, 3.5, 3.0, 5.0), ("Amphibolite", 2.5, 4.0, 3.0, 5.0),
    ("Serpentinite", 2.5, 3.0, 3.0, 5.0), ("Marble", 2.0, 3.0, 2.5, 3.5),
    ("Clean Gravel, Dry", 1.0, 1.3, 2.5), ("Heterometric Gravel with Sand, Wet", 1.0,
2.0, 2.0, 4.0),
```

```
    ("Sand, Dry", 0.15, 0.25, 0.80), ("Sand, Moist", 0.20, 0.70, 0.80),
    ("Medium Sand, Wet", 0.10, 0.25, 0.80), ("Silty Sand/Sandy Silt, Wet", 0.15, 0.30,
0.20, 0.40),
    ("Silt, Dry", 0.10, 0.25, 0.15, 0.35), ("Silt and Clayey Silt, Wet", 0.15, 0.30,
0.20, 0.40),
    ("Clay, Dry", 0.15, 0.25, 0.20, 0.50), ("Plastic Clay, Wet", 0.20, 0.40, 0.25,
0.60),
    ("Till/Loam", 0.10, 0.30, 0.15, 0.40), ("Organic Materials: Peat", 0.05, 0.25,
0.10, 0.30)
]

# Set up the figure and axis
fig, ax = plt.subplots(figsize=(12, 20))

for i, (rock, min_dry, max_dry, min_sat, max_sat) in enumerate(data):
    # Dry thermal conductivity range (blue)
    rect_dry = patches.Rectangle((min_dry, i - 0.25), max_dry - min_dry, 0.4,
                                 edgecolor='black', facecolor='blue', alpha=0.5,
                                 label="Dry" if i == 0 else "")

    ax.add_patch(rect_dry)

    # Saturated thermal conductivity range (yellow)
    rect_sat = patches.Rectangle((min_sat, i + 0.15), max_sat - min_sat, 0.4,
                                 edgecolor='black', facecolor='yellow', alpha=0.5,
                                 label="Saturated" if i == 0 else "")

    ax.add_patch(rect_sat)

ax.set_yticks(range(len(data)))
ax.set_yticklabels([rock for rock, _, _, _, _ in data])

# Set labels and title
ax.set_xlabel("Thermal Conductivity (W/m·K)")
ax.set_title("Rock Types vs Thermal Conductivity Ranges (Dry and Saturated)")

ax.legend(loc="upper right")

plt.grid(axis='x')
plt.xlim(0, 8)

# Show the plot
plt.tight_layout()
plt.show()
```

Thermal conductivity Ranges for Various Rock Types (Figure 32):

```
import matplotlib.pyplot as plt
import numpy as np
import matplotlib.cm as cm

# Data: rock types with their thermal conductivity ranges
rock_data = {
    "Conglomerate": (1.0, 2.5),
    "Sandstone": (1.0, 4.0),
    "Claystone": (1, 3),
    "Limestone": (1.0, 2.5),
    "Travertine": (0.5, 1.5),
    "Dolomite": (2.0, 4.0),
```

```python
        "Marl": (0.5, 1.5),
        "Gypsum": (0.2, 0.5),
        "Clay": (0.2, 1.0),
        "Anhydrite": (2.5, 3.5),
        "Granite": (2.5, 5.0),
        "Diorite": (2.5, 4.5),
        "Syenite": (3.0, 4.5),
        "Gabbro": (3.0, 6.0),
        "Rhyolite": (1.5, 3.0),
        "Dacite": (1.5, 3.0),
        "Andesite": (1.5, 3.0),
        "Granodiorite": (2.5, 3.5),
        "Trachyte": (2.0, 3.0),
        "Basalt": (2.5, 6.0),
        "Tuff/Tuffstone": (0.5, 2.0),
        "Quartzite Schist": (3.0, 5.0),
        "Micaschist": (2.5, 4.0),
        "Calcschists": (2.5, 3.5),
        "Metavolcanite": (2.5, 3.5),
        "Gneiss": (2.5, 4.0),
        "Phyllite": (2.5, 3.5),
        "Amphibolite": (2.5, 4.0),
        "Serpentinite": (2.5, 3.0),
        "Marble": (2.0, 3.0),
        "Clean Gravel, Dry": (1.0, 2.0),
        "Heterometric Gravel with Sand, Wet": (1.0, 2.0),
        "Sand, Dry": (0.15, 0.50),
        "Sand, Moist": (0.20, 0.70),
        "Medium Sand, Wet": (0.10, 0.50),
        "Silty Sand/Sandy Silt, Wet": (0.10, 0.50),
        "Silt, Dry": (0.10, 0.25),
        "Silt and Clayey Silt, Wet": (0.15, 0.30),
        "Clay, Dry": (0.15, 0.25),
        "Plastic Clay, Wet": (0.20, 0.40),
        "Till/Loam": (0.10, 0.30),
        "Organic Materials: Peat": (0.05, 0.25),
}

# Extract rock types and their corresponding conductivity ranges
rock_types = list(rock_data.keys())
min_conductivities = [value[0] for value in rock_data.values()]
max_conductivities = [value[1] for value in rock_data.values()]

# Set positions for x-axis
x_pos = np.arange(len(rock_types))

# Generate colors for each rock type
colors = cm.viridis(np.linspace(2, -2, len(rock_types)))  # Using Viridis colormap

# Create a figure
plt.figure(figsize=(14, 8))

# Plot each rock type with a unique color
for i, color in zip(range(len(rock_types)), colors):
    plt.fill_between([i - 0.3, i + 0.3], min_conductivities[i], max_conductivities[i],
color=color, alpha=1)
    plt.plot([i, i], [min_conductivities[i], max_conductivities[i]], color="black",
linewidth=1.5)

# Customize plot
plt.xlabel("Type of Rock")
```

```python
plt.ylabel("Thermal Conductivity (W/m·K)")
plt.title("Thermal Conductivity Ranges of Different Rock Types")
plt.xticks(x_pos, rock_types, rotation=90, ha="center")

# Set y-axis limits to data range
plt.ylim(min(min_conductivities) - 0.1, max(max_conductivities) + 0.5)

# Display plot
plt.tight_layout()
plt.show()
```

Thermal diffusivity Ranges for Various Rock Types (Figure 33):

```python
import matplotlib.pyplot as plt
import numpy as np
import matplotlib.cm as cm

# rock types with their thermal diffusivity ranges
rock_data = {
    "Conglomerate": (0.1, 0.3),
    "Sandstone": (0.1, 0.3),
    "Clay-Mudstone": (0.05, 0.1),
    "Limestone": (0.1, 0.4),
    "Travertine": (0.05, 0.1),
    "Dolomite": (0.1, 0.2),
    "Marl": (0.1, 0.3),
    "Gypsum": (0.05, 0.1),
    "Clay": (0.05, 0.1),
    "Anhydrite": (0.1, 0.2),
    "Granite": (0.5, 1.0),
    "Diorite": (0.5, 1.0),
    "Syenite": (0.5, 1.0),
    "Gabbro": (0.5, 1.0),
    "Rhyolite": (0.3, 0.5),
    "Dacite": (0.3, 0.5),
    "Andesite": (0.3, 0.5),
    "Granodiorite": (0.5, 1.0),
    "Trachyte": (0.5, 0.8),
    "Basalt": (0.5, 1.0),
    "Tuff/Tuffstone": (0.05, 0.1),
    "Quartzite Schist": (0.5, 1.0),
    "Micaschist": (0.5, 1.0),
    "Calcschists": (0.5, 1.0),
    "Metavolcanite": (0.5, 1.0),
    "Gneiss": (0.5, 1.0),
    "Phyllite": (0.5, 1.0),
    "Amphibolite": (0.5, 1.0),
    "Serpentinite": (0.5, 1.0),
    "Marble": (0.5, 1.0),
    "Clean Gravel, Dry": (0.1, 0.3),
    "Heterometric Gravel with Sand, Wet": (0.1, 0.3),
    "Sand, Dry": (0.01, 0.05),
    "Sand, Moist": (0.01, 0.05),
    "Medium Sand, Wet": (0.01, 0.05),
    "Silty Sand/Sandy Silt, Wet": (0.01, 0.05),
    "Silt, Dry": (0.01, 0.05),
    "Silt and Clayey Silt, Wet": (0.01, 0.05),
    "Clay, Dry": (0.01, 0.05),
    "Plastic Clay, Wet": (0.01, 0.05),
    "Till/Loam": (0.01, 0.05),
```

```
        "Organic Materials: Peat": (0.01, 0.05),
}

# Extract rock types and their corresponding thermal diffusivity ranges
rock_types = list(rock_data.keys())
min_diffusivities = [value[0] for value in rock_data.values()]
max_diffusivities = [value[1] for value in rock_data.values()]

# Set the positions for the x-axis
x_pos = np.arange(len(rock_types))

# Create a figure
plt.figure(figsize=(12, 8))

# Generate a list of colors
colors = cm.viridis(np.linspace(2, -2, len(rock_types)))  # Using the viridis colormap

# Create bars for thermal diffusivity ranges using rectangles
for i in range(len(rock_types)):
    plt.fill_between([i, i], min_diffusivities[i], max_diffusivities[i],
color=colors[i], alpha=0.8)
    plt.plot([i, i], [min_diffusivities[i], max_diffusivities[i]], color=colors[i],
linewidth=10)

# Customize the plot
plt.xlabel("Type of Rock")
plt.ylabel("Thermal Diffusivity (m²/s)")
plt.title("Thermal Diffusivity Ranges of Different Rock Types")
plt.xticks(x_pos, rock_types, rotation=90, ha="center")

# Set the y-axis limits to match only the range of data (not starting from 0)
plt.ylim(min(min_diffusivities) - 0.01, max(max_diffusivities) + 0.1)

# Optionally, add a grid for better readability
plt.grid(axis="y", linestyle="--", alpha=0.7)

# Display the plot
plt.tight_layout()
plt.show()
```

Thermal conductivity and thermal diffusivity of different rock types (Figure 34):

```
import matplotlib.pyplot as plt

import numpy as np

import pandas as pd


# Data as a list of dictionaries
data = [
    {"Rock Type": "Conglomerate", "Lithology": "Sedimentary", "Thermal Conductivity":
(1.0, 2.5), "Thermal Diffusivity": (0.1, 0.3)},
    {"Rock Type": "Sandstone", "Lithology": "Sedimentary", "Thermal Conductivity": (1.0,
4.0), "Thermal Diffusivity": (0.1, 0.3)},
    {"Rock Type": "Claystone", "Lithology": "Sedimentary", "Thermal Conductivity": (1,
3), "Thermal Diffusivity": (0.05, 0.1)},
```

```
{"Rock Type": "Limestone", "Lithology": "Sedimentary", "Thermal Conductivity": (1.0,
2.5), "Thermal Diffusivity": (0.1, 0.4)},
    {"Rock Type": "Travertine", "Lithology": "Sedimentary", "Thermal Conductivity":
(0.5, 1.5), "Thermal Diffusivity": (0.05, 0.1)},
    {"Rock Type": "Dolomite", "Lithology": "Sedimentary", "Thermal Conductivity": (2.0,
4.0), "Thermal Diffusivity": (0.1, 0.2)},
    {"Rock Type": "Marl", "Lithology": "Sedimentary", "Thermal Conductivity": (0.5,
1.5), "Thermal Diffusivity": (0.1, 0.3)},
    {"Rock Type": "Gypsum", "Lithology": "Sedimentary", "Thermal Conductivity": (0.2,
0.5), "Thermal Diffusivity": (0.05, 0.1)},
    {"Rock Type": "Clay", "Lithology": "Sedimentary", "Thermal Conductivity": (0.2,
1.0), "Thermal Diffusivity": (0.05, 0.1)},
    {"Rock Type": "Anhydrite", "Lithology": "Sedimentary", "Thermal Conductivity": (2.5,
3.5), "Thermal Diffusivity": (0.1, 0.2)},

    {"Rock Type": "Granite", "Lithology": "Igneous", "Thermal Conductivity": (2.5, 5.0),
"Thermal Diffusivity": (0.5, 1.0)},
    {"Rock Type": "Diorite", "Lithology": "Igneous", "Thermal Conductivity": (2.5, 4.5),
"Thermal Diffusivity": (0.5, 1.0)},
    {"Rock Type": "Syenite", "Lithology": "Igneous", "Thermal Conductivity": (3.0, 4.5),
"Thermal Diffusivity": (0.5, 1.0)},
    {"Rock Type": "Gabbro", "Lithology": "Igneous", "Thermal Conductivity": (3.0, 6.0),
"Thermal Diffusivity": (0.5, 1.0)},
    {"Rock Type": "Rhyolite", "Lithology": "Igneous", "Thermal Conductivity": (1.5,
3.0), "Thermal Diffusivity": (0.3, 0.5)},
    {"Rock Type": "Dacite", "Lithology": "Igneous", "Thermal Conductivity": (1.5, 3.0),
"Thermal Diffusivity": (0.3, 0.5)},
    {"Rock Type": "Andesite", "Lithology": "Igneous", "Thermal Conductivity": (1.5,
3.0), "Thermal Diffusivity": (0.3, 0.5)},
    {"Rock Type": "Granodiorite", "Lithology": "Igneous", "Thermal Conductivity": (2.5,
3.5), "Thermal Diffusivity": (0.5, 1.0)},
    {"Rock Type": "Trachyte", "Lithology": "Igneous", "Thermal Conductivity": (2.0,
3.0), "Thermal Diffusivity": (0.5, 0.8)},
    {"Rock Type": "Basalt", "Lithology": "Igneous", "Thermal Conductivity": (2.5, 6.0),
"Thermal Diffusivity": (0.5, 1.0)},
    {"Rock Type": "Tuff/Tuffstone", "Lithology": "Igneous", "Thermal Conductivity":
(0.5, 2.0), "Thermal Diffusivity": (0.05, 0.1)},

    {"Rock Type": "Quartzite Schist", "Lithology": "Metamorphic", "Thermal
Conductivity": (3.0, 5.0), "Thermal Diffusivity": (0.5, 1.0)},
```

```python
    {"Rock Type": "Micaschist", "Lithology": "Metamorphic", "Thermal Conductivity":
(2.5, 4.0), "Thermal Diffusivity": (0.5, 1.0)},


    {"Rock Type": "Clean Gravel, Dry", "Lithology": "Unconsolidated", "Thermal
Conductivity": (1.0, 2.0), "Thermal Diffusivity": (0.1, 0.3)},
    {"Rock Type": "Heterometric Gravel with Sand, Wet", "Lithology": "Unconsolidated",
"Thermal Conductivity": (1.0, 2.0), "Thermal Diffusivity": (0.1, 0.3)},
    {"Rock Type": "Sand, Dry", "Lithology": "Unconsolidated", "Thermal Conductivity":
(0.15, 0.50), "Thermal Diffusivity": (0.01, 0.05)},
]


# Create a DataFrame
df = pd.DataFrame(data)

# Extract the average values for thermal conductivity and diffusivity
df["Avg Thermal Conductivity"] = df["Thermal Conductivity"].apply(lambda x: (x[0] +
x[1]) / 2)
df["Avg Thermal Diffusivity"] = df["Thermal Diffusivity"].apply(lambda x: (x[0] + x[1])
/ 2)


# Plotting
x = np.arange(len(df["Rock Type"]))  # the label locations
width = 0.35  # the width of the bars

fig, ax = plt.subplots(figsize=(14, 8))

# Create bars for thermal conductivity and diffusivity
bars1 = ax.bar(x, df["Avg Thermal Conductivity"], width, label="Thermal Conductivity
(W/mK)", color="lightskyblue")
bars2 = ax.bar(x + width, df["Avg Thermal Diffusivity"], width, label="Thermal
Diffusivity (m²/s)", color="greenyellow")

# Add some text for labels, title and custom x-axis tick labels, etc.
ax.set_ylabel("Values")
ax.set_title("Thermal Conductivity and Diffusivity of Different Rock Types")
ax.set_xticks(x)
ax.set_xticklabels(df["Rock Type"], rotation=90)
ax.legend()

ax.grid(axis="y")
```

```python
# Show the plot
plt.tight_layout()
plt.show()
```

Volumetric heat capacity ranges of different rock types (Figure 35):

```python
import matplotlib.pyplot as plt
import numpy as np
import matplotlib.cm as cm

# Data: rock types with their heat capacity ranges
rock_data = {
    "Conglomerate": (800, 1000),
    "Sandstone": (800, 1000),
    "Claystone": (1000, 2200),
    "Limestone": (800, 1000),
    "Travertine": (1000, 2200),
    "Dolomite": (800, 1000),
    "Marl": (1000, 2200),
    "Gypsum": (800, 1400),
    "Clay": (1000, 2200),
    "Anhydrite": (800, 1400),
    "Granite": (800, 1200),
    "Diorite": (800, 1200),
    "Syenite": (800, 1200),
    "Gabbro": (800, 1200),
    "Rhyolite": (800, 1000),
    "Dacite": (800, 1000),
    "Andesite": (800, 1000),
    "Granodiorite": (800, 1200),
    "Trachyte": (800, 1200),
    "Basalt": (800, 1200),
    "Tuff/Tuffstone": (800, 2200),
    "Quartzite Schist": (800, 1200),
    "Micaschist": (800, 1200),
    "Calcschists": (800, 1200),
    "Metavolcanite": (800, 1200),
    "Gneiss": (800, 1200),
    "Phyllite": (800, 1200),
    "Amphibolite": (800, 1200),
    "Serpentinite": (800, 1200),
    "Marble": (800, 1200),
    "Clean Gravel, Dry": (800, 2000),
    "Heterometric Gravel with Sand, Wet": (800, 2000),
    "Sand, Dry": (800, 2000),
    "Sand, Moist": (800, 2000),
    "Medium Sand, Wet": (800, 2000),
    "Silty Sand/Sandy Silt, Wet": (800, 2000),
    "Silt, Dry": (800, 2000),
    "Silt and Clayey Silt, Wet": (800, 2000),
    "Clay, Dry": (800, 2000),
    "Plastic Clay, Wet": (800, 2000),
    "Till/Loam": (800, 2000),
    "Organic Materials: Peat": (1500, 2500),
}
```

```python
# Extract rock types and their corresponding heat capacity ranges
rock_types = list(rock_data.keys())
min_heat_capacity = [value[0] for value in rock_data.values()]
max_heat_capacity = [value[1] for value in rock_data.values()]

# Set the positions for the x-axis
x_pos = np.arange(len(rock_types))

# Create a figure
plt.figure(figsize=(12, 8))

# Generate a list of colors
colors = cm.viridis(np.linspace(2, -2, len(rock_types)))  # Using the viridis colormap

# Create bars for heat capacity ranges using rectangles
for i in range(len(rock_types)):
    plt.fill_between([i, i], min_heat_capacity[i], max_heat_capacity[i],
color=colors[i], alpha=0.4)
    plt.plot([i, i], [min_heat_capacity[i], max_heat_capacity[i]], color=colors[i],
linewidth=10)

# Customize the plot
plt.xlabel("Type of Rock")
plt.ylabel("Volumetric Heat Capacity (J/kg·K)")
plt.title("Volumetric Heat Capacity Ranges of Different Rock Types")
plt.xticks(x_pos, rock_types, rotation=90, ha="center")

# Set the y-axis limits to match only the range of data (not starting from 0)
plt.ylim(min(min_heat_capacity) - 100, max(max_heat_capacity) + 100)

# Optionally, add a grid for better readability
plt.grid(axis="y", linestyle="--", alpha=0.7)

# Display the plot
plt.tight_layout()
plt.show()
```

Create a figure